

AWARD NUMBER: W81XWH-11-1-0491

TITLE: Role of microRNA in aggressive prostate cancer

PRINCIPAL INVESTIGATOR: Hsieh, Jer-Tsong

CONTRACTING ORGANIZATION: University of Texas
Southwestern Medical Center
Dallas, TX 75390

REPORT DATE: September 2015

TYPE OF REPORT: Final

PREPARED FOR: U.S. Army Medical Research and Materiel Command
Fort Detrick, Maryland 21702-5012

DISTRIBUTION STATEMENT: Approved for Public Release;
Distribution Unlimited

The views, opinions and/or findings contained in this report are those of the author(s) and should not be construed as an official Department of the Army position, policy or decision unless so designated by other documentation.

REPORT DOCUMENTATION PAGE			<i>Form Approved</i> <i>OMB No. 0704-0188</i>		
Public reporting burden for this collection of information is estimated to average 1 hour per response, including the time for reviewing instructions, searching existing data sources, gathering and maintaining the data needed, and completing and reviewing this collection of information. Send comments regarding this burden estimate or any other aspect of this collection of information, including suggestions for reducing this burden to Department of Defense, Washington Headquarters Services, Directorate for Information Operations and Reports (0704-0188), 1215 Jefferson Davis Highway, Suite 1204, Arlington, VA 22202-4302. Respondents should be aware that notwithstanding any other provision of law, no person shall be subject to any penalty for failing to comply with a collection of information if it does not display a currently valid OMB control number. PLEASE DO NOT RETURN YOUR FORM TO THE ABOVE ADDRESS.					
1. REPORT DATE September 2015		2. REPORT TYPE Final		3. DATES COVERED 15 Jun 2011 - 14 Jun 2015	
4. TITLE AND SUBTITLE Role of microRNA in aggressive prostate cancer			5a. CONTRACT NUMBER		
			5b. GRANT NUMBER W81XWH-11-1-0491		
			5c. PROGRAM ELEMENT NUMBER		
6. AUTHOR(S) Jer-Tsong Hsieh E-Mail: jt.hsieh@utsouthwestern.edu			5d. PROJECT NUMBER		
			5e. TASK NUMBER		
			5f. WORK UNIT NUMBER		
7. PERFORMING ORGANIZATION NAME(S) AND ADDRESS(ES) UT Southwestern Medical Center 5323 Harry Hines Blvd., Dallas, TX 75390			8. PERFORMING ORGANIZATION REPORT NUMBER		
9. SPONSORING / MONITORING AGENCY NAME(S) AND ADDRESS(ES) U.S. Army Medical Research and Materiel Command Fort Detrick, Maryland 21702-5012			10. SPONSOR/MONITOR'S ACRONYM(S)		
			11. SPONSOR/MONITOR'S REPORT NUMBER(S)		
12. DISTRIBUTION / AVAILABILITY STATEMENT Approved for Public Release; Distribution Unlimited					
13. SUPPLEMENTARY NOTES					
14. ABSTRACT The majority of mortality of prostate cancer (PCa) is due to the recurrent metastasized castration resistance PCa. The acquisition of epithelial-to-mesenchymal transition (EMT) in PCa signifies the initial process of cancer metastasis. Our previous findings unveiled that DAB2IP is down-regulated in high-grade PCa specimens and this novel tumor suppressor can block EMT leading to lymph node metastasis. It has recently been associated with the onset of cancer stem cell (CSC) that is considered as cancer initiating cell with a survival advantage during the course of cancer therapy. However, the mechanism of action is not fully characterized. Using microRNA microarray screening, we found microRNA-363 (miR363) is significantly down regulated in several DAB2IP knockdown (KD) prostate cells. In particular, miR363 is predominately expressed in normal prostate and belongs to the miR106a-363 cluster that is closely resembled to the oncogenic miR17-92 cluster in their seed sequence. It appears that DAB2IP significantly regulates the expression of a unique miR-363; the profile of miR-363 expression appears to be highly specific in normal prostate. The objective of this project is to delineate the functional links of miR-363 with the appearance of CSC and its clinical correlation in aggressive PCa.					
15. SUBJECT TERMS					
16. SECURITY CLASSIFICATION OF:			17. LIMITATION OF ABSTRACT	18. NUMBER OF PAGES	19a. NAME OF RESPONSIBLE PERSON USAMRMC
a. REPORT U	b. ABSTRACT U	c. THIS PAGE U			19b. TELEPHONE NUMBER (include area code)
			UU		

Table of Contents

	<u>Page</u>
1. Introduction.....	1
2. Keywords.....	2
3. Accomplishments.....	2
4. Impact.....	3
5. Changes/Problems.....	4
6. Products.....	4
7. Participants & Other Collaborating Organizations.....	4
8. Special Reporting Requirements.....	4
9. Appendices.....	5

INTRODUCTION

MicoRNA (miR) is a large family of a short sequence of single-stranded noncoding RNAs and known to regulate approximate 60% protein-coding genes by post-transcriptional suppression, target mRNA degradation, or translational inhibition (1, 2). Until now, many miRs have been identified to be associated with different stages of tumor development. Based on their seed sequence of 2-7 nucleotides are grouped into different family for predicting the potential target gene(s), the function of miRs could be divided into onco-miR and tumor suppressor miR. However, only handful of them has been demonstrated experimentally (*Appendix: Review Article*)

In general, similar to most protein-coding genes, miRNA genes can be regulated at transcriptional or post-transcriptional level (3). Unlike most eukaryotic protein genes, several miRNAs such as miR-106a-363 (4) and miR-17-92 are clustered together to generate a polycistronic primary transcript (5-7), which further complicates the regulatory scheme of miRNA biogenesis because each individual miRNA derived from one cluster may have different functional roles as well as expression levels in any given cell or tissue. For example, miR-363 belongs to the polycistronic miR-106a-363 cluster containing six miRNAs (miR-106a, miR-18b, miR-20b, miR-19b-2, miR-92a-2 and miR-363), located on chromosome X. Unlike the other five miRNAs with similar seed sequences and similar functions as the oncogenic miR-17-92 cluster (8), we demonstrated that miR-363 is a tumor suppressor miRNA capable of suppressing epithelial-to-mesenchymal transition (EMT) in prostate cancer (PCa).

In this project, we unveiled a new post-transcriptional regulatory machinery of miR turnover by a novel protein complex- Interferon-induced protein with tetratricopeptide repeats 5 (IFIT5) (9, 10) and exoribonuclease XRN1. This machinery is very specific to miR-363 but not other member miRNAs in miR-106a-363 cluster. Also, elevated IFIT5 is correlated with PCa tumor grade. In addition, IFIT5 complex can regulate the turnover of other tumor suppressor miRNAs, particularly, involved in regulating cancer stem cell.

Taken together, IFIT5-XRN1 complex mediates a specific degradation of tumor suppressor miRNA from its cluster, which could provide a new understanding of miRNA biogenesis. IFIT5 also represents a potential target for metastatic PCa.

REFERENCES

1. Aalto AP, Pasquinelli AE. (2012) Small non-coding RNAs mount a silent revolution in gene expression. *Current Opinion In Cell Biol.* 24:333-340.
2. Schickel R, Boyerinas B, Park SM, Peter ME. (2008) MicroRNAs: key players in the immune system, differentiation, tumorigenesis and cell death. *Oncogene* 27:5959-5974.
3. Thiery JP (2002) Epithelial-mesenchymal transitions in tumour progression. *Nat. Rev. Cancer* 2:442-454.
4. Yang J, Weinberg RA (2008) Epithelial-mesenchymal transition: at the crossroads of development and tumor metastasis. *Dev. Cell* 14:818-829.
5. Mani SA, et al. (2008) The epithelial-mesenchymal transition generates cells with properties of stem cells. *Cell* 133:704-715.

6. Xie, D, et al. (2009) DAB2IP/AIP1, a novel tumor suppressor, coordinates both PI3K-Akt and ASK1 pathways. Proc. Natl. Acad. Sci., USA 106:19878-19883.
7. Xie, D, et al. (2010) The role of DAB2IP in modulating epithelial-to-mesenchymal transition and prostate cancer metastasis. Proc. Natl. Acad. Sci., USA 107:2485-2490.
8. Landais S, et al. (2007) Oncogenic potential of the miR-106-363 cluster and its implication in human T-cell leukemia. Cancer Res. 67:5699-5707.
9. Abbas YM, et al. (2013) Structural basis for viral 5'-PPP-RNA recognition by human IFIT proteins. Nature 494:60-64.
10. Katibah GE, et al. (2013) tRNA binding, structure, and localization of the human interferon-induced protein IFIT5. Molecular Cell 49:743-750.

KEYWORDS

Prostate cancer, metastasis, epithelial-to-mesenchymal transition, cancer stem cell, microRNA-363, microRNA turnover, Interferon-induced protein with tetratricopeptide repeats 5 (IFIT5), exoribonuclease XRN1

ACCOMPLISHMENTS

A. PROJECT ACCOMPLISHMENTS

Goal 1: Study the regulation of miR-363 gene expression by DAB2IP.

- IFIT5-XRN1 complex represents unique machinery for miR-363 turnover (*Appendix: Figure 1 and Manuscript draft*).
- IFIT5 complex can specifically degrade mature miR-363 from miR-106a-363 cluster in PCa cells (*Appendix: Manuscript draft-Figure 1-3, and Additional file 1-2*).
- DAB2IP regulates the expression of IFIT5-XRN1 protein complex (*Appendix: Manuscript draft-Figure 2 and 4*)

Goal 2: Delineate the functional role of miR-363 in modulating Cancer Stem cell (CSC) phenotype.

- IFIT5-XRN1 complex specifically modulates the turnover of miRNAs with 5'-overhanging sequence (*Appendix: Manuscript draft-Figure 3-5, and Additional file 3-5*).
- MiR-363 can inhibit EMT leading to PCa metastases by targeting Slug mRNA (*Appendix: Manuscript draft-Figure 5-7 and Additional file 6*).
- IFIT5 complex also degrades miR-101, miR-128, miR-203, and miR-345 that are targeting Bmi-1 mRNA associated with CSC (*Appendix: Figure 2, 4 and 5*).

Goal 3: Study the correlation of DAB2IP and miR-363 in PCa progression.

- Loss of miR-363 expression is correlated with clinical PCa development mRNA (*Appendix: Manuscript draft-Figure 8 and Additional file 8*).
- Increased IFIT5 expression is correlated with clinical PCa development (*Appendix: Manuscript draft-Figure 8 and Additional file 8*).
- A positive correlation between IFIT5 and XRN1 expression is detected in PCa specimens (*Appendix: Manuscript draft-Additional file 8*)

B. OTHER ACHIEVEMENTS

- IFIT5 complex also degrades miR-101, miR-128, miR-203, and miR-345 that are targeting Bmi-1 mRNA in Glioblastoma (GBM) cells (*Appendix: Figure 2 and 4*).
- A positive correlation between IFIT5 and Bmi-1 expression was observed in clinical GBM database (*Appendix: Figure 4*).
- IFIT5 is able to increase stemness phenotype of PCa via Bmi-1-mediated pathway (*Appendix: Figure 5*).
- Dr. Lo has received a 2-years postdoctoral training award from DOD-PCRP in 2014.

IMPACT

MiRNA is initially transcribed into a long primary transcript (pri-miRNA) and subsequently processed by Drosha and Dicer-mediated endonuclease cleavage to generate mature miRNA. The miRNA biogenesis becomes more complicated when differential expression of individual miRNA located in the same polycistronic cluster is observed. In this project, we identify the tumor suppressive effect of miR-363, from a cluster that contains the rest of miRNAs characterized as onco-miRs, on intervening the EMT process in PCa cells. Most significantly, a new miRNA degradation machinery associated with IFIT5 that specifically recognizes a unique 5'-end structure of miRNA and recruits exoribonuclease (XRN1) to degrade this miRNA is identified (*Appendix: Figure 1*) from this project, which could provide a new aspect of miRNA biogenesis for the regulation of other tumor suppressor miRNA genes as well.

Despite of completing 3 specific aims proposed in original project, we extended our effort to discover the specificity of IFIT5 in modulating miRNA biogenesis. In addition to PCa, we also found IFIT5 elevation in GBM cells. Therefore, we profile miRNA expression in both PCa and GBM cells by manipulating IFIT5 levels. Indeed, the majority of miRNA modulated by IFIT3 contain the 5'-overhanging sequence (*Appendix: Figure 2*). Among that, we found 4 different miRNAs (101, 128, 203, 345) consistently decreased in the presence of IFIT5 from all the PCa and GBM cells examined in this experiment (*Appendix: Figure 3A*) and validated by additional PCa and GBM cells (*Appendix: Figure 4*). Interestingly, all these miRs appear to target Bmi-1 (*Appendix: Figure 3A*) that is involved in stem cell formation. From TCGA database, we also observed a significant correlation between IFIT5 and Bmi-1 expression (*Appendix: Figure 3B*). Furthermore, data from prostatesphere formation study using PCa cells concluded that the presence of IFIT5 is critical for increasing stemness phenotype in PCa in which Bmi-1 is a key downstream factor (*Appendix: Figure 5*). Taken together, the overall project discovers a new regulation of microRNA biogenesis that is related with PCa progression.

Interferon-induced tetratricopeptide repeat (IFIT) protein family is first identified as viral RNAs binding protein that is a part of antiviral defense mechanisms by reducing virus replication or disrupt protein-protein interactions in host translation-initiation machinery. Among IFIT orthologs, IFIT1, IFIT2 and IFIT3 form a complex through its tetratricopeptide repeats (TPR). On the contrary, IFIT5 acts solely as a monomer and binds directly to RNA molecules via its convoluted RNA-binding cleft. In addition, IFIT5

has been shown to directly bind to endogenous cellular RNA with a 5'-end phosphate cap, including transfer RNA (tRNA), which partially shared a structural similarity with the precursor form of small RNAs such as small hairpin RNA (shRNA) and miRs. We have demonstrated the first time that IFIT5 is able to specifically recognize a unique structure in the precursor miR-363 and recruit XRN1 to degrade miR363. We have also shown that the significant elevation of IFIT5 is detected in several PCa cells undergone EMT leading to highly metastatic potential and the expression level of IFIT5 is correlated with that of miR-363 in PCa specimens.

Furthermore, IFIT5 is also elevated in GBM. Using both PCa and GBM cell models to profile IFIT5-mediated miRs, a subset of miRs (101, 128, 203, 345) is identified and shares a common target Bmi-1 mRNA that is involved in stem cell development. Indeed, the presence of IFIT5 can elicit CSC phenotype that is correlated with Bmi-1 expression. Overall, this study unveils a new mechanism of miRNA degradation, particularly, tumor suppressor miR involved in EMT and CSC. Most significantly, this is the first study to unveil this miRNA turnover machinery in PCa research community. There are several major impact: developing new reagents for the area of miRNA research, identifying new prognostic marker for PCa patients, unveiling new function of IFIT5, training postdoctor to become independent investigator, and expanding new research horizon to other diseases.

CHANGES/PROBLEMS

N/A

PRODUCTS

Publications, Conference papers, and Presentations

1. Review article: Lo, U., Yang, D., Hsieh, J.T. (2013) The role of microRNAs in prostate cancer progression. *Trans. Androl. Urol.*, 2: 228-241 (Appendix: Review article).
2. Peer-reviewed article: Lo, U., Pong, R.C., Yang, D., Gandee, L., Zhou, J.C., Tseng, S-F., Hsieh, J.T. (2015) A new microRNA turnover machinery mediated by IFIT4 complex leading to epithelial-to-mesenchymal transition. *Genome Biology* (Appendix: Manuscript draft).
3. AACR podium presentation: Lo, R.C. Pong, D. Yang, J. Zhou, S.F. Tseng & J.T. Hsieh (2015) The specific regulation of miR-363 turnover from miR-106a-363 cluster by IFIT5 complex leading to epithelial-to-mesenchymal transition (EMT). Podium Presentation, *The 2015 annual meeting of American Association of Cancer Research (AACR)*, Philadelphia, PA, USA. (Appendix: AACR Podium presentation)
4. Abstract: Lo, R.C. Pong, D. Yang, J. Zhou, S.F. Tseng & J.T. Hsieh (2015) The role of IFIT5 in miR-363 turnover. Poster Session, *The 2015 Keystone Symposium of MicroRNAs and Noncoding RNAs in Cancer*, Keystone, CO, USA.

PARTICIPANTS AND OTHER COLLABORATING ORGANIZATIONS

N/A

SPECIAL REPORTING REQUIREMENTS

N/A

APPENDICES

Figure 1 Schematic representation of IFIT5-mediated pre-miR-363 turnover leading to EMT.

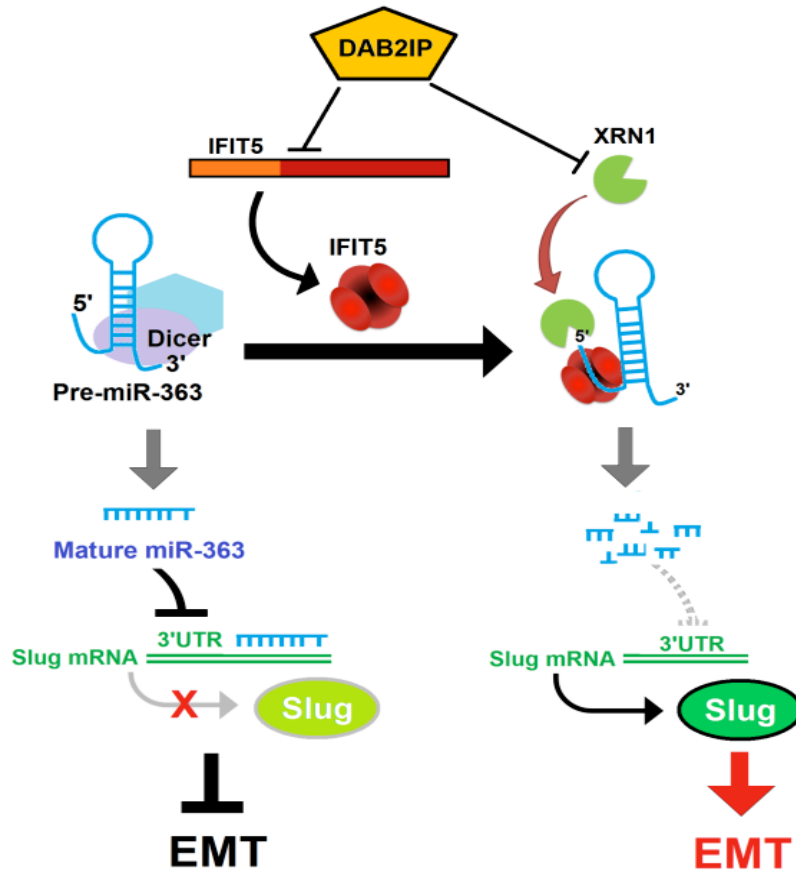


Figure 2 Profiling miR mediated by IFIT5 degradation complex from PCa and GBM cells. Small RNA was prepared from PCa or GBM cells by either knocking down endogenous IFIT5 or overexpressing IFIT5 and subjected to microRNA microarray. By comparing each set, the miR candidates were chosen and their secondary structure were deduced. Based on the 5'-sequences of each miRNA was divided into SN (single-nucleotide overhanging), MN (multiple-nucleotides overhanging), and DS: double-stranded overhanging.

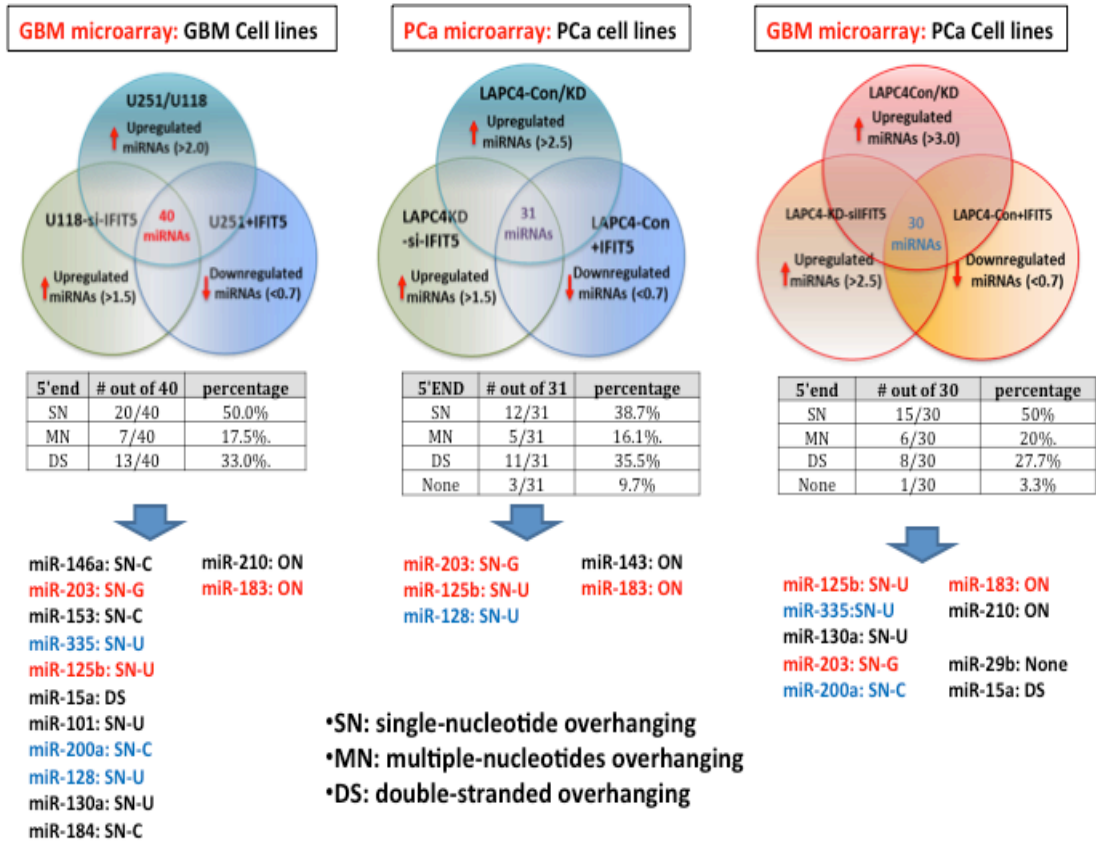


Figure 3 Bmi-1 as a common target and its clinical correlation between IFIT5 expression in PCa and GBM. (A) Identification of common miRNAs in PCa and GBM cells modulated by IFIT5 and their potential target mRNA (B) Clinical correlation between IFIT5 and Bmi-1 in clinical PCa and brain cancer.

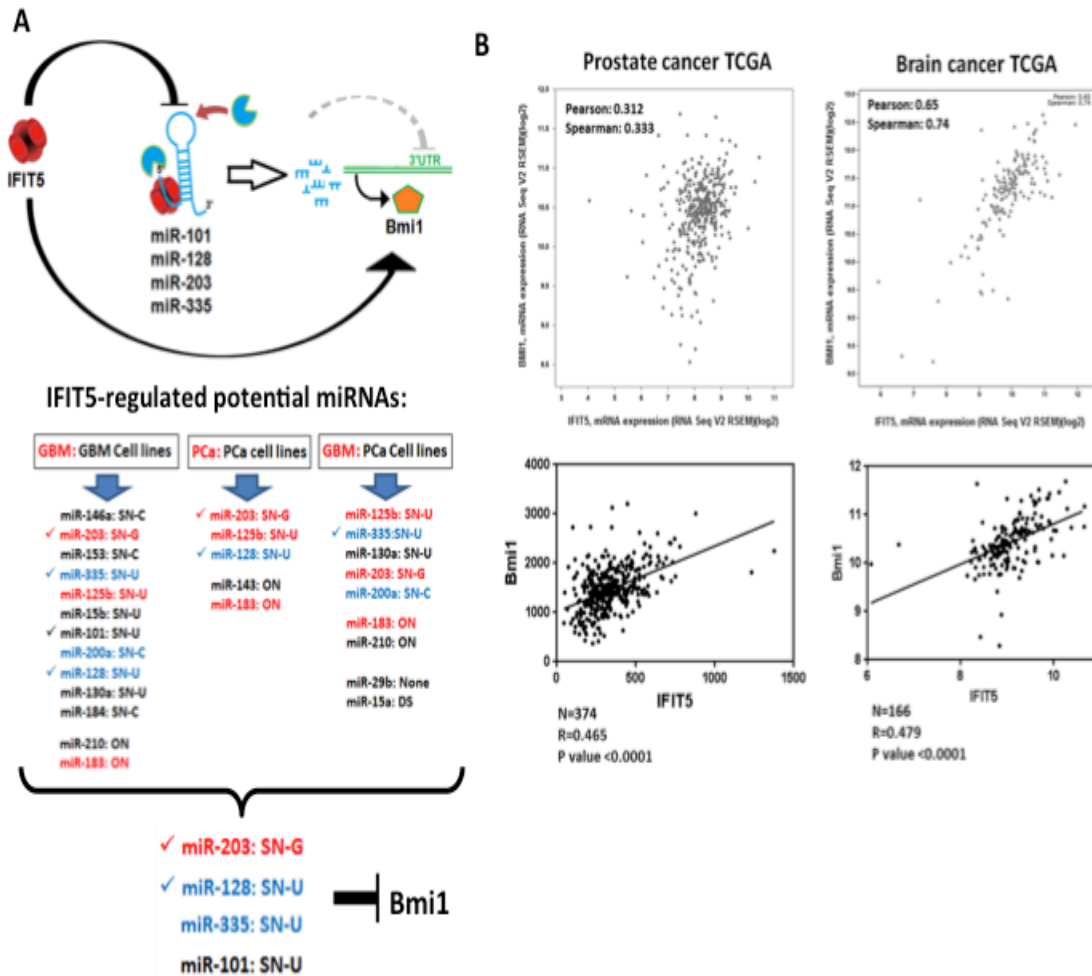


Figure 4 Validation of miRNA expression modulated by IFIT5 in PCa and GBM cells. By knocking down endogenous IFIT5 expression in several PCa cell lines, the expression level of Bmi-1 and Sox4 proteins were determined by western blot analyses. These cells were also subjected to ultralow attachment plate for their sphere formation.

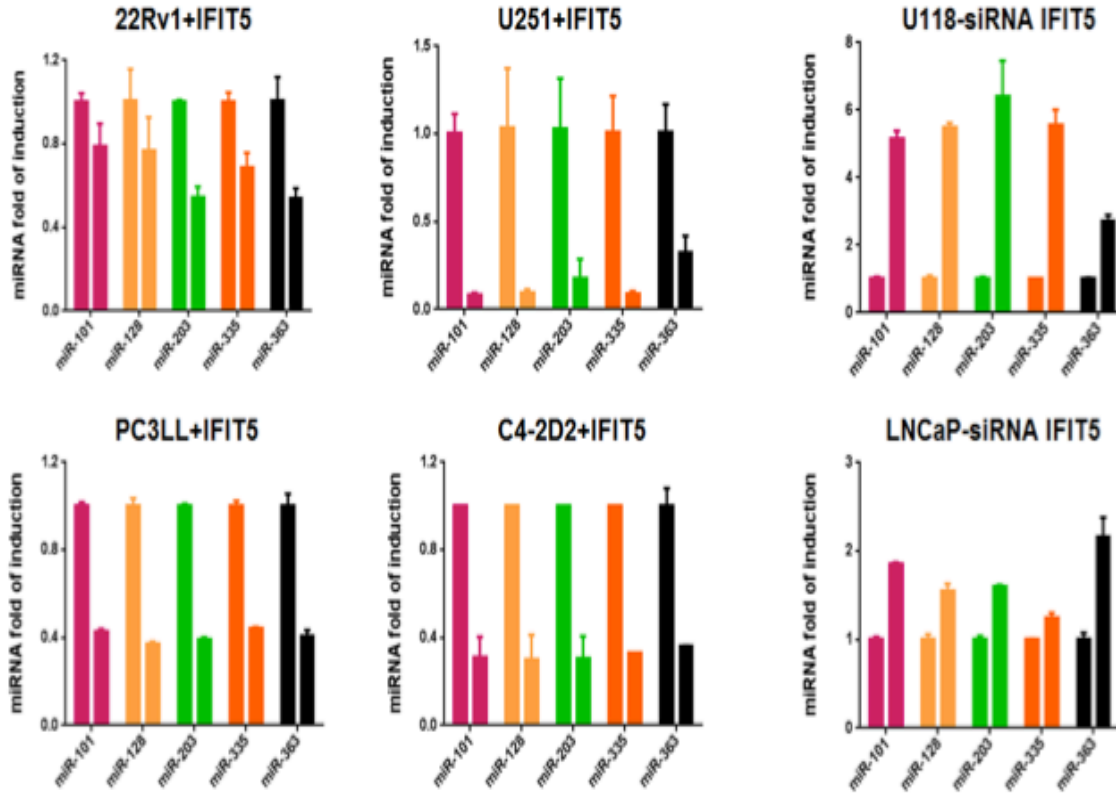
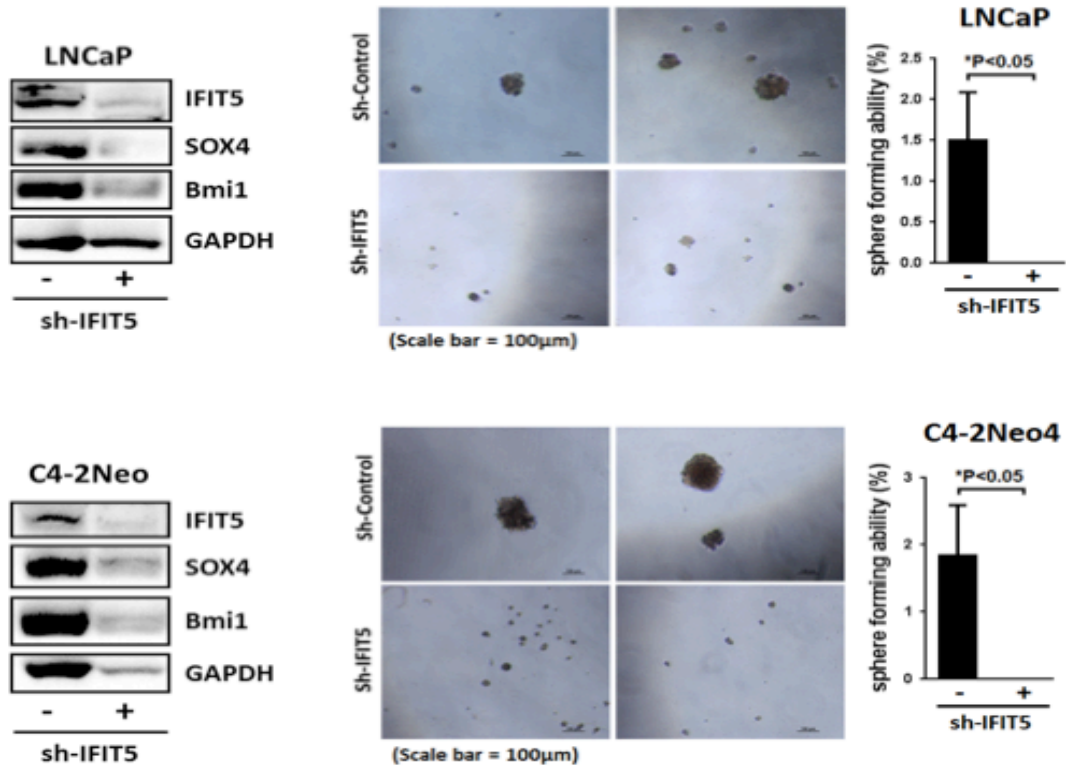


Figure 5 The role of IFIT5 in prostasphere formation of PCa cells. By modulating IFIT5 expression in several PCa and GBM cell lines by transfecting either cDNA for increasing protein expression or specific shRNA for decreasing protein expression, the expression level of each candidate miRNAs was determined using quantitative real-time reverse transcription polymerase chain reaction.



The role of microRNAs in prostate cancer progression

U-Ging Lo, Diane Yang, Jer-Tsong Hsieh

Departments of Urology, University of Texas Southwestern Medical Center, Dallas, TX 75390, USA

Corresponding to: Jer-Tsong Hsieh. 5323 Harry Hines Blvd. Dallas, TX 75390, USA. Email: JT.Hsieh@UTSouthwestern.edu.

Abstract: Prostate cancer (PCa) is the most common male malignancy and the second highest cause of cancer-related mortality in United States. MicroRNAs (miRNAs) are small non-coding RNAs that represent a new mechanism to regulate mRNA post-transcriptionally. It is involved in diverse physiological and pathophysiological process. Dysregulation of miRNAs has been associated with the multistep progression of PCa from prostatic intraepithelial neoplasia (PIN), localized adenocarcinoma to metastatic castration-resistance PCa (CRPC). Identification of unique miRNA could provide new biomarkers for PCa and develop into therapeutic strategies. In this review, we will summarize a broad spectrum of both tumor suppressive and oncogenic miRNAs, and their mechanisms contribute to prostate carcinogenesis.

Key Words: Androgen receptor (AR); castration-resistant prostate cancer (CRPC); epithelial-to-mesenchymal transition (EMT); microRNA (miRNA)



Submitted Aug 01, 2013. Accepted for publication Aug 05, 2013.

doi: 10.3978/j.issn.2223-4683.2013.08.01

Scan to your mobile device or view this article at: <http://www.amepc.org/tau/article/view/2550/3635>

Introduction

Prostate cancer (PCa) is a typical hormone-dependent disease (1); however, almost all PCa patients with androgen-ablation therapy ultimately become castration-resistant prostate cancer (CRPC), which contributes to the majority of mortality in PCa. Androgen receptor (AR) is known as a key mitogen for the growth and morphogen for the development of prostate. In PCa, AR activity is critical for the disease progression and becomes hyperactivated in CRPC. Mounting evidences indicate that the development of PCa is highly associated with aberrant AR activity resulted from AR gene amplification and/or mutation, alternative splicing (2-7), the cross talk with growth factor signaling pathways (8-13), and the presence of AR co-activators and AR co-repressors (14-17). In particular, Dicer-mediated maturation of microRNAs (miRNAs) suppresses the expression level of AR co-repressors, NCoR and SMRT, leading to enhance AR transcriptional activity (18). Based on the interaction between Dicer and AR, the correlation between AR and microRNA signaling has been broadly examined to investigate the fundamental role of miRNAs in PCa progression.

miRNAs are a large family of small 20-25 nt single stranded noncoding RNAs, which can interfere with the expression of ~60% protein coding genes by post-transcriptional suppression, target mRNA degradation, or translational inhibition (19). In the past two decades, significant advances have been achieved in miRNA research. miRNAs are found to be highly conserved among the animal phylogeny. Based on their conserved sequences, miRNAs shared an identical seed region of 2-7 nucleotides are grouped into different family. Up to date, 63 miRNA families have been categorized and more than 1,000 miRNAs have been fully characterized in their expression, epigenetic regulation, biogenesis and functions. In general, miRNAs are either derived from non-coding RNA transcripts or located within the introns of protein-coding genes (20,21). Multiple miRNAs can be clustered in close proximity and encoded together as a single polycistronic primary transcript, such as miR-106a-363 (22) and miR-17-92 clusters (23). The transcriptional mechanism of microRNA is similar to that of mRNA. miRNA gene promoters are regulated by transcriptional factors that also regulate protein-coding gene expression. For example, the promoter region of miR-21 can be regulated by AR, activation protein 1 (AP-1) and

signal transducer and activator of transcription 3 (STAT-3) (24,25). Hence elevation of miR-21 in cancer is partially due to aberrant activation of AR and AP-1. Meanwhile, c-Myc is a well-known oncogene that is suggested to regulate an oncogenic miR-17-92 cluster. Overexpression of both c-Myc and miR-17-92 cluster is indicated to enhance the tumor aggressiveness (26). Moreover, the genomic organization of miRNAs reveals that about 52% of miRNA genes are localized at the fragile chromosomal regions, which are susceptible to amplification, deletion and translocation associated with cancer. A recent study indicates that let-7 miRNAs family is located in the genomic regions that are frequently deleted in multiple cancer types including PCa (27). Moreover, the miR-15a/miR-16-1 cluster is located at chromosome 13q14. The frequency of allelic loss at 13q increases from early, advanced to metastatic PCa (28). In addition, aberrant DNA hypermethylation at the CpG island is often observed in the promoter region or transcriptional start site of tumor suppressive miRNAs such as miR-200/-141, miR-205, miR-34, miR-143 and miR-145 associated with PCa (29-32). Thus epigenetic regulation is also a key regulatory mechanism for miRNA gene expression.

In addition to the regulation of miRNA gene expression, the biosynthetic process of miRNA maturation becomes an emerging area. The biogenesis of miRNAs composes sequential steps of RNase III-mediated endonucleolytic cleavage mechanisms (33,34). In brief, the primary transcripts of miRNAs are transcribed by RNA polymerase II and processed in the nucleus by Drosha and Pasha (DGCR8) into a 70-100 nucleotides-long precursor miRNAs (pre-miRNAs) (35). Pre-miRNAs are exported to the cytoplasm through Exportin 5 and further processed by Dicer, generating a 20-25 nt RNA duplex comprise of a matured guide strand and a complementary passenger strand (miRNA*). The single stranded matured miRNA is then incorporated into the RNA-induced silencing complex (RISC) associated with Agonaut (AGO2), and bound to the complementary sequence on the 3' untranslated region (3' UTR) of target mRNA, leading to mRNA degradation (36-38). Based on their post-transcriptional regulation on a variety of target genes, miRNA is expected to be involved in virtually every biologic process in cell. In cancer, based on their post-transcriptional repression on a variety of oncogenes or tumor suppressor genes, miRNAs are also divided into onco-miRNAs (oncomirs) and tumor suppressors miRNAs (*Figure 1*). Overall, the importance of microRNAs has become a key to gain more understanding of molecular mechanisms associated with prostatic

carcinogenesis. In this review, we will focus on key unique miRNAs (*Tables 1,2*) involved in PCa.

Tumor suppressive miRNAs

Let-7 family

The let-7 gene encodes a highly conserved miRNA family of let-7a, let-7b, let-7c, let-7d, let-7e, let-7f, let-7g, let-7i and miR-98, which are significantly down-regulated in localized PCa, compared to adjacent benign tissues (39). The functionality of let-7 has been shown to target oncogenes involved in cell-cycle regulation, cell migration, proliferation, differentiation, and epithelial-to-mesenchymal transition (EMT) progression. In particular, let-7g can inhibit tumor growth via post-transcriptional suppression on RAS oncogene (44). On the other hand, loss of let-7 miRNAs is corresponded with elevated level of Enhancer of Zeste homolog 2 (Ezh2) correlated with PCa progression (45). Ectopic expression of let-7 results in the reduction of Ezh2, accompanied with diminished clonogenic ability and sphere formation in PCa cells (45). Another let-7 target gene is High-mobility group AT-hook 2 (HMGA2) (89) that is highly expressed in PCa compared to adjacent benign tissues. Indeed, HMGA2 was found de-repressed upon let-7 inhibition (43). Meanwhile, co-regulation of HMGA2 and Smad were found to orchestrate an EMT transcriptional network via targeting the promoter of SNAI1 in human hepatocarcinoma cell line (90). These results suggest a possibility that let-7 could inhibit EMT via targeting HMGA2 during PCa progression. Moreover, another study also imply that let-7 can induce cell cycle arrest and xenograft PCa tumor development by suppressing E2F2 and CCND2, which are found to be the direct target of let-7 (43). Lin-28 is a well-identified post-transcriptional suppressor of precursor let-7 maturation (91,92); An inverse correlation between lin28 and let-7 is also found in many cancer cell lines including PC3 (93). Based on these observations, lin28-mediated let-7 biogenesis has become an important mechanism to impact tumorigenesis. Conversely, let-7 can target the lin28 mRNA, suggesting that a reciprocal feedback loop exists between let-7 and lin28 (94-97). In addition, c-Myc is found to be a key factor involved in this interaction. c-Myc acts as a transcriptional activator for lin-28 gene expression and c-Myc is also found to be a target gene of let-7 family in multiple cancer types (40,98,99). Overall, the orchestrated interaction between lin28, let-7 and c-Myc is a complicated network of gene

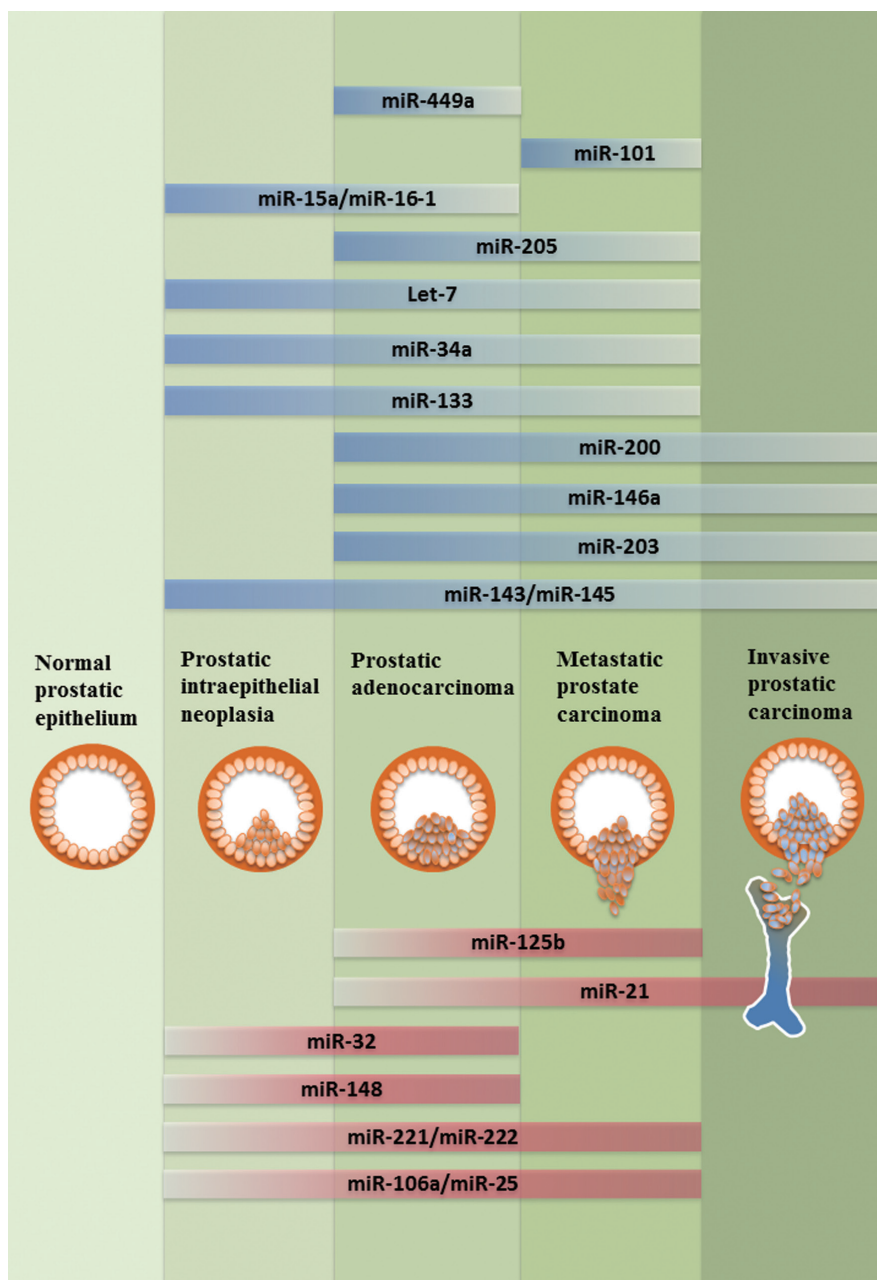


Figure 1 Schematic representation of tumor suppressive miRNAs (blue) and oncogenic miRNAs (red) in the prostatic tumorigenesis progression from PIN to metastatic CRPC

regulation, which is often altered in cancer cells (100). Also, let-7c is shown to antagonize AR expression by targeting c-Myc (101). Overexpression of let-7 leads to AR suppression, accompanied with attenuated cell proliferation, clonogenicity and anchorage-independent growth in PCa cells (39,41). Overall, the let-7 miRNA family exerts tumor suppressor characteristics via targeting multiple oncogenes including RAS,

HMGA2, Ezh2, Lin28 and c-Myc. Therefore, let-7 could be a potential diagnostic biomarker and further developed into a new therapeutic strategy for PCa.

miR-143 and miR-145

Both miR-143 and miR-145 are derived from the same

Table 1 Tumor suppressive miRNAs in PCa

miRNA	Target genes	Function	Ref.
Let-7	AR, c-MYC	Suppress cell proliferation, clonogenicity and anchorage-independent growth	(39-41)
	HMGA2	Suppress advanced tumor progression	(42)
	E2F2, CCND2	Induce cell cycle arrest <i>in vitro</i> and suppress tumor development <i>in vivo</i>	(43)
	RAS	Inhibit tumor growth	(44)
	EZH2	Inhibit clonogenicity and sphere formation	(45)
miR-143	KRAS	Suppress cell proliferation, migration <i>in vitro</i> Attenuate bone metastatic invasion <i>in vivo</i>	(46,47)
	ERK5	Arrest cell proliferation and abrogate tumor growth	(48)
	CD133, CD44, OCT4, KLF4, c-MYC	Suppress tumor sphere formation	(49)
miR-145	FSCN1	Inhibit cell proliferation, invasion, migration and arrest cell cycle	(50)
	OCT4, SOX2, KLF4	Suppress tumor stemness by inhibiting sphere formation	(51)
miR-200	ZEB1 ZEB2	Prevent PDGF-D induced EMT	(52)
	SLUG	Inhibit TGF- β induced EMT and suppress mesenchymal differentiation	(53,54)
miR-203	CKAP2, LASP1, WASF1, BIRC5, ASAP1	Suppress cell proliferation, promote cell apoptosis and inhibit metastasis dissemination	(55)
	RUNX2	Inhibit tumor invasion destined for bone metastasis	(55,56)
	PARK7, BRCA1	Impair cell growth by promoting apoptosis and cell cycle arrest	(57)
	ZEB2, Bmi, Survivin	Suppress bone metastasis via inhibition of cell motility, invasion and EMT	(56)
miR-205	ErbB3, E2F1, E2F5, PKC ϵ ,	Counteract EMT by attenuate cell migration and invasion	(58)
	BCL2	Promote cell apoptosis and cell cycle arrest in response to DNA damage	(59)
	PSAP, ARA24, HRAS, PARK7	Induce apoptosis and cell cycle arrest	(57)
	AR, NR4A2, EPCAM	Impair cell growth by promoting apoptosis and cell cycle arrest	(60)
miR-34a	CD44	Inhibit tumor progenitor cells and suppress metastasis	(61)
	AR	Suppress tumor metastasis	(62)
	CDK6	Induce cell-cycle arrest, cell senescence and apoptosis	(32)
	c-MYC	Inhibit cell proliferation and cell invasion	(63)
	BCL2, SIRT1	Induce cell senescence and apoptosis	(64,65)
miR-101	EZH2	Attenuate tumor cell invasiveness	(66,67)
miR-133	EGFR	Reduce cell proliferation, migration and invasiveness	(68)
miR-146a	ROCK1	Suppress cell metastasis to bone marrow endothelium	(69) N.Y.
	EGFR, MMP2	Inhibit cell growth, colony formation and migration <i>in vitro</i> Reduce tumorigenicity and angiogenesis <i>in vivo</i>	(70)
miR-15	FGF-2, FGFR1	Impair the tumor-supportive capability of stromal cells	(71)
miR-16	WNT3A	Attenuate tumor expansion and invasiveness	(72)
	BCL2, CCND1	Induce growth arrest, apoptosis	(72)
miR-449	HDAC1, CCND1	Induce cell cycle arrest and loss of clonogenicity	(73,74)

miR-143/-145 cluster, which are found down-regulated in metastatic PCa samples (29). Both miR-143 and miR-145 share similar functions in tumor suppression.

First, miR-143 is found to exhibit a negative effect on PCa cell proliferation and migration by targeting ERK5 and KRAS, and inactivating subsequent epidermal growth

Table 2 Oncogenic miRNAs in PCa

miRNA	Target genes	Function	Ref.
miR-21	RECK	Promote tumor invasiveness, support xenograft tumor growth and induce castration-resistance phenotype	(75,76)
	MARCKS, PDCD4, TPM1	Promote cell apoptosis resistance, motility, and invasion	(77)
miR-125b	p53, Puma, BAK1	Promote xenograft tumor growth	(78,79)
	p14ARF	Enhance cell proliferation	(80)
miR-221	ARHI	Enhance cell proliferation, colony formation, invasion, and cell survival	(81,82)
miR-222	p27	Promote cell cycle progression and increase clonogenicity. Enhance tumorigenicity <i>in vivo</i>	(83,84)
miR-32	BTG2, PIK3IP1	Facilitate cell growth by inhibit apoptosis and enhance proliferation	(85,86)
miR-148	CAND1	Facilitate tumor growth by enhance cell proliferation	(87)
miR-106a	CASP7	Facilitate tumor progression	(88)
miR-25			

factor receptor (EGFR)-RAS-MAPK signaling pathway (46,48). On the other hand, miR-145 is shown to inhibit PCa cell proliferation by targeting Fascin homolog 1 (FSCN1) that is an actin bundling protein involved in cell motility, adhesion and cellular interactions during tumorigenesis and metastasis (50). Second, overexpression of both miRNAs in PC3 cells represses fibronectin and enhances E-cadherin expression and both can reverse EMT and further attenuate the tumor invasiveness in an *in vivo* bone metastasis model (47). Third, a recent study indicates that both miR-143 and miR-145 can suppress the stem cell characteristics in PC3 cell lines by inhibiting the stem cell markers or factors including CD133, CD44, Oct4, c-Myc and Klf4 (49). Similarly, some studies of embryonic stem cell (ESCs) indicate that miR-145 has been identified to repress pluripotency by targeting Oct4, Sox2, and Klf4 (51,102). Taken together, both miR-143 and miR-145 can suppress several cancer behaviors of PCa cells from tumor proliferation, invasion/metastasis and stemness.

miR-200 family

During embryogenesis, EMT is established to determine the transition between epithelial and mesenchymal phenotypes at different developmental stages (103,104). However, during prostatic carcinogenesis, EMT has been highly implicated in PCa progression by initiating the tumor invasiveness (105-107). The consequences of EMT result in the suppression of epithelial markers by transcriptional repressors including ZEB1, ZEB2, SNAI1 and SNAI2, which are found to be the target genes of

several tumor suppressive miRNAs including the miR-200 family. The miR-200 family consists of miR-200a, miR-200b, miR-200c, miR-141 and miR-449, which are significantly down-regulated during PCa progression and identified to suppress PCa tumor metastasis particularly via inhibiting EMT. A recent study using PC3 cell line indicates that miR-200 can inhibit the platelet-derived growth factor-D (PDGF-D)-induced acquisition of EMT via targeting of both ZEB1 and ZEB2 (52). Another group studying benign prostate hyperplasia (BPH) also shows that miR-200 can reverse the TGF β -induced EMT phenotype in BPH cell line (53). Meanwhile, in kidney epithelial cell line, all miR-200 family members have been shown to suppress TGF β -induced EMT via targeting ZEB1, ZEB2 and SNAI2 *in vitro* (108,109); Similar result is also found in unilateral urethral obstruction (UUO) model that miR-200 can protect renal tubular epithelial cells from mesenchymal transition via suppressing ZEB1 and ZEB2 *in vivo* (110). In addition, a regulatory feedback loop has been demonstrated between SNAI2 and the miR-200 family. While miR-200 can target SNAI2 mRNA, SNAI2 protein acts as a repressor to suppress miR-200 gene expression (54). Thus, down-regulation of miR-200 may disrupt the homeostasis between SNAI2 and miR-200. Overall, loss of the miR-200 family in PCa initiates EMT process, which is critical for PCa invasiveness.

miR-203

miR-203 is a well-characterized tumor suppressor and shared the similar anti-metastatic function to miR-200

family (111,112). MiR-203 has been demonstrated to induce MET in PC3 and DU145 cell lines via targeting CKAP2, LASP1, BIRC5, WASF1, ASAP1, and RUNX2, which are critical effectors involved in cell proliferation, migration, invasion and EMT (55). Meanwhile, other study also suggests that miR-203 exhibits its negative effect on multiple steps of the PCa metastatic cascade via targeting on pro-metastatic molecules including ZEB2, Bmi, survivin, and Runx2. As a result, restoration of miR-203 in PC3, VCaP, and MDA-PCa-2b cell lines attenuates the invasiveness of PCa bone metastasis *in vivo* (56). This evidence suggests miR-203 play an important role in the metastatic progression of PCa and that loss of miR-203 may further enhance the invasive characteristics of advanced PCa.

miR-205

Similar to miR-203, miR-205 regulates PCa progression by targeting EMT signaling mechanisms (113). Restoration of miR-205 in PCa cells can induce MET phenotype by up-regulation of E-cadherin, along with attenuated cell invasiveness. In a more detailed study, miR-205 is suggested to attenuate cell invasion and migration via targeting ErbB3, E2F1, E2F5 and protein kinase C ϵ (PKC ϵ) (58). Meanwhile, another study using xenograft model with tail vein injection also demonstrates that miR-205 can inhibit PCa lung metastasis *in vivo* by targeting ZEB1 and vimentin (114). In addition to EMT regulation, miR-205 can also promote PCa cell apoptosis and cell-cycle arrest by targeting the anti-apoptotic gene BCL2 (59). Moreover, miR-205 is able to inhibit tumor cell growth by inducing apoptosis and cell cycle arrest via targeting AR co-regulators (DJ-1, PSAP, ARA24) and MAPK signaling components (57). These accumulating findings indicate that both miR-203 and miR-205 may suppress metastatic progression of PCa by impairing the EMT-induced invasiveness.

miR-34a

In PCa, miR-34a is identified as a tumor suppressor by inhibiting the stemness characteristics of prostate cancer stem cells (CSC) (61). The study demonstrates that miR-34a is down-regulated in the CD44 + PCa cells purified from xenograft tumors; overexpression of miR-34a can attenuate clonogenic expansion, tumor regeneration, and metastasis in CD44 + PCa cells. These results suggest that miR-34a is a negative regulator of prostate CSC and may exert its suppressive effect on PCa progression

before the onset of metastatic CRPC. Moreover, miR-34a appears to be a p53-regulated gene from a study (115) using doxorubicin and camptothecin-induced p53 activation that a significant up-regulation of both miR-34a and miR-34c is shown. However, this p53-mediated miR-34a up-regulation is abolished in both AR-knockdown LNCaP cells and AR-negative cell lines including PC3 and DU145, suggesting miR-34a expression is AR-dependent. On the other hand, AR has been identified as a direct target gene of miR-34a (62); AR activity can be repressed by de-methylation of epigenetically silenced miR-34a promoter in PCa cells. Overall, these findings imply a reciprocal transcriptional regulatory network among miR-34a, p53 and AR in PCa cells. However, whether this network is involved in PCa progression and its clinical significance require further investigation. Another target gene of miR-34a is c-Myc (63). By targeting the c-Myc expression, miR-34a is shown to suppress the signaling cascade of c-Myc-Skp2-Miz1, which leads to RhoA gene expression and subsequent attenuates cell migration and invasion. In addition to PCa stemness and metastasis, miR-34a also affect the PCa tumor growth by inducing cell-cycle arrest, cell senescence and apoptosis via targeting cell-cycle regulatory gene, such as CDK6 (32), and anti-apoptosis genes including Bcl-2 and SIRT1 (64,65). Overall, miR-34a may exert its tumor suppressor role via targeting various signaling molecules at different stages of PCa progression.

miR-101

Ezh2 is a histone methyltransferase that regulates epigenetic silencing and early studies have demonstrated that overexpression of Ezh2 in PCa contributes to the enhanced aggressiveness and metastatic potential of PCa cells (116-119). A study shows an inverse correlation between miR-101 and Ezh2 expression has been observed in human PCa. Meanwhile, miR-101 is found to suppress the expression and function of Ezh2 in PCa cell lines (66) and the overexpression of miR-101 in PC3, DU145 and LNCaP cells also results in the suppression of Ezh2, along with attenuated cell invasion and migration of these PCa cell lines *in vitro* (67,117). These findings clearly indicate the role of miR-101 in the epigenetic regulation critical for PCa progression via targeting Ezh2 expression.

miR-133 and miR-146a

Epidermal growth factor (EGF) and EGFR are known

to be key tumor promoter for PCa (120). A recent study indicates that, under hypoxia condition, EGFR can interrupt the biogenesis of mHESM (miRNAs regulated by hypoxia-dependent EGFR-suppressed maturation) resulted in reducing Dicer binding and abolishing miRNA maturation via targeting AGO2 phosphorylation (121). Implying that EGFR may certainly contribute to the modification of miRNA processing. On the other hand, both miR-133 and miR-146a have been shown to suppress PCa tumor progression via targeting EGFR. Down-regulation of miR-133 has been observed in PC3 and DU-145 cell lines. Ectopic expression of miR-133 can reduce cell proliferation, migration and invasiveness by targeting EGFR (68). Similar to miR-133, expression level of miR-146a is also significantly down-regulated in PCa (122,123). Overexpression of miR-146a has been demonstrated to suppress PCa cell growth, colony formation and migration *in vivo* via targeting EGFR. Additional studies also reveal that miR-146a can inhibit angiogenesis and bone metastasis *in vivo* by suppressing both matrix metalloproteinase-2 (MMP2) and Rho-associated, coiled-coil containing protein kinase 1 (ROCK1) expression (69,70). These findings indicate that loss of both miR-133 and miR-146a in PCa may attribute to enhancement of EGFR signaling, leading to aggressive PCa progression.

miR-15a and miR-16-1

miR-15a and miR-16-1 are in the same cluster; the expression of miR-15a/miR-16-1 is often down-regulated in PCa due to chromosomal deletion at 13q14, which is highly correlated with the progression of PCa (124). A study has demonstrated that miR-15a/miR-16-1 level is inversely correlated with B-cell lymphoma 2 (BCL2), cyclin-D1 (CCND1) and wingless-type 3A (WNT3A) in advanced PCa (72). The same group also found that both CCND1 and WNT3A are putative target genes of miR-15a/miR-16-1. As a result, restoration of miR-15a and miR-16 is shown to arrest cell growth and induce apoptosis and knockdown of miR-15a/miR-16-1 can promote survival, proliferation and invasiveness of PCa xenograft tumor *in vivo*. On the other hand, miR-15a and miR-16-1 also exert tumor suppressive effects by interfering the stromal support in the tumor microenvironment since interaction between tumor cells and the surrounding cellular components is critical for tumor development (125,126). It has been indicated that down-regulation of miR-15a and miR-16 in cancer-associated fibroblasts results in tumor expansion and invasion (72), which is supported by the

reconstitution of both miRNAs in fibroblast can interrupt the stromal support by targeting FGF-2 and FGFR1 (71). All these data indicate that the tumor suppressor role of miR-15a/ miR-16-1 is to suppress cancer cells or interrupt their communication with the microenvironment.

miR-449a

miR-449a is inversely correlated with the expression of histone deacetylase 1 (HDAC1)-an enzyme critical for epigenetic regulation. It has been indicated that increased expression of miR-449a in PCa cell lines leads to both cell cycle arrest and loss of clonogenicity by targeting HDAC1 (73). In addition, miR-449 can initiate cell cycle arrest and induce cell senescence by targeting cyclinD1 (74).

Oncogenic miRNAs

miR-21

The recurrence of CRPC is often associated with hyperactivation of AR. Recent studies have suggested that several oncogenic miRNAs is correlated with aberrant AR activation. In particular, miR-21 is an AR-regulated miRNA and its expression level is consistently elevated from androgen-dependent PCa to CRPC (127). Overexpression of miR-21 can support xenograft tumor growth and induce castration-resistant phenotype (75). In addition to androgen response element (ARE), other cis-elements such as AP-1 and STAT-3 are also found in the promoter region of miR-21 (24,25). AP-1 activity is closely associated with CRPC recurrence (128) and STAT-3 is also shown to be involved in PCa metastasis (129). Overall, the highly elevation of miR-21 may be attributed to the aberrant expression of transcriptional activators such as AR and AP-1. The subsequent effect of miR-21 overexpression in turn contributes to the development of prostate tumorigenesis. Several target genes of miR-21 have been shown to suppress tumor progression by inhibiting invasiveness, promoting apoptosis and cell cycle arrest. For example, myristoylated alanine-rich protein kinase c substrate (MARCKS) is a direct target of miR-21, which plays key role in cell motility, membrane trafficking and mitogenesis. Thus, miR-21 promotes the apoptosis resistance, cell motility and invasiveness of PC3 and DU-145 cells partly via targeting MARCKS (77). Meanwhile, a recent study demonstrates that reversion-inducing cysteine-rich protein with Kazal motifs (RECK) is another novel target of miR-21; An

inverse correlation between RECK and miR-21 has been shown from different stages of PCa (76).

miR-125b

Similar to miR-21, miR-125b is also an AR-induced miRNA. The induction of miR-125b in LNCaP cells inhibits apoptosis and enhances cell proliferation. Mechanistically, miR-125b promotes PCa xenograft tumor growth by targeting major pro-apoptotic genes including p53, Puma and BAK1 (78). Consistent with this observation, miR-125b is shown to modulate the p53 network by interrupting Mdm2 degradation via targeting p14^{ARF}, which mediates the Mdm2 sequestration (80). Overall, miR-125b can target the p53-p21 and Puma signaling network, leading to enhanced cell proliferation in both LNCaP and CWR22Rv1 PCa cell lines through p53-dependent and p53-independent manner, respectively.

miR-221 and miR-222

Both miR-221 and miR-222 belong to the same miRNA cluster. Overexpression of miR-221/miR-222 has been often found in PCa. The aberrant elevation of miR-221/miR-222 is highly correlated with metastatic CRPC phenotypes. Moreover, an inverse correlation between miR-221/miR-222 expression and p27^{Kip1} level has been observed in primary PCa. Several studies demonstrated that miR-221/miR-222 can up-regulate S-phase kinase associated protein 2 (Skp2), cyclin A and cyclin D1 via targeting p27^{Kip1} suppression, leading to cell cycle progression at G1-to -S phase, increased clonogenicity *in vitro* and enhanced tumorigenicity *in vivo* (83,84,130). Meanwhile, Ras homolog member I (ARHI), a tumor suppressor identified in ovarian cancer (131), is also identified as the target gene of miR-221/miR-222. Overexpression of ARHI in PC3 cells results in the inhibition of cell proliferation, colony formation, cell invasion and survival (81,82,132), suggesting decreased ARHI mRNA could be an additional mechanism for miR-221/miR-222 contributing to the accelerated tumor growth in PCa. Thus, these data conclude the functional role of miR-221/miR-222 as PCa promoter by targeting tumor suppressor genes such as p27^{Kip1} and ARHI.

miR-32

miR-32 is highly expressed in CRPC specimens compared

to BPH specimens (85). A study demonstrated that miR-32 exerts oncogenic characteristics by targeting on both B-cell translocation gene 2 (BTG-2) and phosphoinositide-3-kinase interacting protein 1 (PIK3IP1), which regulates the inhibition of PI3K, a well-known regulator of cell proliferation, migration and survival (85). An inverse correlation between miR-32 and BTG-2 has been found in the CRPC specimens (85). In addition, numerous studies have identified BTG-2 as a critical target gene of AR-regulated miRNAs including miR-32, miR-148 and miR-21 (85,86). Loss of BTG-2 was implicated in the progression of PCa accompanied by the appearance of EMT markers (133). Meanwhile, a study using LNCaP cells demonstrated that miR-32 facilitates cell growth by inhibiting cell apoptosis and enhancing cell proliferation, respectively. Overall, miR-32 exerts its oncogenic characteristics by targeting on tumor suppressors critical for cell proliferation, survival and migration.

miR-148a

Similar to miR-32, miR-148 is elevated in advanced PCa compared to primary tumor (134). However, in contrast to the distinctive oncogenic role of miR-32, the role of miR-148a in PCa progression is more controversial. For example, miR-148a was identified as an androgen-responsive miRNA and facilitates LNCaP cell proliferation via targeting cullin-associated and neddylation-dissociated 1 (CAND1) (87). In contrast, miR-148a is shown to be down-regulated in both DU-145 and PC3 cell lines. Furthermore, overexpression of miR-148a in PC3 cells attenuates cell growth, migration, invasion, and enhances the drug sensitivity to Paclitaxel. This phenomenon is paralleled with the effect in MSK1-knockdown PC3 cells. In particular, MSK1 has been identified as the target gene of miR-148a, suggesting miR-148a attenuates the drug-resistance of CRPC cells via targeting MSK1 (135). Apparently, miR-148a represents a unique miRNA with dual function in PCa. Although the exact mechanism remains undetermined, AR may be an important factor involved in miR-148a function or the presence of different target genes of miRNA-148a in PCa cells derived from different origins.

miR-106b/miR-25

A study (136) using computational approach to identify PTEN-target miRNAs has identified miR-106b/miR-25 as a candidate that is concomitantly overexpressed with

its host gene, minichromosome maintenance protein 7 (MCM7), which result in enhanced cell transformation and initiated prostatic intraepithelial neoplasia (PIN) progression of PCa. This study has a significant finding to show a cooperative expression of an oncomir cluster with its oncogenic host gene, which could simultaneously generate “two-hits” effect on the malignant transformation of normal cells. In addition, a study using LNCaP cell line has demonstrated that miR-106b/miR-25 cluster is associated with PCa progression by targeting caspase 7, apoptosis-related cysteine peptidase (CASP7) mRNA, which is down-regulated in both primary PCa and metastatic lesions (134). Overall, miR-106b/miR-25 cluster is an oncomir cluster and it is often found altered in its expression level between PIN, primary, and metastatic PCa (86,137).

Conclusions

miRNA represents a new mechanism of regulating gene expression at either post-transcriptional or translational levels. Aberrant alteration of miRNAs has been clearly demonstrated in PCa. However, knowing complex regulatory mechanism and relationship of miRNAs and their multiple target genes have further complicated their functionality during carcinogenesis. Therefore, carefully dissecting the mechanisms and functional role of each miRNA in heterogeneous PCa cells will certainly generate new information that could be applied as biomarker(s) and developed into novel therapeutic strategies.

Acknowledgements

This work was supported in part by grants from the United States Army (W81XWH-11-1-0491 to JTH).

Disclosure: The authors declare no conflict of interest.

References

1. Siegel R, Naishadham D, Jemal A. Cancer statistics, 2012. *CA Cancer J Clin.* 2012;62:10-29.
2. Koivisto P, Kononen J, Palmberg C, et al. Androgen receptor gene amplification: a possible molecular mechanism for androgen deprivation therapy failure in prostate cancer. *Cancer Res* 1997;57:314-9.
3. Ruizeveld de Winter JA, Janssen PJ, Sleddens HM, et al. Androgen receptor status in localized and locally progressive hormone refractory human prostate cancer. *Am J Pathol* 1994;144:735-46.
4. Henshall SM, Quinn DI, Lee CS, et al. Altered expression of androgen receptor in the malignant epithelium and adjacent stroma is associated with early relapse in prostate cancer. *Cancer Res* 2001;61:423-7.
5. Watson PA, Chen YF, Balbas MD, et al. Constitutively active androgen receptor splice variants expressed in castration-resistant prostate cancer require full-length androgen receptor. *Proc Natl Acad Sci U S A* 2010;107:16759-65.
6. Dehm SM, Tindall DJ. Alternatively spliced androgen receptor variants. *Endocr Relat Cancer* 2011;18:R183-96.
7. Li Y, Chan SC, Brand LJ, et al. Androgen receptor splice variants mediate enzalutamide resistance in castration-resistant prostate cancer cell lines. *Cancer Res* 2013;73:483-9.
8. Bonaccorsi L, Muratori M, Carloni V, et al. Androgen receptor and prostate cancer invasion. *Int J Androl* 2003;26:21-5.
9. Zhu ML, Kyprianou N. Role of androgens and the androgen receptor in epithelial-mesenchymal transition and invasion of prostate cancer cells. *FASEB J* 2010;24:769-77.
10. Wu JD, Haugk K, Woodke L, et al. Interaction of IGF signaling and the androgen receptor in prostate cancer progression. *J Cell Biochem* 2006;99:392-401.
11. Léotoing L, Manin M, Monte D, et al. Crosstalk between androgen receptor and epidermal growth factor receptor-signalling pathways: a molecular switch for epithelial cell differentiation. *J Mol endocrinol* 2007;39:151-62.
12. Culig Z, Hobisch A, Cronauer MV, et al. Androgen receptor activation in prostatic tumor cell lines by insulin-like growth factor-I, keratinocyte growth factor, and epidermal growth factor. *Cancer Res* 1994;54:5474-8.
13. Gregory CW, Johnson RT Jr, Presnell SC, et al. Androgen receptor regulation of G1 cyclin and cyclin-dependent kinase function in the CWR22 human prostate cancer xenograft. *J Androl* 2001;22:537-48.
14. Ikonen T, Palvimo JJ, Janne OA. Interaction between the amino- and carboxyl-terminal regions of the rat androgen receptor modulates transcriptional activity and is influenced by nuclear receptor coactivators. *J Biol Chem* 1997;272:29821-8.
15. Voegel JJ, Heine MJ, Tini M, et al. The coactivator TIF2 contains three nuclear receptor-binding motifs and mediates transactivation through CBP binding-dependent and -independent pathways. *EMBO J* 1998;17:507-19.
16. Zhou G, Hashimoto Y, Kwak I, et al. Role of the steroid receptor coactivator SRC-3 in cell growth. *Mol Cell Biol*

- 2003;23:7742-55.
17. Chua SS, Ma Z, Ngan E, et al. Cdc25B as a steroid receptor coactivator. *Vitam Horm* 2004;68:231-56.
 18. Narayanan R, Jiang J, Gusev Y, et al. MicroRNAs are mediators of androgen action in prostate and muscle. *PLoS One* 2010;5:e13637.
 19. Aalto AP, Pasquinelli AE. Small non-coding RNAs mount a silent revolution in gene expression. *Curr Opin Cell Biol* 2012;24:333-40.
 20. Saini HK, Griffiths-Jones S, Enright AJ. Genomic analysis of human microRNA transcripts. *Proc Natl Acad Sci U S A* 2007;104:17719-24.
 21. Rodriguez A, Griffiths-Jones S, Ashurst JL, et al. Identification of mammalian microRNA host genes and transcription units. *Genome Res* 2004;14:1902-10.
 22. Landais S, Landry S, Legault P, et al. Oncogenic potential of the miR-106-363 cluster and its implication in human T-cell leukemia. *Cancer Res* 2007;67:5699-707.
 23. Hayashita Y, Osada H, Tatematsu Y, et al. A polycistronic microRNA cluster, miR-17-92, is overexpressed in human lung cancers and enhances cell proliferation. *Cancer Res* 2005;65:9628-32.
 24. Fujita S, Ito T, Mizutani T, et al. miR-21 Gene expression triggered by AP-1 is sustained through a double-negative feedback mechanism. *J Mol Biol* 2008;378:492-504.
 25. Iliopoulos D, Jaeger SA, Hirsch HA, et al. STAT3 activation of miR-21 and miR-181b-1 via PTEN and CYLD are part of the epigenetic switch linking inflammation to cancer. *Mol Cell* 2010;39:493-506.
 26. Mu P, Han YC, Betel D, et al. Genetic dissection of the miR-17~92 cluster of microRNAs in Myc-induced B-cell lymphomas. *Genes Dev* 2009;23:2806-11.
 27. Wang Y, Hu X, Greshock J, et al. Genomic DNA copy-number alterations of the let-7 family in human cancers. *PLoS One* 2012;7:e44399.
 28. Dong JT, Boyd JC, Frierson HF Jr. Loss of heterozygosity at 13q14 and 13q21 in high grade, high stage prostate cancer. *Prostate* 2001;49:166-71.
 29. Suh SO, Chen Y, Zaman MS, et al. MicroRNA-145 is regulated by DNA methylation and p53 gene mutation in prostate cancer. *Carcinogenesis* 2011;32:772-8.
 30. Vrba L, Jensen TJ, Garbe JC, et al. Role for DNA methylation in the regulation of miR-200c and miR-141 expression in normal and cancer cells. *PLoS One* 2010;5:e8697.
 31. Hulf T, Sibbritt T, Wiklund ED, et al. Epigenetic-induced repression of microRNA-205 is associated with MED1 activation and a poorer prognosis in localized prostate cancer. *Oncogene* 2013;32:2891-9.
 32. Lodygin D, Tarasov V, Epanchintsev A, et al. Inactivation of miR-34a by aberrant CpG methylation in multiple types of cancer. *Cell Cycle* 2008;7:2591-600.
 33. Bartel DP. MicroRNAs: genomics, biogenesis, mechanism, and function. *Cell* 2004;116:281-97.
 34. Winter J, Jung S, Keller S, et al. Many roads to maturity: microRNA biogenesis pathways and their regulation. *Nat Cell Biol* 2009;11:228-34.
 35. Feng Y, Zhang X, Song Q, et al. Drosha processing controls the specificity and efficiency of global microRNA expression. *Biochim Biophys Acta* 2011;1809:700-7.
 36. Maniatakis E, Mourelatos Z. A human, ATP-independent, RISC assembly machine fueled by pre-miRNA. *Genes Dev* 2005;19:2979-90.
 37. Kawamata T, Yoda M, Tomari Y. Multilayer checkpoints for microRNA authenticity during RISC assembly. *EMBO Rep* 2011;12:944-9.
 38. Liu J, Carmell MA, Rivas FV, et al. Argonaute2 is the catalytic engine of mammalian RNAi. *Science* 2004;305:1437-41.
 39. Nadiminty N, Tummala R, Lou W, et al. MicroRNA let-7c is downregulated in prostate cancer and suppresses prostate cancer growth. *PLoS One* 2012;7:e32832.
 40. Kim HH, Kuwano Y, Srikantan S, et al. HuR recruits let-7/RISC to repress c-Myc expression. *Genes Dev* 2009;23:1743-8.
 41. Nadiminty N, Tummala R, Lou W, et al. MicroRNA let-7c suppresses androgen receptor expression and activity via regulation of Myc expression in prostate cancer cells. *J Biol Chem* 2012;287:1527-37.
 42. Lee YS, Dutta A. The tumor suppressor microRNA let-7 represses the HMGA2 oncogene. *Genes Dev* 2007;21:1025-30.
 43. Dong Q, Meng P, Wang T, et al. MicroRNA let-7a inhibits proliferation of human prostate cancer cells in vitro and in vivo by targeting E2F2 and CCND2. *PLoS One* 2010;5:e10147.
 44. Johnson SM, Grosshans H, Shingara J, et al. RAS is regulated by the let-7 microRNA family. *Cell* 2005;120:635-47.
 45. Kong D, Heath E, Chen W, et al. Loss of let-7 up-regulates EZH2 in prostate cancer consistent with the acquisition of cancer stem cell signatures that are attenuated by BR-DIM. *PLoS One* 2012;7:e33729.
 46. Xu B, Niu X, Zhang X, et al. miR-143 decreases prostate cancer cells proliferation and migration and enhances their sensitivity to docetaxel through suppression of KRAS. *Mol*

- Cell Biochem 2011;350:207-13.
47. Peng X, Guo W, Liu T, et al. Identification of miRs-143 and -145 that is associated with bone metastasis of prostate cancer and involved in the regulation of EMT. *PloS One* 2011;6:e20341.
 48. Clapé C, Fritz V, Henriquet C, et al. miR-143 interferes with ERK5 signaling, and abrogates prostate cancer progression in mice. *PloS One* 2009;4:e7542.
 49. Huang S, Guo W, Tang Y, et al. miR-143 and miR-145 inhibit stem cell characteristics of PC-3 prostate cancer cells. *Oncol Rep* 2012;28:1831-7.
 50. Fuse M, Nohata N, Kojima S, et al. Restoration of miR-145 expression suppresses cell proliferation, migration and invasion in prostate cancer by targeting FSCN1. *Int J Oncol* 2011;38:1093-101.
 51. Xu N, Papagiannakopoulos T, Pan G, et al. MicroRNA-145 regulates OCT4, SOX2, and KLF4 and represses pluripotency in human embryonic stem cells. *Cell* 2009;137:647-58.
 52. Kong D, Li Y, Wang Z, et al. miR-200 regulates PDGF-D-mediated epithelial-mesenchymal transition, adhesion, and invasion of prostate cancer cells. *Stem Cells* 2009;27:1712-21.
 53. Slabáková E, Pernicová Z, Slavíčková E, et al. TGF-beta1-induced EMT of non-transformed prostate hyperplasia cells is characterized by early induction of SNAI2/Slug. *Prostate* 2011;71:1332-43.
 54. Liu YN, Yin JJ, Abou-Kheir W, et al. MiR-1 and miR-200 inhibit EMT via Slug-dependent and tumorigenesis via Slug-independent mechanisms. *Oncogene* 2013;32:296-306.
 55. Viticchiè G, Lena AM, Latina A, et al. MiR-203 controls proliferation, migration and invasive potential of prostate cancer cell lines. *Cell Cycle* 2011;10:1121-31.
 56. Saini S, Majid S, Yamamura S, et al. Regulatory role of mir-203 in prostate cancer progression and metastasis. *Clin Cancer Res* 2011;17:5287-98.
 57. Boll K, Reiche K, Kasack K, et al. MiR-130a, miR-203 and miR-205 jointly repress key oncogenic pathways and are downregulated in prostate carcinoma. *Oncogene* 2013;32:277-85.
 58. Gandellini P, Folini M, Longoni N, et al. miR-205 Exerts tumor-suppressive functions in human prostate through down-regulation of protein kinase Cepsilon. *Cancer Res* 2009;69:2287-95.
 59. Verdoodt B, Neid M, Vogt M, et al. MicroRNA-205, a novel regulator of the anti-apoptotic protein Bcl2, is downregulated in prostate cancer. *Int J Oncol* 2013;43:307-14.
 60. Hagman Z, Hafliðadóttir BS, Ceder JA, et al. miR-205 negatively regulates the androgen receptor and is associated with adverse outcome of prostate cancer patients. *Br J Cancer* 2013;108:1668-76.
 61. Liu C, Kelnar K, Liu B, et al. The microRNA miR-34a inhibits prostate cancer stem cells and metastasis by directly repressing CD44. *Nat Med* 2011;17:211-5.
 62. Kong D, Heath E, Chen W, et al. Epigenetic silencing of miR-34a in human prostate cancer cells and tumor tissue specimens can be reversed by BR-DIM treatment. *Am J Transl Res* 2012;4:14-23.
 63. Yamamura S, Saini S, Majid S, et al. MicroRNA-34a modulates c-Myc transcriptional complexes to suppress malignancy in human prostate cancer cells. *PloS One* 2012;7:e29722.
 64. Ji Q, Hao X, Zhang M, et al. MicroRNA miR-34 inhibits human pancreatic cancer tumor-initiating cells. *PloS One* 2009;4:e6816.
 65. Yamakuchi M, Ferlito M, Lowenstein CJ. miR-34a repression of SIRT1 regulates apoptosis. *Proc Natl Acad Sci U S A* 2008;105:13421-6.
 66. Varambally S, Cao Q, Mani RS, et al. Genomic loss of microRNA-101 leads to overexpression of histone methyltransferase EZH2 in cancer. *Science* 2008;322:1695-9.
 67. Cao P, Deng Z, Wan M, et al. MicroRNA-101 negatively regulates Ezh2 and its expression is modulated by androgen receptor and HIF-1alpha/HIF-1beta. *Mol Cancer* 2010;9:108.
 68. Tao J, Wu D, Xu B, et al. microRNA-133 inhibits cell proliferation, migration and invasion in prostate cancer cells by targeting the epidermal growth factor receptor. *Oncol Rep* 2012;27:1967-75.
 69. Lin SL, Chiang A, Chang D, et al. Loss of mir-146a function in hormone-refractory prostate cancer. *RNA* 2008;14:417-24.
 70. Xu B, Wang N, Wang X, et al. MiR-146a suppresses tumor growth and progression by targeting EGFR pathway and in a p-ERK-dependent manner in castration-resistant prostate cancer. *Prostate* 2012;72:1171-8.
 71. Musumeci M, Coppola V, Addario A, et al. Control of tumor and microenvironment cross-talk by miR-15a and miR-16 in prostate cancer. *Oncogene* 2011;30:4231-42.
 72. Bonci D, Coppola V, Musumeci M, et al. The miR-15a-miR-16-1 cluster controls prostate cancer by targeting multiple oncogenic activities. *Nat Med* 2008;14:1271-7.
 73. Noonan EJ, Place RF, Pookot D, et al. miR-449a targets

- HDAC-1 and induces growth arrest in prostate cancer. *Oncogene* 2009;28:1714-24.
74. Noonan EJ, Place RF, Basak S, et al. miR-449a causes Rb-dependent cell cycle arrest and senescence in prostate cancer cells. *Oncotarget* 2010;1:349-58.
 75. Ribas J, Lupold SE. The transcriptional regulation of miR-21, its multiple transcripts, and their implication in prostate cancer. *Cell Cycle* 2010;9:923-9.
 76. Reis ST, Pontes-Junior J, Antunes AA, et al. miR-21 may acts as an oncomir by targeting RECK, a matrix metalloproteinase regulator, in prostate cancer. *BMC Urol* 2012;12:14.
 77. Li T, Li D, Sha J, et al. MicroRNA-21 directly targets MARCKS and promotes apoptosis resistance and invasion in prostate cancer cells. *Biochem Biophys Res Commun* 2009;383:280-5.
 78. Shi XB, Xue L, Ma AH, et al. miR-125b promotes growth of prostate cancer xenograft tumor through targeting pro-apoptotic genes. *Prostate* 2011;71:538-49.
 79. Shi XB, Xue L, Yang J, Ma AH, Zhao J, Xu M, et al. An androgen-regulated miRNA suppresses Bak1 expression and induces androgen-independent growth of prostate cancer cells. *Proc Natl Acad Sci U S A* 2007;104:19983-8.
 80. Amir S, Ma AH, Shi XB, et al. Oncomir miR-125b suppresses p14(ARF) to modulate p53-dependent and p53-independent apoptosis in prostate cancer. *PloS One* 2013;8:e61064.
 81. Chen Y, Zaman MS, Deng G, et al. MicroRNAs 221/222 and genistein-mediated regulation of ARHI tumor suppressor gene in prostate cancer. *Cancer Prev Res (Phila)* 2011;4:76-86.
 82. Lin D, Cui F, Bu Q, et al. The expression and clinical significance of GTP-binding RAS-like 3 (ARHI) and microRNA 221 and 222 in prostate cancer. *J Int Med Res* 2011;39:1870-5.
 83. Mercatelli N, Coppola V, Bonci D, et al. The inhibition of the highly expressed miR-221 and miR-222 impairs the growth of prostate carcinoma xenografts in mice. *PloS One* 2008;3:e4029.
 84. le Sage C, Nagel R, Egan DA, et al. Regulation of the p27(Kip1) tumor suppressor by miR-221 and miR-222 promotes cancer cell proliferation. *EMBO J* 2007;26:3699-708.
 85. Jalava SE, Urbanucci A, Latonen L, et al. Androgen-regulated miR-32 targets BTG2 and is overexpressed in castration-resistant prostate cancer. *Oncogene* 2012;31:4460-71.
 86. Ambs S, Prueitt RL, Yi M, et al. Genomic profiling of microRNA and messenger RNA reveals deregulated microRNA expression in prostate cancer. *Cancer Res* 2008;68:6162-70.
 87. Murata T, Takayama K, Katayama S, et al. miR-148a is an androgen-responsive microRNA that promotes LNCaP prostate cell growth by repressing its target CAND1 expression. *Prostate Cancer Prostatic Dis* 2010;13:356-61.
 88. Hudson RS, Yi M, Esposito D, et al. MicroRNA-106b-25 cluster expression is associated with early disease recurrence and targets caspase-7 and focal adhesion in human prostate cancer. *Oncogene* 2013;32:4139-47.
 89. Motoyama K, Inoue H, Nakamura Y, et al. Clinical significance of high mobility group A2 in human gastric cancer and its relationship to let-7 microRNA family. *Clin Cancer Res* 2008;14:2334-40.
 90. Thuault S, Tan EJ, Peinado H, et al. HMGA2 and Smads co-regulate SNAIL1 expression during induction of epithelial-to-mesenchymal transition. *J Biol Chem* 2008;283:33437-46.
 91. Newman MA, Thomson JM, Hammond SM. Lin-28 interaction with the Let-7 precursor loop mediates regulated microRNA processing. *RNA* 2008;14:1539-49.
 92. Nam Y, Chen C, Gregory RI, et al. Molecular basis for interaction of let-7 microRNAs with Lin28. *Cell* 2011;147:1080-91.
 93. Iliopoulos D, Hirsch HA, Struhl K. An epigenetic switch involving NF-kappaB, Lin28, Let-7 MicroRNA, and IL6 links inflammation to cell transformation. *Cell* 2009;139:693-706.
 94. Rybak A, Fuchs H, Smirnova L, et al. A feedback loop comprising lin-28 and let-7 controls pre-let-7 maturation during neural stem-cell commitment. *Nat Cell Biol* 2008;10:987-93.
 95. Viswanathan SR, Powers JT, Einhorn W, et al. Lin28 promotes transformation and is associated with advanced human malignancies. *Nat Genet* 2009;41:843-8.
 96. Boyerinas B, Park SM, Shomron N, et al. Identification of let-7-regulated oncofetal genes. *Cancer Res* 2008;68:2587-91.
 97. Wu L, Belasco JG. Micro-RNA regulation of the mammalian lin-28 gene during neuronal differentiation of embryonal carcinoma cells. *Mol Cell Biol* 2005;25:9198-208.
 98. Sampson VB, Rong NH, Han J, et al. MicroRNA let-7a down-regulates MYC and reverts MYC-induced growth in Burkitt lymphoma cells. *Cancer Res* 2007;67:9762-70.
 99. Akao Y, Nakagawa Y, Naoe T. let-7 microRNA functions as a potential growth suppressor in human colon cancer

- cells. *Biol Pharm Bull* 2006;29:903-6.
100. Chang TC, Zeitels LR, Hwang HW, et al. Lin-28B transactivation is necessary for Myc-mediated let-7 repression and proliferation. *Proc Natl Acad Sci U S A* 2009;106:3384-9.
 101. Kung HJ, Evans CP. Oncogenic activation of androgen receptor. *Urol oncol* 2009;27:48-52.
 102. Yamaguchi S, Yamahara K, Homma K, et al. The role of microRNA-145 in human embryonic stem cell differentiation into vascular cells. *Atherosclerosis* 2011;219:468-74.
 103. Ahmed S, Nawshad A. Complexity in interpretation of embryonic epithelial-mesenchymal transition in response to transforming growth factor-beta signaling. *Cells Tissues Organs* 2007;185:131-45.
 104. Eastham AM, Spencer H, Soncin F, et al. Epithelial-mesenchymal transition events during human embryonic stem cell differentiation. *Cancer Res* 2007;67:11254-62.
 105. Wei J, Xu G, Wu M, et al. Overexpression of vimentin contributes to prostate cancer invasion and metastasis via src regulation. *Anticancer Res* 2008;28:327-34.
 106. Luo Y, He DL, Ning L. Expression of "epithelial-mesenchymal transition" associated proteins in prostate cancer cell lines with different metastatic potentials and its significance. *Zhonghua Nan Ke Xue* 2006;12:696-700.
 107. Drake JM, Strohschein G, Bair TB, et al. ZEB1 enhances transendothelial migration and represses the epithelial phenotype of prostate cancer cells. *Mol Biol Cell* 2009;20:2207-17.
 108. Gregory PA, Bert AG, Paterson EL, et al. The miR-200 family and miR-205 regulate epithelial to mesenchymal transition by targeting ZEB1 and SIP1. *Nat Cell Biol* 2008;10:593-601.
 109. Gregory PA, Bracken CP, Smith E, et al. An autocrine TGF-beta/ZEB/miR-200 signaling network regulates establishment and maintenance of epithelial-mesenchymal transition. *Mol Biol Cell* 2011;22:1686-98.
 110. Xiong M, Jiang L, Zhou Y, et al. The miR-200 family regulates TGF-beta1-induced renal tubular epithelial to mesenchymal transition through Smad pathway by targeting ZEB1 and ZEB2 expression. *Am J Physiol Renal Physiol* 2012;302:F369-79.
 111. Moes M, Le Behec A, Crespo I, et al. A novel network integrating a miRNA-203/SNAI1 feedback loop which regulates epithelial to mesenchymal transition. *PloS One* 2012;7:e35440.
 112. Qu Y, Li WC, Hellem MR, et al. MiR-182 and miR-203 induce mesenchymal to epithelial transition and self-sufficiency of growth signals via repressing SNAI2 in prostate cells. *Int J Cancer* 2013;133:544-55.
 113. Bhatnagar N, Li X, Padi SK, et al. Downregulation of miR-205 and miR-31 confers resistance to chemotherapy-induced apoptosis in prostate cancer cells. *Cell Death Dis* 2010;1:e105.
 114. Tucci P, Agostini M, Grespi F, et al. Loss of p63 and its microRNA-205 target results in enhanced cell migration and metastasis in prostate cancer. *Proc Natl Acad Sci U S A* 2012;109:15312-7.
 115. Rokhlin OW, Scheinker VS, Taghiyev AF, et al. MicroRNA-34 mediates AR-dependent p53-induced apoptosis in prostate cancer. *Cancer Biol Ther* 2008;7:1288-96.
 116. Kobayashi Y, Absher DM, Gulzar ZG, et al. DNA methylation profiling reveals novel biomarkers and important roles for DNA methyltransferases in prostate cancer. *Genome Res* 2011;21:1017-27.
 117. Varambally S, Dhanasekaran SM, Zhou M, et al. The polycomb group protein EZH2 is involved in progression of prostate cancer. *Nature* 2002;419:624-9.
 118. Hoffmann MJ, Engers R, Florl AR, et al. Expression changes in EZH2, but not in BMI-1, SIRT1, DNMT1 or DNMT3B are associated with DNA methylation changes in prostate cancer. *Cancer Biol Ther* 2007;6:1403-12.
 119. Ren G, Baritaki S, Marathe H, et al. Polycomb protein EZH2 regulates tumor invasion via the transcriptional repression of the metastasis suppressor RKIP in breast and prostate cancer. *Cancer Res* 2012;72:3091-104.
 120. Sherwood ER, Van Dongen JL, Wood CG, et al. Epidermal growth factor receptor activation in androgen-independent but not androgen-stimulated growth of human prostatic carcinoma cells. *Br J Cancer* 1998;77:855-61.
 121. Shen J, Xia W, Khotskaya YB, et al. EGFR modulates microRNA maturation in response to hypoxia through phosphorylation of AGO2. *Nature* 2013;497:383-7.
 122. Man YG, Fu SW, Liu AJ, et al. Aberrant expression of chromogranin A, miR-146a, and miR-146b-5p in prostate structures with focally disrupted basal cell layers: an early sign of invasion and hormone-refractory cancer? *Cancer genomics proteomics* 2011;8:235-44.
 123. Xu B, Feng NH, Li PC, et al. A functional polymorphism in Pre-miR-146a gene is associated with prostate cancer risk and mature miR-146a expression in vivo. *Prostate* 2010;70:467-72.
 124. Hyytinen ER, Frierson HF Jr, Boyd JC, et al. Three distinct regions of allelic loss at 13q14, 13q21-22, and

- 13q33 in prostate cancer. *Genes chromosomes cancer* 1999;25:108-14.
125. Tuxhorn JA, Ayala GE, Smith MJ, et al. Reactive stroma in human prostate cancer: induction of myofibroblast phenotype and extracellular matrix remodeling. *Clin Cancer Res* 2002;8:2912-23.
126. Chung LW, Chang SM, Bell C, et al. Co-inoculation of tumorigenic rat prostate mesenchymal cells with non-tumorigenic epithelial cells results in the development of carcinosarcoma in syngeneic and athymic animals. *Int J Cancer* 1989;43:1179-87.
127. Ribas J, Ni X, Haffner M, et al. miR-21: an androgen receptor-regulated microRNA that promotes hormone-dependent and hormone-independent prostate cancer growth. *Cancer Res* 2009;69:7165-9.
128. Kajanne R, Miettinen P, Tenhunen M, et al. Transcription factor AP-1 promotes growth and radioresistance in prostate cancer cells. *Int J Oncol* 2009;35:1175-82.
129. Abdulghani J, Gu L, Dagvadorj A, et al. Stat3 promotes metastatic progression of prostate cancer. *Am J Pathol* 2008;172:1717-28.
130. Galardi S, Mercatelli N, Giorda E, et al. miR-221 and miR-222 expression affects the proliferation potential of human prostate carcinoma cell lines by targeting p27Kip1. *J Biol Chem* 2007;282:23716-24.
131. Badgwell DB, Lu Z, Le K, et al. The tumor-suppressor gene ARHI (DIRAS3) suppresses ovarian cancer cell migration through inhibition of the Stat3 and FAK/Rho signaling pathways. *Oncogene* 2012;31:68-79.
132. Li Y, Liu M, Zhang Y, et al. Effects of ARHI on breast cancer cell biological behavior regulated by microRNA-221. *Tumour Biol* 2013. [Epub ahead of print].
133. Coppola V, Musumeci M, Patrizii M, et al. BTG2 loss and miR-21 upregulation contribute to prostate cell transformation by inducing luminal markers expression and epithelial-mesenchymal transition. *Oncogene* 2013;32:1843-53.
134. Walter BA, Valera VA, Pinto PA, et al. Comprehensive microRNA profiling of prostate cancer. *J Cancer* 2013;4:350-7.
135. Fujita Y, Kojima K, Ohhashi R, et al. MiR-148a attenuates paclitaxel resistance of hormone-refractory, drug-resistant prostate cancer PC3 cells by regulating MSK1 expression. *J Biol Chem* 2010;285:19076-84.
136. Poliseno L, Salmena L, Riccardi L, et al. Identification of the miR-106b~25 microRNA cluster as a proto-oncogenic PTEN-targeting intron that cooperates with its host gene MCM7 in transformation. *Sci Signal* 2010;3:ra29.
137. Szczyrba J, Loprich E, Wach S, et al. The microRNA profile of prostate carcinoma obtained by deep sequencing. *Mol Cancer Res* 2010;8:529-38.

Cite this article as: Lo UG, Yang D, Hsieh JT. The role of microRNAs in prostate cancer progression. *Transl Androl Urol* 2013;2(3):228-241. doi: 10.3978/j.issn.2223-4683.2013.08.01

Genome Biology

A new microRNA turnover machinery mediated by IFIT5 complex leading to epithelial-to-mesenchymal transition --Manuscript Draft--

Manuscript Number:					
Full Title:	A new microRNA turnover machinery mediated by IFIT5 complex leading to epithelial-to-mesenchymal transition				
Article Type:	Research				
Funding Information:	<table border="1"> <tr> <td>Medical Research and Materiel Command, U.S. Army Medical Department (W81XWH-11-1-0491)</td> <td>Dr. Jer-Tsong Hsieh</td> </tr> <tr> <td>Medical Research and Materiel Command, U.S. Army Medical Department (W81XWH-14-1-0249)</td> <td>Dr. U-ging Lo</td> </tr> </table>	Medical Research and Materiel Command, U.S. Army Medical Department (W81XWH-11-1-0491)	Dr. Jer-Tsong Hsieh	Medical Research and Materiel Command, U.S. Army Medical Department (W81XWH-14-1-0249)	Dr. U-ging Lo
Medical Research and Materiel Command, U.S. Army Medical Department (W81XWH-11-1-0491)	Dr. Jer-Tsong Hsieh				
Medical Research and Materiel Command, U.S. Army Medical Department (W81XWH-14-1-0249)	Dr. U-ging Lo				
Abstract:	<p>Background: MicroRNAs (miRNA) are small noncoding RNA molecules regulating multiple biological processes via post-transcriptional suppression, mRNA degradation or translational inhibition. Functionally, miRNAs can either promote or inhibit cancer development. For example, each member of miR17-92 cluster is characterized as oncogenic miRNA. In contrast, miR-363 belongs to the polycistronic miR106a-363 cluster that is closely resembled to the oncogenic miR17-92 cluster. However, no miR-363 homolog is present in the miR-17-92 cluster and its regulation and functional role in cancer are not well understood.</p> <p>Results: The acquisition of epithelial-to-mesenchymal transition (EMT) is a hallmark of cancer cells to increase their invasive potentials leading to the initiation of metastases. We unveil the function of miRNA-363 (miR-363) as a potent anti-EMT miRNA in prostate cancer (PCa), renal cancer and liver cancer, which is distinct from the rest of miRNAs in miR106a-363 cluster. Noticeably, our work provides a new mechanistic insight of miR-363 regulation within the miR-106a-363 cluster by interferon-induced protein with tetratricopeptide repeats 5 (IFIT5) first characterized as a viral RNA binding protein. IFIT5 appears to recognize the unique 5'-end sequence of miR-363 and coordinates with XRN1 to specifically degrade miR-363 but not other miRNAs in this cluster. We further demonstrate that IFIT5 can elicit EMT via miR-363 turnover in PCa. Clinically, IFIT5 is highly elevated in high-grade PCa with an inverse correlation of miR-363</p> <p>Conclusion: Our finding unveils miR-363 as anti-EMT miRNA and identifies IFIT5 complex as a new machinery of miRNA turnover that is specific for the degradation of a tumor suppressive miRNA derived from a cluster containing mostly oncogenic miRNAs.</p>				
Corresponding Author:	Jer-Tsong Hsieh UT Southwestern Medical Center Dallas, TX UNITED STATES				
Corresponding Author Secondary Information:					
Corresponding Author's Institution:	UT Southwestern Medical Center				
Corresponding Author's Secondary Institution:					
First Author:	U-ging Lo				
First Author Secondary Information:					
Order of Authors:	<table border="1"> <tr> <td>U-ging Lo</td> </tr> <tr> <td>Rey-Chen Pong</td> </tr> <tr> <td>Diane Yang</td> </tr> <tr> <td>Leah Gandee</td> </tr> </table>	U-ging Lo	Rey-Chen Pong	Diane Yang	Leah Gandee
U-ging Lo					
Rey-Chen Pong					
Diane Yang					
Leah Gandee					

	Jiancheng Zhou
	Shu-Fen Tseng
	Jer-Tsong Hsieh
Order of Authors Secondary Information:	
Suggested Reviewers:	Jindan Yu jindan-yu@northwestern.edu
	Rajvir Dahiya RDahiya@ucsf.edu
	Leland Chung leland.chung@cshs.org
	Martin Gleave m.gleave@ubc.ca
	Robert Matusik robert.matusik@mcmail.vanderbilt.edu
	George Thalmann George.Thalmann@insel.ch
	Kathleen Collins kcollins@berkeley.edu
	Natasha Kyprianou nkypr2@uky.edu
Additional Information:	
Question	Response
Has this manuscript been submitted to this journal before?	No
Experimental design and statistics	Yes
Full details of the experimental design and statistical methods used should be given in the Methods section, as detailed in our Minimum Standards Reporting Checklist . Information essential to interpreting the data presented should be made available in the figure legends.	
Have you included all the information requested in your manuscript?	
Resources	Yes
A description of all resources used, including antibodies, cell lines, animals and software tools, with enough information to allow them to be uniquely identified, should be included in the Methods section. Authors are strongly encouraged to cite Research Resource Identifiers (RRIDs) for antibodies, model organisms and tools, where possible.	

<p>Have you included the information requested as detailed in our Minimum Standards Reporting Checklist?</p>	
<p>Availability of data and materials</p> <p>All datasets and code on which the conclusions of the paper rely must be either included in your submission or deposited in publicly available repositories (where available and ethically appropriate), referencing such data using a unique identifier in the references and in the “Availability of Data and Materials” section of your manuscript.</p> <p>Have you have met the above requirement as detailed in our Minimum Standards Reporting Checklist?</p>	<p>Yes</p>

[Click here to view linked References](#)

1
2
3
4 **A new microRNA turnover machinery mediated by IFIT5 complex leading to**
5 **epithelial-to-mesenchymal transition**
6
7

8
9 **U-Ging Lo¹, Rey-Chen Pong¹, Diane Yang¹, Leah Gandee¹, Jiancheng Zhou², Shu-Fen**
10 **Tseng³, and Jer-Tsong Hsieh^{1,4}**
11
12
13
14

15 ¹Department of Urology, University of Texas Southwestern Medical Center, Dallas, TX 75390,
16 USA; ²Department of Urology, The First Affiliated Hospital, Medical School of Xi'an Jiaotong
17 University, Xi'an 710049, China; ³Department of Bioengineering, University of Texas at
18 Arlington, Arlington, TX 76019, USA; ⁴Graduate Institute of Cancer Biology, China Medical
19 University Hospital, Taichung 40447, Taiwan, Republic of China
20
21
22
23
24

25 **Corresponding author:**
26

27
28 Jer-Tsong Hsieh, Ph.D., jt.hsieh@utsouthwestern.edu, Phone: 214-648-3988; Fax: 214-648-

29
30 8786; 5323 Harry Hines Blvd., J8-134 Dallas, TX 75390, USA.
31
32
33
34
35
36
37
38
39
40
41
42
43
44
45
46
47
48
49
50
51
52
53
54
55
56
57
58
59
60
61
62
63
64
65

1
2
3
4 **ABSTRACT**
5
6

7 **Background:** MicroRNAs (miRNA) are small noncoding RNA molecules regulating multiple
8 biological processes via post-transcriptional suppression, mRNA degradation or translational
9 inhibition. Functionally, miRNAs can either promote or inhibit cancer development. For
10 example, each member of miR17-92 cluster is characterized as oncogenic miRNA. In contrast,
11 miR-363 belongs to the polycistronic miR106a-363 cluster that is closely resembled to the
12 oncogenic miR17-92 cluster. However, no miR-363 homolog is present in the miR-17-92 cluster
13 and its regulation and functional role in cancer are not well understood.
14
15
16
17
18
19
20

21 **Results:** The acquisition of epithelial-to-mesenchymal transition (EMT) is a hallmark of cancer
22 cells to increase their invasive potentials leading to the initiation of metastases. We unveil the
23 function of miRNA-363 (miR-363) as a potent anti-EMT miRNA in prostate cancer (PCa), renal
24 cancer and liver cancer, which is distinct from the rest of miRNAs in miR106a-363 cluster.
25 Noticeably, our work provides a new mechanistic insight of miR-363 regulation within the miR-
26 106a-363 cluster by interferon-induced protein with tetratricopeptide repeats 5 (IFIT5) first
27 characterized as a viral RNA binding protein. IFIT5 appears to recognize the unique 5'-end
28 sequence of miR-363 and coordinates with XRN1 to specifically degrade miR-363 but not other
29 miRNAs in this cluster. We further demonstrate that IFIT5 can elicit EMT via miR-363 turnover
30 in PCa. Clinically, IFIT5 is highly elevated in high-grade PCa with an inverse correlation of
31 miR-363.
32
33
34
35
36
37
38
39
40
41

42 **Conclusion:** Our finding unveils miR-363 as anti-EMT miRNA and identifies IFIT5 complex as
43 a new machinery of miRNA turnover that is specific for the degradation of a tumor suppressive
44 miRNA derived from a cluster containing mostly oncogenic miRNAs.
45
46
47
48

49 **Key Words:** IFIT5, XRN1, microRNA-363, EMT
50
51
52
53
54
55
56
57
58
59
60
61
62
63
64
65

BACKGROUND

MicroRNAs (miRNA) are a large family of short sequence single-stranded noncoding RNAs, which has been shown to regulate approximate 60% protein-coding genes via post-transcriptional suppression by facilitating mRNA degradation, or translational inhibition[1, 2]. Until now, many miRNAs have been identified to be associated with different stages of tumor development. Based on the seed sequence of 2-7 nucleotides, miRNAs are grouped into different families for predicting the potential target gene(s); the function of miRNAs could be divided into onco-miRNAs and tumor suppressor miRNAs. However, only handfuls of them have been validated experimentally. In this study, we clearly identify a unique miR-363 that is able to inhibit EMT in PCa by targeting Slug/SNAI2 mRNA. Clinically, a reduced miR-363 expression is correlated with PCa malignancy.

In general, similar to most protein-coding genes, miRNA genes can be regulated at transcriptional or post-transcriptional level [3]. Unlike most eukaryotic protein genes, several miRNAs such as miR-106a-363 [4] and miR-17-92 are clustered together to generate a polycistronic primary transcript [5-7], which further complicates the regulatory scheme of miRNA biogenesis because each individual miRNA derived from one cluster may have different functional roles as well as expression levels in any given cell or tissue. For example, miR-363 belongs to the polycistronic miR-106a-363 cluster containing six miRNAs (miR-106a, miR-18b, miR-20b, miR-19b-2, miR-92a-2 and miR-363), located on chromosome X. Unlike the other five miRNAs with similar seed sequences and similar functions as the oncogenic miR-17-92 cluster [8], miR-363 has been implicated to play a tumor suppressor role in nasal-type natural killer/T-cell lymphoma [9], hepatocellular carcinoma [10] and colorectal cancer [11]. In this study, we unveil a new post-transcriptional regulatory mechanism specific to miR-363 turnover by a novel protein complex- Interferon-induced protein with tetratricopeptide repeats 5 (IFIT5), and our results further support the tumor suppressive role of miR-363 in several cancer cells.

IFIT protein family was first identified as a viral RNA binding protein [12] as a part of antiviral defense mechanisms by intervening viral replication and/or disrupting viral RNA translation in host cells. Among IFIT orthologs, human IFIT1, IFIT2 and IFIT3 form a complex through the tetratricopeptide repeats (TPR) to degrade viral RNA. On the contrary, IFIT5 acts solely as a monomer and binds directly to RNA molecules via its convoluted RNA-binding cleft. In a recent

1
2
3
4 study, IFIT5 has been shown to directly bind to endogenous cellular RNA with a 5'-end
5 phosphate cap, including transfer RNA (tRNA) [13, 14], which partially shared a structural
6 similarity with the precursor form of small RNAs such as small hairpin RNA (shRNA) and
7 primary or precursor miRNAs. This is the first time in the literature to demonstrate that IFIT5 is
8 able to specifically recognize a unique structure in the precursor miR-363 (pre-miR-363) and can
9 facilitate the recruitment of XRN1 to degrade pre-miR-363. Also, the expression level of IFIT5
10 is inversely correlated with that of miR-363 in PCa specimens. In addition, a significant
11 elevation of IFIT5 is detected in several cancer cells expressing EMT phenotypes associated with
12 invasiveness. Thus, IFIT5-XRN1 complex mediates a specific degradation of tumor suppressor
13 miRNA from its cluster, which could provide a new understanding of miRNA biogenesis for
14 other tumor suppressor miRNAs.
15
16
17
18
19
20
21
22
23
24
25
26
27
28
29
30
31
32
33
34
35
36
37
38
39
40
41
42
43
44
45
46
47
48
49
50
51
52
53
54
55
56
57
58
59
60
61
62
63
64
65

RESULTS AND DISCUSSION

The specific correlation between DAB2IP and miR-363 expression. DAB2IP is known as a potent regulator in EMT leading to cancer metastases [15, 16]. However, the detailed mechanism of action of DAB2IP is not fully characterized. As emerging evidence demonstrates the critical role of miRNA in the EMT process of PCa, we therefore performed miRNA microarray screening (Additional file 1A and 1B) that resulted in the identification of a unique miRNA-miR-363 that is significantly decreased in DAB2IP-knockdown (KD) cells. The down-regulation of miR-363 in DAB2IP-KD cells was further validated in not only prostate cell lines (LAPC-4, RWPE1, PC3 and PNT1A) (Fig. 1A) but also renal cell lines such as 786-O-KD and HK2-KD (Fig. S1C). Ectopic expression of DAB2IP in C4-2Neo or LAPC4-KD cells (Fig. 1B), or HEK293 (Fig. S1D) was able to induce mature miR-363 levels in a dose-dependent manner, indicating that DAB2IP could modulate miR-363 expression.

MiR-363 is located in the polycistronic miR-106a-363 cluster that is first transcribed into a single primary miRNA containing the entire sequence of the cluster genes. We therefore examined the effect of DAB2IP on the expression levels of primary transcript of miR-106a-363. In contrast to the significant down-regulation of mature miR-363 in DAB2IP-KD cells, the expression levels of primary miR-106a-363 were similar between DAB2IP-positive and -negative cells (Fig. 1C). Also, the expression levels of precursor miR-363 (pre-miR-363) showed no significant difference between these cells (Fig. 1D). Noticeably, only the mature miR-363 levels dramatically decreased in DAB2IP-KD cells (i.e., LAPC4-KD and RWPE1-KD) (Fig. 1E). On the other hand, only the mature miR-363 levels increased significantly in DAB2IP-expressing cells (i.e., C4-2D2) (Fig. 1E). Similar result was also observed in HEK293 cells (Additional file 1E). These findings indicate that DAB2IP specifically regulates miR-363 maturation process from the miR-106a-363 cluster.

The impact of IFIT5 on miR-363 biogenesis distinct from miR-106a-363 cluster. In order to elucidate the machinery responsible for miR-363 maturation process, the protein candidates were pulled down by precursor miR-363 and analyzed by LC-MS/MS (Additional file 9, Table 1) to unveil IFIT5 protein as a potential hit. Indeed, the steady-state levels of IFIT5 mRNA and protein were inversely correlated with DAB2IP (Additional file 2A). IFIT5 is characterized as viral RNA or cellular tRNA binding protein and has not been known for its binding ability to

1
2
3
4 microRNA. Therefore, the specific association between pre-miR-363 and IFIT5 was further
5 validated using RNA pull-down (Fig. 2A). This inhibitory effect of DAB2IP on IFIT5 expression
6 was further confirmed by the ectopic expression of DAB2IP in LAPC4-KD (Fig. 2B), C4-2Neo
7 (Fig. 2C), LNCaP (Additional file 2B), and HEK293 cells (Additional file 2C).
8
9

10
11
12 To further examine whether IFIT5 plays a critical role in DAB2IP-mediated miR-363
13 maturation, ectopic expression of IFIT5 in DAB2IP-positive cells resulted in a significant
14 reduction of mature miR-363 levels but not the other mature miRNAs from the same cluster (Fig.
15 2D, 2E, and 2F). In addition, applying 3 different IFIT5 small interfering RNA (siRNA) onto
16 LAPC4-KD cells, the levels of mature miR-363 were correlated with the knockdown efficiency
17 of each siRNA on endogenous IFIT5 mRNA levels (Additional file 2D). Thus, the IFIT5-C
18 siRNA was chosen; and the reduced IFIT5 resulted in a significant elevation of mature miR-363
19 in a dose-dependent manner (Additional file 2E). Despite of the significantly elevated mature
20 miR-363 in IFIT5-KD cells, the levels of mature miR-106a, miR-18b, miR-20b, miR-19b-2 and
21 miR-92a-2 remained relatively unchanged (Fig. 2G, 2H, 2I and Additional file 2F). Meanwhile,
22 the expression levels of pre-miR-363 and other pre-miRNAs from the same cluster remained
23 unchanged in these IFIT5-KD cells (Additional file 2G). Taken together, IFIT5 can specifically
24 inhibit the miR-363 maturation from miR-106a-363 cluster.
25
26
27
28
29
30
31
32
33
34
35
36

37 **The effect of IFIT5 on miR-363 turnover at precursor stage.** In a recent study, IFIT5 has
38 been suggested to suppress virus replication by targeting 5'-phosphate single stranded viral RNA
39 for rapid turnover [14]. Thus, we examined whether IFIT5 has a direct impact on the stability of
40 pre-miR-363. In fact, pre-miR-363 RNA prepared from *in vitro* transcription was relatively
41 stable at 37°C (Additional file 3A). However, the presence of IFIT5 protein immunoprecipitated
42 (IP) from LAPC4-Con cells significantly increased the turnover rate of pre-miR-363 RNA
43 (Additional file 3A), indicating that the degradation of pre-miR-363 is accelerated by IFIT5
44 complex. To examine the specificity of IFIT5 in the acceleration of pre-miR-363 turnover, we
45 determined the turnover rate of pre-miR-92a-2 (immediate adjacent to miR-363) in the presence
46 of IFIT5 and found no significant change (Fig. 3A). Previous studies [12, 13] indicate that IFIT5
47 protein binds to viral RNA molecules at either 5'-phosphate cap or 5'-tri-phosphate group. By
48 comparing the 5'-end structure between pre-miR-92a-2 and pre-miR-363, we hypothesized that a
49 single nucleotide (uracil) overhang in pre-miR-363, in contrast to the double-stranded blunt end
50
51
52
53
54
55
56
57
58
59
60
61
62
63
64
65

1
2
3
4 in pre-miR-92a-2 is critical for IFIT5 recognition. Therefore, we generated 2 mutant pre-miR-
5 363 constructs: one with 5'-end six nucleotides single stranded overhang (SS⁶Mut pre-miR-363)
6 and the other with double-stranded blunt end (DSMut pre-miR-363) (Fig. 3B) to test their
7 stabilities. The result (Fig. 3B) indicated that the expression levels of primary miR-363 from
8 either native or mutants were similar. However, the expression levels of pre-miR363 or mature
9 miR-363 derived from SS⁶Mut were significantly lower than those from native or DSMut form
10 (Fig. 3B), indicating that the 5'-end structure of pre-miR-363 dictates the stability of miR-363
11 maturation. Similar pattern of mature miR-363 expression was also detected in RWPE1-KD cells
12 (Additional file 3B). By determining the *in vitro* degradation rates of pre-miR-363, SS⁶Mut and
13 DSMut pre-miR-363 RNA molecules, as we expected, SS⁶Mut pre-miR-363 was very sensitive
14 to IFIT5 whereas DSMut pre-miR-363 was the most resistant one (Fig. 3C). Furthermore, we
15 observed a steady elevation of SS⁶Mut -derived mature miR-363 level in a dose-dependent
16 manner in the presence of an incremental IFIT5 siRNA, while the expression of DSMut-derived
17 mature miR-363 remained at high levels and was not affected by IFIT5 siRNA (Fig. 3D).
18 Meanwhile, using RNA pull-down assay, SS⁶Mut pre-miR-363 exhibited higher affinity to IFIT5
19 than DSMut pre-miR-363 (Fig. 3E). In contrast, DICER, one of the key endoribonuclease for
20 miRNA maturation, exhibited higher interaction with DSMut pre-miR-363 than SS⁶Mut pre-
21 miR-363. These data conclude that IFIT5 recognizes the unique 5'-end overhanging structure in
22 pre-miR-363 to elicit its degradation activities.
23
24
25
26
27
28
29
30
31
32
33
34
35
36
37
38
39

40 To further this specific recognition between the unique 5'end structure of pre-miRNA and IFIT5
41 complex, we also generated a mutant construct of pre-miR-92a-2 with single nucleotide at
42 5'overhang (SS¹Mut pre-miR-92a-2) (Fig. 3F), which shared a structural similarity to the 5'-end
43 of pre-miR-363 (Fig. 3B). Using RNA pull-down assay, we observed significantly higher
44 interaction between SS¹Mut pre-miR-92a-2 and IFIT5 protein than pre-miR-92a-2 (Fig. 3F).
45 Moreover, the degradation rate of SS¹Mut pre-miR-92a-2 increased in the presence of IFIT5
46 complex, compared to that of pre-miR-92a-2 (Additional file 3C). In addition, we generated a
47 mutant pre-miR-18b with double nucleotide overhang at its 5'end (SS²Mut pre-miR-18b).
48 Similarly, the significantly higher interaction between SS²Mut pre-miR-18b and IFIT5
49 protein was observed (Fig. 3G) and the degradation rate of SS²Mut pre-miR-18b RNA molecule
50 was significantly elevated as well (Additional file 3D). Overall data indicate that IFIT5-mediated
51 precursor miRNAs turnover is determined by the 5'-end overhanging structure.
52
53
54
55
56
57
58
59
60
61
62
63
64
65

1
2
3
4 **The role of XRN1 in IFIT5-mediated miR-363 turnover.** Although IFIT5 can elicit miR-363
5 turnover, IFIT5 doesn't possess ribonuclease activity. We further examined LC-MS/MS results
6 and identified an exoribonuclease candidate-XRN1. XRN1 is known to regulate mRNA stability
7 and identified an exoribonuclease candidate-XRN1. XRN1 is known to regulate mRNA stability
8 via cleavage of de-capped 5'-monophosphorylated mRNA [17, 18] and a recent study also
9 implied its potential role in miRNA turnover [19]. Indeed, an interaction was observed between
10 IFIT5 and XRN1 protein in LAPC4-Con cells (Fig. 4A). Also, XRN1 exhibited a similar
11 expression pattern as that of IFIT5 between DAB2IP-negative and DAB2IP-positive cells
12 (Additional file 4A) and the presence of DAB2IP was able to inhibit XRN1 expression (Fig. 4B
13 and Additional file 4B). Using 3 different XRN1 siRNAs in LAPC4-KD cells, the elevated
14 expression levels of miR-363 were correlated with the diminished level of XRN1 protein (Fig.
15 4C and Additional file 4C). Similar to IFIT5-KD, data from XRN1-KD cells clearly
16 demonstrated only mature miR-363 exhibited a significant accumulation whereas other mature
17 miRNAs (miR-106a, miR-18b, miR-20b, miR-19b-2, and miR-92a-2) remained relatively
18 unchanged (Fig. 4D).

19
20
21
22
23
24
25
26
27
28
29
30
31 Also, by incubating XRN1 proteins from IP (Additional file 4D) with native, SS⁶Mut or DSMut
32 pre-miR-363 RNA molecules, a significant increase of both native and SS⁶Mut pre-miR-363
33 degradation was detected in a time-dependent manner, whereas DSMut pre-miR-363 remained
34 unchanged (Fig. 4E and Additional file 4D), implying that IFIT5 binding structure in the 5'-end
35 of pre-miR-363 is critical for recruiting XRN1. Indeed, by ectopic transfection IFIT5 cDNA into
36 XRN1-expressing LAPC4-Con cells, the presences of IFIT5 significantly facilitated the turnover
37 rate of SS⁶Mut -pre-miR-363 (Fig. 4F and Additional file 4E). On the other hand, by knocking
38 down XRN1 in IFIT5-expressing LAPC4-Con cells, loss of XRN1 diminished the degradation
39 rate of SS⁶Mut pre-miR-363 (Fig. 4G and Additional file 4F) and rescued the mature miR-363
40 levels (Fig. 4H). These findings provide further evidence for the specific function of IFIT5-
41 XRN1 complex in miR-363 turnover.

42
43
44
45
46
47
48
49
50
51
52 XRN family has been identified as a 5'- to 3'-exoribonuclease responsible for the fidelity of
53 mRNA turnover in eukaryotes [20, 21]. In particular, XRN1 mainly targets the degradation of de-
54 capped mRNA or long non-coding RNAs (lncRNAs), whereas XRN2 is required to degrade a
55 nascent pre-mRNA to prevent long aberrant mRNA formation [18]. Several studies indicated the
56 correlation between XRN family and miRNA biogenesis. For example, XRN2 has been
57
58
59
60
61
62
63
64
65

1
2
3
4 identified to regulate mature miRNA turnover during *C. elegans* development [22], while XRN1
5 is shown to regulate miR-277-3p expression in *Drosophila* [19] and mediates a selective decay of
6 miR-382 in human HEK293 cells [23]. Nevertheless, our data further unveil the specific action
7 of XRN1 as the key ribonuclease in miRNA degradation.
8
9

10 11 12 13 14 **The C-terminal TPR domain of IFIT5 is required for docking XRN1 on pre-miR-363.**

15 Structurally, the C-terminal TPR helices, especially the TPR7 and 8, of IFIT5 are key binding
16 domains for 5'-phosphate capped RNA [12, 13]. Indeed, our data (Fig. 5A and Additional file
17 5A) clearly demonstrated that Δ TPR7-8 (Δ 7-8) mutant of IFIT5 lost its ability to degrade miR-
18 363 compared to wild type (WT) IFIT5 because both domains appeared to be critical for the
19 binding to pre-miR-363 RNA and the interacting with XRN1 protein (Fig. 5B and Additional file
20 5B), which was further confirmed by IP (Fig. 5C). Previously single amino acid mutation
21 (K415A and K422A) in the helix domain between TPR7 and 8 domain of IFIT5 can abolish its
22 binding ability [13], however, our data indicated that both still retained the most of inhibitory
23 activities (Fig. 5A and Additional file 5A) as well as their interaction with XRN1 protein (Fig.
24 5B and Additional file 5B)
25
26
27
28
29
30
31
32
33

34
35 We further determined whether SS⁶Mut or DSMut pre-miR-363 could influence the *in vitro*
36 interaction of IFIT5 and XRN1 in which IFIT5-XRN1 complex was determined by IP with IFIT5
37 in the presence of incremental amounts of SS⁶Mut or DSMut pre-miR363. Clearly, only SS⁶Mut
38 but neither DSMut nor pre-miR-92a-2 could facilitate the complex formation between IFIT5 and
39 XRN1 (Fig. 5D and Additional file 5C). Taken together, the C-terminal TPR7-8 domain of IFIT5
40 protein is critical for not only recognizing the 5'-end overhang structure in pre-miR-363 RNA
41 but also facilitating the docking of XRN1 on pre-miR-363.
42
43
44
45
46
47

48
49 **The functional role of miR-363 in EMT.** DAB2IP is known to inhibit EMT process via
50 regulating several of the embryonic development genes [16] that can be potential target gene(s)
51 of miR-363 based on predicted sequences. From profiling genes modulated by miR-363 in
52 LAPC4-KD cells and RWPE1-KD cells, Slug/SNAI2 mRNA appears to be a potential candidate
53 target gene. Indeed, the suppression of Slug/SNAI2 mRNA and protein levels was detected in
54 miR-363 expressing cells as compared to their controls (Fig. 6A and Additional file 6A).
55 Moreover, the six nucleotides sequence in 3'-end un-translational region (3'-UTR) of
56
57
58
59
60
61
62
63
64
65

1
2
3
4 Slug/SNAI2 mRNA matches the seed region of mature miR-363 (Additional file 6B). By
5 constructing both wild type Slug/SNAI2 3'UTR (Slug-WT3'UTR) and mutant Slug/SNAI2
6 3'UTR (Slug-Mut³⁶³3'UTR) reporter genes, a significant reduction of the Slug-WT3'UTR but
7 not the Slug-Mut³⁶³3'UTR activity was detected in LAPC4-KD (Fig. 6B) and RWPE1-KD cells
8 (Additional file 6C).
9

10
11
12
13
14 Slug/SNAI2 is able to suppress the expression of epithelial marker such as E-Cadherin. As
15 expected, an elevation of E-cadherin mRNA and protein was observed in miR-363
16 overexpressing LAPC4-KD (Fig. 6C) and RWPE1-KD cells (Additional file 6D). In contrast, the
17 expression of both mRNA and protein levels of Vimentin, a mesenchymal marker, were
18 suppressed in both cell lines compared to their controls (Fig. 6C and Additional file 6D).
19 Functionally, miR-363 significantly reduced cell migration in both miR-363 expressing LAPC4-
20 KD (Fig. 6D) and RWPE1-KD cells (Additional file 6E). We also noticed that cells collected
21 from the lower chamber of Transwell exhibited lower miR-363 levels than the upper chamber
22 (Fig. 6D). In contrast, knocking down of miR-363 by an antagomir (Anti-miR-363) enhanced the
23 cell migration of C4-2D2 and RWPE1-Con cells (Additional file 6F). We further confirmed
24 Slug/SNAI2 as the key target gene of miR-363-inhibited EMT, by restoring Slug/SNAI2 level in
25 miR-363-expressing cells that resulted in a dose-dependent reduction of E-Cadherin mRNA and
26 protein levels in both LAPC4-KD (Fig. 6E) and RWPE1-KD cells (Additional file 6G). On the
27 other hand, a dose-dependent elevation of Vimentin mRNA and protein levels was also observed
28 (Fig. 6E and Additional file 6G). Given that the stability of mature miR-363 is dependent on its
29 5'-end overhang structure, we examined the effect of SS⁶Mut or DSMut pre-miR-363 on EMT
30 and found the significant effects of DSMut on inhibiting the expression of Slug/SNAI2 and
31 Vimentin mRNA and enhancing the mRNA expression of E-cadherin (Fig. 6F), which resulted
32 in diminishing both cell migration and invasion (Fig. 6G).
33
34
35
36
37
38
39
40
41
42
43
44
45
46
47
48
49

50 **The effect of IFIT5 on EMT.** To gain more insights whether IFIT5 is able to facilitate EMT via
51 increasing miR-363 turnover, we transfected IFIT5 expression vector in LAPC4-Con cells that
52 express low level of IFIT5. The data clearly showed a significant elevation of Slug/SNAI2 and
53 Vimentin expression along with the suppression of E-cadherin gene expression in IFIT5-
54 expressing cells (Fig. 7A). Ectopic expression of IFIT5 in LAPC4-Con cells was able to alternate
55 E-cadherin, Vimentin and Slug protein levels in a dose-dependent manner (Additional file 6H).
56
57
58
59
60
61
62
63
64
65

1
2
3
4 Moreover, we also observed the morphological change from a cuboidal epithelium-like to an
5 elongated fibroblast-like shape in LAPC4-Con cell (Additional file 6I). On the other hand,
6 knocking down IFIT5 in LAPC4-KD cells significantly increased E-cadherin expression and
7 decreased the expression of both Slug/SNAI2 and Vimentin (Fig. 7B), which led to the reduction
8 of cell motility in LAPC4-KD cells (Fig. 7C). In addition to prostate cell lines, the effect of both
9 IFIT5 and miR-363 on cancer metastasis is also examined in several other cancer cell lines. We
10 observed a significantly lower level of miR-363 in HepG2, 293T and 786O cell lines, which
11 express relatively higher level of IFIT5 protein compared to LAPC4-Con cells (Additional file
12 7A). Knocking down of IFIT5 in these cell lines result in a significant elevation of mature miR-
13 363 level (Additional file 7B). In the absence of IFIT5, E-cadherin was further upregulated and
14 both Vimentin and slug were downregulated at mRNA and protein level (Fig. 7D, 7F and 7H),
15 which led to reduced cell motility in all three cell lines (Fig. 7E, 7G and 7I). On the other hand,
16 the outcome of overexpressing miR-363 in HepG2, 293T and 786O cell lines (Additional file
17 7C) was similar to that of IFIT5 knockdown (Additional file 7D-7J). This data imply that IFIT5
18 may elicit a global oncogenic impact in cancer via regulating EMT-targeting miRNAs. We
19 further demonstrated that IFIT5-elicited EMT is mediated through miR-363 turnover (Fig. 7J and
20 7K) and XRN1 is a key component in the IFIT5 degradation machinery (Fig. 7L).

21
22
23
24
25
26
27
28
29
30
31
32
33
34
35
36 **The clinical correlation of IFIT5.** In general, high-grade PCa is associated with disease
37 progression and poor clinical outcome. We therefore investigated the status of IFIT5 or miR-363
38 in different grades of PCa specimens. Our data (Fig. 8A) indicated that IFIT5 mRNA levels were
39 significantly elevated in the high-grade PCa (G9), compared to both benign and low-grade (G6)
40 tumors, in contrast, the pattern of miR-363 mRNA levels was opposite to that of IFIT5 (Fig. 8B);
41 there appeared to be an inverse correlation between the expression of both genes (Fig. 8C).
42 Meanwhile, both miR-92a-2 and miR-19b-2, immediately adjacent to miR-363, exhibited an
43 elevation pattern in PCa tissues compared with benign tissues (Additional file 8A, 8B), implying
44 a differential regulation or function associated with these miRNAs as compared to miR-363 in
45 PCa. In addition, analyses from TCGA PCa dataset provided further support of our clinical
46 observations; there are the positive correlation between IFIT5 and XRN1 (Additional file 8C) or
47 Slug/SNAI2 or Vimentin (Fig. 8D) and the negative correlation between XRN1 and DAB2IP
48 (Additional file 8D).

1
2
3
4 **The differential regulation of miRNA cluster.** In general, miRNA synthesis including miRNA
5 cluster is under the control of single promoter similar to cellular genes [24, 25]. For example, the
6 presence of two miR-17-92 cluster paralogs including miR-106b-25 and miR-106a-363 in
7 mammals might be due to gene duplication [26]. MiR-17-92 is characterized as an onco-miR
8 cluster from a variety types of cancers such as colon cancer [27, 28], Ewing Sarcoma [4], lung
9 cancer [29, 30] and Burkitt's lymphoma [31]. The pleiotropic functions of miR-17-92 cluster are:
10 promoting proliferation, inhibiting apoptosis, increasing angiogenesis, and maintaining cell
11 survival. In contrast, miR-106a-363 cluster contains 5 miRNAs (miR-106a, miR-18b, miR-20b,
12 miR-19b, miR-92a-2) similar to the oncogenic miR-17-92 cluster plus one additional miR-363
13 that doesn't have a miRNA homolog in miR-17-92 cluster. Our data not only demonstrate the
14 tumor suppressive function of miR-363 in targeting Slug/SNAI2-mediated EMT in several
15 cancer types but also unveil a unique regulation of miRNA cluster via degradation machinery.
16 All together, this study provides not only a new knowledge of miRNA biogenesis but also a
17 potential application of miR-363 as a therapeutic agent in preventing cancer progression.
18
19
20
21
22
23
24
25
26
27
28
29
30
31
32
33
34
35
36
37
38
39
40
41
42
43
44
45
46
47
48
49
50
51
52
53
54
55
56
57
58
59
60
61
62
63
64
65

1
2
3
4 **CONCLUSIONS**
5

6 In this study, we identify the tumor suppressive effect of miR-363, from a cluster that contains
7 the rest of miRNAs characterized as onco-miRs, on intervening EMT. Most interestingly, a
8 miRNA degradation machinery associated with IFIT5 that specifically recognizes a unique 5'-
9 end structure of miRNA and recruits exoribonuclease (XRN1) to degrade this miRNA is
10 delineated in this study, which could provide a new aspect of miRNA biogenesis for other
11 miRNA genes (Fig. 8E). Meanwhile, we also dissect the tumor suppressive function of miR-363
12 in preventing EMT by targeting SNAI2/Slug in PCa. Overall, our finding delineates a new
13 mechanism of miRNA turnover machinery specific for the degradation of a tumor suppressive
14 miRNA derived from a cluster containing oncogenic miRNAs. We believe that this machinery
15 can also work on other tumor suppressor miRNAs as well.
16
17
18
19
20
21
22
23
24
25
26
27
28
29
30
31
32
33
34
35
36
37
38
39
40
41
42
43
44
45
46
47
48
49
50
51
52
53
54
55
56
57
58
59
60
61
62
63
64
65

1
2
3
4
5
6
7 **METHODS**

8 **Cell lines, Clinical specimens, and Plasmid constructs**

9
10 Stable DAB2IP knockdown (KD) and control (Con) cells were generated from RWPE-1, PC-3
11 and LAPC4 cell lines using shRNA [16]. LAPC4 derived from PCa patients with lymph node
12 metastasis was maintained in Iscove Dulbecco's Modified Eagle's Medium (Invitrogen)
13 containing 10% fetal bovine serum (FBS). RWPE-1 derived from normal prostate epithelial cells
14 immortalized with human papillomavirus 18 was maintained in Keratinocyte medium
15 (Invitrogen) containing 10% FBS. The androgen-sensitive LNCaP cell line derived from PCa
16 patients with lymph node metastasis was maintained in RPMI-1640 medium (Invitrogen)
17 containing 10% FBS. C4-2 and PC-3, androgen-independent lines, were maintained in RPMI-
18 1640 medium containing 10% FBS.

19
20 A total of 41 PCa specimens obtained from UT Southwestern Tissue Bank. All the specimens
21 were collected from 6-mm core punch from radical prostatectomy and each punch was divided in
22 half for snap-freeze and paraffin embedding then examined by pathologist to evaluate tumor
23 grade. The Institutional Review Board of UT Southwestern approved the tissue procurement
24 protocol for this study, and appropriate informed consent was obtained from all patients.

25
26 All the plasmid constructs are described in Supplemental information.

27
28
29
30
31
32
33 **Plasmid or siRNA transfection**

34
35 Cells (2.5×10^5) were seeded in 60-mm dish at 60-70% confluence before transfection. According
36 to manufacturer's protocol, transfection of plasmids was using either Xfect Reagent (Clontech)
37 or EZ Plex transfection reagent (EZPLEX), and transfection of siRNA was using
38 Lipofectamine® RNAiMAX reagent (Life Technology). Transient transfection was carried out
39 48 hrs post-transfection to harvest cell for further analyses. In addition, the stable clones (CL)
40 were established after 2 weeks in the selective medium.

41
42
43
44
45
46
47
48
49
50
51
52
53
54
55 **RNA isolation and quantitative real-time RT-PCR (qRT-PCR)**

56
57 Small and large RNA were isolated and purified using mirVana miRNA Isolation Kit (Life
58 Technologies). Small RNA (250 ng) was subjected to miScript II RT kit (QIAGEN) then 2.5 μ l
59
60
61
62
63
64
65

1
2
3
4 cDNA was applied to a 25- μ L reaction volume using miScript SYBR Green PCR kit (QIAGEN)
5
6 in iCycler thermal cycler (Bio-Rad). All primer sequences are listed in Additional file 10, Table
7
8 2. The relative expression levels of precursor and matured miRNAs from each sample were
9
10 determined by normalizing to SNORD95 small RNA. Large RNA (2 μ g) was subjected to
11
12 SuperScript VILO cDNA synthesis kit (Invitrogen) then 2.5 μ l cDNA was applied to 25- μ l
13
14 reaction volume using SYBR Green ER qPCR SuperMix (Invitrogen). The relative expression
15
16 levels of DAB2IP, IFIT5, E-cadherin, and Vimentin, and Slug/SNAI2 mRNA from each sample
17
18 were determined by normalizing to 18S mRNA.
19
20

21 **Western blot analysis**

22
23 Cells were washed with PBS and lysed in lysis buffer [50mMTris-HCl (pH 7.5), 150 mM NaCl,
24
25 0.1% Triton X-100, 1 mM sodium orthovanadate, 1 mM sodium fluoride, 1 mM sodium
26
27 pyrophosphate, 10 mg/mL, aprotinin, 10 mg/mL leupeptin, 2 mM phenylmethylsulfonyl fluoride,
28
29 and 1 mM EDTA] for 60 mins on ice. Cell lysates were spin down at 20,000 xg for 20 mins at
30
31 4°C. Protein extracts were subjected to SDS-PAGE using Bolt 4-12% Bis-Tris Plus gel
32
33 (Invitrogen), and transferred to nitrocellulose membrane using Trans-Blot Turbo Transfer system
34
35 (BIORAD). Membranes were incubated with primary antibodies against DAB2IP, E-Cadherin,
36
37 Vimentin, Slug/SNAI2, XRN1, IFIT5 and Flag at 4 °C for 16-18 hrs, and horseradish
38
39 peroxidase-conjugated secondary antibodies at room temperature for 1.5 hrs. Results were
40
41 visualized with ECL chemiluminescent detection system (Pierce ThermoScientific). The relative
42
43 protein expression level in each sample was normalized to actin or GAPDH.
44

45 **Immunoprecipitation (IP) assay**

46
47 Cells were harvested and protein lysates were prepared freshly before performing IP assay. Flag
48
49 antibody (Sigma) or XRN1 antibody (AbCam) was incubated with 50 μ l of Dynabeads[®] protein
50
51 G (Novex, Life Technology) at room temperature for 15 mins. Subsequently, total 300 μ g of
52
53 protein lysate was incubated with the Dynabead-conjugated antibody at 4°C for 16-18 hrs. After
54
55 washing, the eluates were subjected to SDS-PAGE using Bolt 4-12% Bis-Tris Plus gel
56
57 (Invitrogen), and transferred to a nitrocellulose membrane using Trans-Blot Turbo Transfer
58
59 system (BIORAD). Membranes were then subjected to western blot probed with different
60
61 antibodies.
62
63
64
65

1
2
3
4
5
6 **Luciferase reporter assay**

7
8 Cells (8×10^4) were seeded onto 12-well plates at 75% confluence before transfection. pCMV-
9 miR-363 plasmid was co-transfected with psiCHECK2-Slug3'UTR-WT or psiCHECK2-
10 Slug3'UTR-Mut³⁶³ plasmid into LAPC4-KD and RWPE-1-KD cells using Xfect Reagent
11 (Clontech). Cells were harvested and lysed with Passive Lysis buffer (Promega) at 48 hrs after
12 transfection. Luciferase activity was measured using the Dual-luciferase reporter assay
13 (Promega) on the Veritas Microplate Luminometer (Turner Biosystems). Results were expressed
14 as the relative light unit by normalizing the firefly luciferase activity with Renilla luciferase
15 activity. Each experiment was performed in triplicates.
16
17
18
19
20
21
22
23

24 ***In vitro* transcription of precursor miRNA**

25
26 The PCR-amplified DNA fragment of T7-promoter-precursor-miRNAs was separated by 2%
27 agarose gel electrophoresis and purified using Mermaid SPIN kit (MP Biomedicals), then
28 subjected to *in vitro* transcription assay using T7 High Yield RNA synthesis kit (New England
29 Biolabs). DNA template (750 ng) was mixed with T7 High Yield 10X buffer, NTP mixture
30 (ATP, GTP, CTP and UTP), and T7 RNA polymerase then incubated at 37°C for 16 hrs. The
31 precursor miRNA molecules was first treated with DNase I for 15 mins at 25° C and purified by
32 acid phenol-chloroform extraction and ethanol precipitation. The molecular size and sequence of
33 each purified precursor miRNA was confirmed by gel electrophoresis and qRT-PCR
34 respectively.
35
36
37
38
39
40
41
42
43

44 **RNA pull-down assay**

45
46 The *in vitro* transcribed precursor miRNA was subjected to RNA pull down assay using Pierce
47 Magnetic RNA-Protein Pull-Down Kit (ThermoScientific). An approximate 100 pmol of
48 precursor miRNA were incubated with 10X RNA Ligase reaction buffer, RNase inhibitor,
49 Biotinylated Cytidine Bisphosphate, and T4 RNA ligase at 16°C for 16 hrs. The biotinylated
50 precursor miRNA was then purified and incubated with streptavidin magnetic beads for 30 mins
51 at room temperature. Whole cell lysates were freshly prepared immediately before RNA pull-
52 down assay and 200 µg of protein extract was mixed with the biotinylated precursor miRNA
53 conjugated to streptavidin magnetic beads and incubated at 4°C for 1 hr. The magnetic beads
54
55
56
57
58
59
60
61
62
63
64
65

1
2
3
4 were washed 4 times before elution. Proteins associated with precursor miRNA were eluted and
5 subjected to SDS-PAGE using Bolt 4-12% Bis-Tris Plus gel. Gel bands were stained with
6 Coomassie blue and subjected to LC-MS/MS analysis.
7
8
9

10 11 ***In vitro* pre-miRNA degradation assay**

12 The *in vitro* transcribed precursor miRNAs were incubated with immunoprecipitated IFIT5 or
13 XRN1 in the elution buffer at 37°C on a thermomixer (Eppendorf), then the RNA-containing
14 buffer were collected at indicated time points and subjected to 15% TBE-Urea gel
15 electrophoresis. To quantify the degradation of precursor miRNA, the 15% TBE-Urea gel was
16 then stained with GelRed™ Nucleic Acid Gel Stains (VWR) and visualized under UV light in
17 the AlphaImager device (Protein Simple). The RNA bands were quantified by Multiplex band
18 analysis (AlphaView Software) and the rate of degradation was calculated from each time point
19 normalized to time zero.
20
21
22
23
24
25
26
27
28
29

30 ***In vitro* Transwell migration and invasion assay**

31 Cells (1×10^5 or 4×10^4) were seeded in the serum-free medium in the upper chamber of 6-well
32 insert or 24-well insert with 8- μ m pore size (Corning) with or without Matrigel coating for
33 invasion or migration assay, respectively, while lower chamber contained medium supplemented
34 with 10% FBS. After 2 days, cells that had transmigrated to the lower chamber were fixed by 4%
35 paraformaldehyde and visualized under microscope. Quantification of transmigrated cells was
36 carried out with crystal violet staining and measurement at OD_{555nm}. Each experiment was
37 performed in triplicates.
38
39
40
41
42
43
44
45

46 **Statistics analysis**

47 Statistics analysis was performed by using GraphPad Prism software. Statistical significance was
48 evaluated using Student t-test. P<0.05 was considered a significant difference between compared
49 groups and marked with an asterisk. The statistical association between miR-363 and IFIT5
50 expression among different grades of human PCa was evaluated with regression correlation
51 analysis.
52
53
54
55
56
57
58
59
60
61
62
63
64
65

1
2
3
4 **Abbreviations**
5

6
7 CRPC castration resistant prostate cancer
8
9 EMT epithelial-to-mesenchymal transition
10
11 IFIT5 Interferon-induced protein with tetratricopeptide repeats 5
12
13
14 KD knock-down
15
16 miRNA microRNA
17
18
19 PCa prostate cancer
20
21 shRNA small hairpin RNA
22
23
24 tRNA transfer RNA
25
26 Vec Vector
27
28
29 WT wild type
30
31 XRN1 exoribonuclease
32
33
34
35
36
37
38
39
40
41
42
43
44
45
46
47
48
49
50
51
52
53
54
55
56
57
58
59
60
61
62
63
64
65

1
2
3
4
5
6
7
8
9
10
11
12
13
14
15
16
17
18
19
20
21
22
23
24
25
26
27
28
29
30
31
32
33
34
35
36
37
38
39
40
41
42
43
44
45
46
47
48
49
50
51
52
53
54
55
56
57
58
59
60
61
62
63
64
65

Competing interests

There are no competing interests.

1
2
3
4
5
6
7
8
9
10
11
12
13
14
15
16
17
18
19
20
21
22
23
24
25
26
27
28
29
30
31
32
33
34
35
36
37
38
39
40
41
42
43
44
45
46
47
48
49
50
51
52
53
54
55
56
57
58
59
60
61
62
63
64
65

AUTHORS' CONTRIBUTIONS

UGL designed and performed experiments and drafted the manuscript. RCP, DY LG, JCZ, and SFT constructed plasmid vectors, performed experiments and processing clinical tissues. All authors contributed to the interpretation of the data. UGL and JTH conceived of the study, participated in its design and coordination, and contributed to data analysis. All of the authors approved this manuscript.

1
2
3
4 **DESCRIPTION OF ADDITIONAL DATA**
5

6 **Additional file 1**
7

8
9 **(A)** Profile of miRNA expression in RWPE1-KD cells compared with RWPE1-Con cells. **(B)**
10 Relative fold change of each miRNA from microarray screening (green and red indicate
11 decreased and increased fold change in RWPE1-KD cells after normalizing with RWPE1-Con
12 cells, respectively). **(C)** The expression levels of mature miR-363 in DAB2IP-KD renal cell lines
13 (786-O and HK2) after normalizing with the vector control (Con). **(D)** Induction of mature miR-
14 363 by ectopic expression of DAB2IP in HEK293 cells. **(E)** Expression levels of precursor and
15 mature miRNAs (miR-106a, iR-18b, miR-20b, miR-19b-2, miR-92a-2 and miR-363) in
16 DAB2IP-expressing HEK293D cells after normalizing with HEK293 cells.
17
18
19
20
21
22
23
24
25
26
27
28
29
30

31 **Additional file 2**
32

33 **(A)** Relative change of IFIT5 mRNA and protein level in pairs of DAB2IP-positive and –
34 negative prostate cells (LAPC4, RWPE1 and C4-2). **(B-C)** Suppression of IFIT5 protein
35 expression by ectopic expression of DAB2IP in LNCaP and HEK293 cell lines after normalizing
36 with the control vector (Vec). **(D)** Induction of mature miR-363 in LAPC4-KD cells transfected
37 with IFIT5 siRNA compared with control siRNA (Con). **(E)** Induction of mature miR-363 in
38 LAPC4-KD and RWPE1-KD cells by IFIT5 siRNA after normalizing with the control siRNA
39 (Con). **(F)** Expression levels of mature miRNAs (miR-106a, miR-18b, miR-20b, miR-19b-2,
40 miR-92a-2 and miR-363) in IFIT5-KD (siRNA-IFIT5/+) LNCaP cells compared with the control
41 siRNA (siRNA-Con/-). **(G)** Expression levels of precursor miRNAs (miR-106a, miR-18b, miR-
42 20b, miR-19b-2, miR-92a-2 and miR-363) in IFIT5-KD (siRNA-IFIT5) LAPC4-KD, C4-2Neo,
43 RWPE1-KD and LNCaP cells after normalizing with the control siRNA (siRNA-Con).
44
45
46
47
48
49
50
51
52
53
54
55
56
57
58
59
60
61
62
63
64
65

1
2
3
4 **Additional file 3**
5

6
7 (A) Left panel: Gel electrophoresis of pre-miR-363 fragment after incubation with IFIT5 protein
8 (IP) or elution buffer at 37°C. Middle panel: Time-dependent change of pre-miR-363
9 degradation normalized with 0 min. Right panel: IP of IFIT5 protein subjected to *in vitro* RNA
10 degradation assay (B) Expression levels of primary, precursor and mature miR-363 in RWPE1-
11 KD cells transfected with native, SS⁶Mut or DSMut pre-miR-363 plasmids for 24 hrs and
12 normalized with the control vector (Vec). (C) Time-dependent change of degraded pre-miR-92a-
13 2 and SS¹Mut pre-miR-92a-2 after incubating with IFIT5 protein complex at 37°C normalized
14 with 0 min. (*P<0.05). (D) Time-dependent change of degraded pre-miR-18b and SS²Mut pre-
15 miR-18b after incubating with IFIT5 protein complex at 37°C normalized with 0 min. (*P<0.05).
16
17
18
19
20
21
22
23
24
25
26
27
28
29
30
31

32 **Additional file 4**
33

34 (A) Relative expression level of XRN1 protein in DAB2IP-positive and -negative cells (LAPC4,
35 RWPE1, C4-2, and HK2). (B) Suppression of XRN1 protein expression by ectopic expression of
36 DAB2IP in LNCaP, RWPE1-KD, and HK2-KD cells and compared with the control vector
37 (Vec). (C) Induction of miR-363 expression in LAPC4-KD cells transfected with XRN1 siRNA
38 and compared with the control siRNA (Con). (D) Left panel: IP of endogenous XRN1 protein
39 subjected to *in vitro* RNA degradation assay. Right panel: Time-dependent change of native,
40 SS⁶Mut and DSMut pre-miR-363 degradation (bracket) after incubation with XRN1 protein at
41 37°C, each time point was normalized with 0 min. (E) Left panel: Western blot from Vector or
42 IFIT5-transfected LAPC4-Con cells. Right panel: Time-dependent change of degraded SS⁶Mut
43 pre-miR-363 fragments in the presence of XRN1 alone (XRN1+Vector) or XRN1-IFIT5
44 complex (XRN1+IFIT5) at 37°C. (F) Left panel: western blot from IFIT5-expressing LAPC4-
45
46
47
48
49
50
51
52
53
54
55
56
57
58
59
60
61
62
63
64
65

1
2
3
4 Con cells transfected with control or XRN1 siRNA. Right panel: Time-dependent change of
5
6 degraded SS⁶Mut pre-miR-363 fragments in the presence of XRN1-IFIT5 complex derived from
7
8 IFIT5 w/ siRNA-Con or IFIT5 w/ siRNA-XRN1 at 37°C.
9
10

11 12 13 14 **Additional file 5**

15
16 (A) Relative expression level of mature miR-363 in RWPE1-Con cells transfected with wild
17 type (WT) and mutant (Δ 7-8, K422A) IFIT5 after normalizing with the control vector. (B)
18 Interaction between pre-miR-363 and wild type (WT) or mutant IFIT5 (Δ 7-8, K415A, K422A)
19 derived from RWPE1-Con cells using RNA pull down. (C) The effect of pre-miR-92a-2
20 molecule on the interaction between XRN1 and IFIT5 using IP with Flag antibodies.
21
22
23
24
25
26
27
28
29
30

31 32 **Additional file 6**

33
34 (A) Reduction of Slug/SNAI2 mRNA and protein levels in miR-363-expressing RWPE1-KD
35 cells after normalizing with the control vector (Vec). (*p<0.05, CL: miR-363 expressing stable
36 clone) (B) Predicted sequence of the putative miR-363 target site in 3'UTR of Slug/SNAI2
37 mRNA (Slug-WT 3'UT) and its mutant sequence (Slug Mut³⁶³ 3'UTR). (C) Luciferase reporter
38 activities in RWPE1-KD cells co-transfected with siCHECK2-slug-WT 3'UTR or -slug-Mut³⁶³
39 3'UTR and pCMV-miR363 or control vector (Vec). (RFU=Renilla to Firefly luciferase activity,
40 each bar represents mean \pm SD of four replicated experiments.) (D) Expression levels of E-
41 cadherin or Vimentin mRNA and protein in miR-363-expressing RWPE1-KD clones. (E) Cell
42 migration of RWPE1-Con, -KD and miR363-expressing RWPE1-KD clones. (F) Cell migration
43 of RWPE1-Con and C4-2D2 cells transfected with anti-miR-363. Cells transmigrated at the
44 lower chamber were stained with crystal violet and quantified at OD 555nm. Each bar represents
45
46
47
48
49
50
51
52
53
54
55
56
57
58
59
60
61
62
63
64
65

1
2
3
4 mean \pm SD of three replicated experiments. (*P<0.05) **(G)** The effect of Slug on the expression
5
6 levels of E-cadherin and Vimentin mRNA and protein in miR-363-expressing RWPE1-KD
7
8 clones (CL2) after normalizing with the control vector (Con). (*P<0.05). **(H)** The dose-
9
10 dependent effect of IFIT5 on the protein levels of E-Cadherin, Vimentin and Slug in LAPC4-Con
11
12 cells. **(I)** The effect of IFIT5 on morphological change in LAPC4-Con cells compared with the
13
14 control vector (Vec).
15
16
17
18
19
20

21 **Additional file 7**

22
23 **(A)** The expression level of miR-363 and IFIT5 protein among prostate (LAPC4), brain (U118),
24
25 kidney (786O, 293T) and liver (HepG2) cancer cell lines. **(B)** Induction of mature miR-363
26
27 levels in IFIT5-shRNA knockdown (sh-IFIT5, +) HepG2, 293T and 786O cell lines, compared to
28
29 the control shRNA (-). **(C, E, G)** Overexpression of miR-363 and its impact on the mRNA level
30
31 of E-cadherin, Slug and Vimentin in HepG2 (C), 293T (E) and 786O cell lines (G), compared to
32
33 control vector (Vec). **(D)** Transwell migration of miR-363 expressing HepG2 cells (363),
34
35 compared to the control vector (Vec). **(F)** Transwell invasion of miR-363 expressing 293T cells
36
37 (363), compared to the control vector (Vec). **(H)** Transwell invasion of miR-363 expressing
38
39 786O cells (363), compared to the control vector (Vec). Migrated or invaded cells at the lower
40
41 chamber were stained with crystal violet and quantified at OD 555nm. Each bar represents mean
42
43 \pm SD of three replicated experiments (* p<0.05).
44
45
46
47
48
49
50

51 **Additional file 8**

52
53 **(A, B)** Expression levels of mature miR-92a-2 and miR-19b-2 in human prostate specimens
54
55 including benign (N=10), G6 (N=9), G7(N=9), G8(N=6) and G9(N=7) (*p<0.05, **p<0.0001).
56
57
58
59
60
61
62
63
64
65

1
2
3
4 **(C,D)** Clinical correlation between IFIT5 and XRN1, as well as XRN1 and DAB2IP mRNA
5
6 level in PCa from TCGA PCa dataset.
7
8
9

10
11 **Additional file 9**
12

13
14 List of protein candidates derived from Mass Spectrometry after using precursor miR-363 to pull
15
16 down protein complex in a variety of pairs (LAPC4, RWPE1 and C4-2) with or without DAB2IP
17
18 expression.
19
20
21

22
23 **Additional file 10**
24

25
26 Primers designed for site-directed mutagenesis and PCR.
27
28
29
30
31
32
33
34
35
36
37
38
39
40
41
42
43
44
45
46
47
48
49
50
51
52
53
54
55
56
57
58
59
60
61
62
63
64
65

1
2
3
4
5
6
7
8
9
10
11
12
13
14
15
16
17
18
19
20
21
22
23
24
25
26
27
28
29
30
31
32
33
34
35
36
37
38
39
40
41
42
43
44
45
46
47
48
49
50
51
52
53
54
55
56
57
58
59
60
61
62
63
64
65

ACKNOWLEDGMENTS

We thank Dr. Collins (University of California, Berkeley) for providing IFIT5 cDNA constructs, Dr. Dong (Emory University, Atlanta) for providing the psiCHECK2-Slug3'UTR plasmid. Drs. Kou-Juey Wu (China Medical University, Taichung, Taiwan) and Dr. Vimal Selvaraj (Cornell University, Ithaca) for the helpful discussion. This work was supported by grants from the United States Army (W81XWH-11-1-0491 to JTH) and (W81XWH-14-1-0249 to UGL)

REFERENCES

1. Aalto AP, Pasquinelli AE: **Small non-coding RNAs mount a silent revolution in gene expression.** *Curr Opin Cell Biol* 2012, **24**:333-340.
2. Schickel R, Boyerinas B, Park SM, Peter ME: **MicroRNAs: key players in the immune system, differentiation, tumorigenesis and cell death.** *Oncogene* 2008, **27**:5959-5974.
3. Obernosterer G, Leuschner PJ, Alenius M, Martinez J: **Post-transcriptional regulation of microRNA expression.** *RNA* 2006, **12**:1161-1167.
4. Dylla L, Jedlicka P: **Growth-promoting role of the miR-106a~363 cluster in Ewing sarcoma.** *PLoS One* 2013, **8**:e63032.
5. Chow TF, Mankaruos M, Scorilas A, Youssef Y, Girgis A, Mossad S, Metias S, Rofael Y, Honey RJ, Stewart R, et al: **The miR-17-92 cluster is over expressed in and has an oncogenic effect on renal cell carcinoma.** *J Urol* 2010, **183**:743-751.
6. Diosdado B, van de Wiel MA, Terhaar Sive Droste JS, Mongera S, Postma C, Meijerink WJ, Carvalho B, Meijer GA: **MiR-17-92 cluster is associated with 13q gain and c-myc expression during colorectal adenoma to adenocarcinoma progression.** *Br J Cancer* 2009, **101**:707-714.
7. Wong P, Iwasaki M, Somervaille TC, Ficara F, Carico C, Arnold C, Chen CZ, Cleary ML: **The miR-17-92 microRNA polycistron regulates MLL leukemia stem cell potential by modulating p21 expression.** *Cancer Res* 2010, **70**:3833-3842.
8. Landais S, Landry S, Legault P, Rassart E: **Oncogenic potential of the miR-106-363 cluster and its implication in human T-cell leukemia.** *Cancer Res* 2007, **67**:5699-5707.
9. Ng SB, Yan J, Huang G, Selvarajan V, Tay JL, Lin B, Bi C, Tan J, Kwong YL, Shimizu N, et al: **Dysregulated microRNAs affect pathways and targets of biologic relevance in nasal-type natural killer/T-cell lymphoma.** *Blood* 2011, **118**:4919-4929.
10. Zhou P, Huang G, Zhao Y, Zhong D, Xu Z, Zeng Y, Zhang Y, Li S, He F: **MicroRNA-363-mediated downregulation of S1PR1 suppresses the proliferation of hepatocellular carcinoma cells.** *Cell Signal* 2014, **26**:1347-1354.
11. Tsuji S, Kawasaki Y, Furukawa S, Taniue K, Hayashi T, Okuno M, Hiyoshi M, Kitayama J, Akiyama T: **The miR-363-GATA6-Lgr5 pathway is critical for colorectal tumorigenesis.** *Nat Commun* 2014, **5**:3150.
12. Abbas YM, Pichlmair A, Gorna MW, Superti-Furga G, Nagar B: **Structural basis for viral 5'-PPP-RNA recognition by human IFIT proteins.** *Nature* 2013, **494**:60-64.
13. Katibah GE, Lee HJ, Huizar JP, Vogan JM, Alber T, Collins K: **tRNA binding, structure, and localization of the human interferon-induced protein IFIT5.** *Mol Cell* 2013, **49**:743-750.
14. Katibah GE, Qin Y, Sidote DJ, Yao J, Lambowitz AM, Collins K: **Broad and adaptable RNA structure recognition by the human interferon-induced tetratricopeptide repeat protein IFIT5.** *Proc Natl Acad Sci U S A* 2014, **111**:12025-12030.
15. Min J, Zaslavsky A, Fedele G, McLaughlin SK, Reczek EE, De Raedt T, Guney I, Strochlic DE, Macconail LE, Beroukhim R, et al: **An oncogene-tumor suppressor cascade drives metastatic prostate cancer by coordinately activating Ras and nuclear factor-kappaB.** *Nat Med* 2010, **16**:286-294.
16. Xie D, Gore C, Liu J, Pong RC, Mason R, Hao G, Long M, Kabbani W, Yu L, Zhang H, et al: **Role of DAB2IP in modulating epithelial-to-mesenchymal transition and prostate cancer metastasis.** *Proc Natl Acad Sci U S A* 2010, **107**:2485-2490.

17. Jones CI, Zabolotskaya MV, Newbury SF: **The 5' --> 3' exoribonuclease XRN1/Pacman and its functions in cellular processes and development.** *Wiley Interdiscip Rev RNA* 2012, **3**:455-468.
18. Nagarajan VK, Jones CI, Newbury SF, Green PJ: **XRN 5'-->3' exoribonucleases: structure, mechanisms and functions.** *Biochim Biophys Acta* 2013, **1829**:590-603.
19. Jones CI, Grima DP, Waldron JA, Jones S, Parker HN, Newbury SF: **The 5'-3' exoribonuclease Pacman (Xrn1) regulates expression of the heat shock protein Hsp67Bc and the microRNA miR-277-3p in Drosophila wing imaginal discs.** *RNA Biol* 2013, **10**:1345-1355.
20. Newbury SF: **Control of mRNA stability in eukaryotes.** *Biochem Soc Trans* 2006, **34**:30-34.
21. Orban TI, Izaurralde E: **Decay of mRNAs targeted by RISC requires XRN1, the Ski complex, and the exosome.** *RNA* 2005, **11**:459-469.
22. Chatterjee S, Grosshans H: **Active turnover modulates mature microRNA activity in Caenorhabditis elegans.** *Nature* 2009, **461**:546-549.
23. Bail S, Swerdel M, Liu H, Jiao X, Goff LA, Hart RP, Kiledjian M: **Differential regulation of microRNA stability.** *RNA* 2010, **16**:1032-1039.
24. Olive V, Jiang I, He L: **mir-17-92, a cluster of miRNAs in the midst of the cancer network.** *Int J Biochem Cell Biol* 2010, **42**:1348-1354.
25. Tanzer A, Stadler PF: **Molecular evolution of a microRNA cluster.** *J Mol Biol* 2004, **339**:327-335.
26. Ventura A, Young AG, Winslow MM, Lintault L, Meissner A, Erkeland SJ, Newman J, Bronson RT, Crowley D, Stone JR, et al: **Targeted deletion reveals essential and overlapping functions of the miR-17 through 92 family of miRNA clusters.** *Cell* 2008, **132**:875-886.
27. Tsuchida A, Ohno S, Wu W, Borjigin N, Fujita K, Aoki T, Ueda S, Takanashi M, Kuroda M: **miR-92 is a key oncogenic component of the miR-17-92 cluster in colon cancer.** *Cancer Sci* 2011, **102**:2264-2271.
28. Dews M, Homayouni A, Yu D, Murphy D, Sevignani C, Wentzel E, Furth EE, Lee WM, Enders GH, Mendell JT, Thomas-Tikhonenko A: **Augmentation of tumor angiogenesis by a Myc-activated microRNA cluster.** *Nat Genet* 2006, **38**:1060-1065.
29. Hayashita Y, Osada H, Tatematsu Y, Yamada H, Yanagisawa K, Tomida S, Yatabe Y, Kawahara K, Sekido Y, Takahashi T: **A polycistronic microRNA cluster, miR-17-92, is overexpressed in human lung cancers and enhances cell proliferation.** *Cancer Res* 2005, **65**:9628-9632.
30. Osada H, Takahashi T: **let-7 and miR-17-92: small-sized major players in lung cancer development.** *Cancer Sci* 2011, **102**:9-17.
31. Onnis A, De Falco G, Antonicelli G, Onorati M, Bellan C, Sherman O, Sayed S, Leoncini L: **Alteration of microRNAs regulated by c-Myc in Burkitt lymphoma.** *PLoS One* 2010, **5**.

1
2
3
4
5
6
7
8
9 **Figure Legends**

10 **Figure 1. The effect DAB2IP on miR-363 expression in prostate cell lines.** (A) Expression
11 levels of miR-363 in DAB2IP-knockdown (KD) prostate cell lines after normalizing with the
12 control (Con). (B) Induction of miR-363 by ectopic expression of DAB2IP in C4-2Neo and
13 LAPC4-KD cell lines after normalizing with the control vector (Vec). (C) Expression levels of
14 primary miR-106a-363 in DAB2IP-positive and-negative sublines. (D) Expression levels of
15 precursor miRNAs (miR-106a, miR-18b, miR-20b, miR-19b-2, miR-92a-2 and miR-363) in
16 DAB2IP-positive and-negative cells. (E) Expression levels of mature miRNAs (miR-106a, miR-
17 18b, miR-20b, miR-19b-2, miR-92a-2 and miR-363) in DAB2IP-positive and-negative cells.

18
19
20
21
22
23
24
25
26
27
28
29
30
31
32 **Figure 2. The impact of IFIT5 on miR-363 maturation from the miR-106a-363 cluster.** (A)
33 The interaction between IFIT5 protein and pre-miR-363 in DAB2IP-positive and –negative cells
34 using RNA pull down assay. (B-C) Suppression of IFIT5 protein expression by ectopic
35 transfecting DAB2IP into LAPC4-KD and C4-2Neo cells after normalizing with the control
36 vector (Vec). (D-F) Expression levels of mature miRNAs (miR-106a, miR-18b, miR-20b, miR-
37 19b-2, miR-92a-2 and miR-363) in IFIT5-expressing (IFIT5) LAPC4-Con, C4-2D2 and RWPE1-
38 Con cells after normalizing with the control vector (Vec). (G-I) Expression levels of mature
39 miRNAs (miR-106a, miR-18b, miR-20b, miR-19b-2, miR-92a-2 and miR-363) in IFIT5-siRNA
40 knockdown (+) LAPC4-KD, C4-2Neo and RWPE1-KD cells compared to the control siRNA (-).
41
42
43
44
45
46
47
48
49
50
51
52
53
54
55
56

57 **Figure 3. IFIT5-mediated precursor miR-363 degradation *in vitro*.** (A) Time-dependent
58 change of degraded pre-miR-92a-2 and pre-miR-363 fragments (bracket) after incubation with
59
60
61
62
63
64
65

1
2
3
4 IFIT5 protein complex at 37°C normalized with 0 min. (*P<0.05) (B) Left panel: Mutation of
5
6 nucleotides (red box) for generating 5'-end 6 nucleotides single stranded pre-miR-363 (SS⁶Mut
7
8 pre-miR-363) and blunt 5'-end double stranded pre-miR-363 (DSMut pre-miR-363). Both
9
10 mature miR-363 and miR-363* sequence are shown in pink. Right panel: Expression levels of
11
12 primary, precursor and mature miR-363 in LAPC4-KD cells transfected with Native, SS⁶Mut or
13
14 DSMut pre-miR-363 plasmids for 24 hrs after normalizing with the vector control. (C) Time-
15
16 dependent change of degraded native, SS⁶Mut and DSMut pre-miR-363 fragments (bracket) after
17
18 incubation with IFIT5 protein at 37°C, each time point was normalized with 0 min. (*p<0.05)
19
20
21
22
23
24
25 (D) Induction of mature miR-363 in cells transfected with SS⁶Mut pre-miR-363 or DSMut pre-
26
27 miR-363 plasmids and IFIT5 siRNA after normalizing with the control vector (Vec).
28
29 (Con=control siRNA). (E) Interaction between IFIT5 protein and SS⁶Mut or DSMut pre-miR-
30
31 363 RNA molecules using RNA pull down assay. (F) Upper panel: predicted structure and
32
33 sequence of pre-miR-92a-2. Middle panel: mutation of nucleotides (red box) for generating
34
35 single nucleotide overhanging structure of pre-miR-92a-2 (SS¹Mut). Lower panel: interaction
36
37 between IFIT5 protein and pre-miR-92a-2 or SS¹Mut pre-miR-92a-2 RNA molecules using RNA
38
39 pull down assay. (G) Upper panel: predicted structure and sequence of pre-miR-18b. Middle
40
41 panel: mutation of nucleotides (red box) for generating double nucleotides overhanging structure
42
43 of pre-miR-18b (SS²Mut). Lower panel: Interaction between IFIT5 protein and pre-miR-18b or
44
45 SS²Mut pre-miR-18b RNA molecules using RNA pull down assay.
46
47
48
49
50
51
52
53
54
55

56 **Figure 4. Interaction between XRN1 with IFIT5 leading to pre-miR-363 degradation *in***

57 ***vitro*.** (A) Interaction between IFIT5 and XRN1 proteins using IP by Flag and XRN1 antibodies,
58
59
60
61
62
63
64
65

1
2
3
4 respectively. **(B)** Suppression of XRN1 protein expression by ectopic transfecting DAB2IP into
5
6 LAPC4-KD and C4-2Neo cells after normalizing with the control vector (Vec). **(C)** Induction of
7
8 mature miR-363 in LAPC4-KD cells transfected with XRN1 siRNA after normalizing with the
9
10 control siRNA (Con). **(D)** Expression levels of precursor and mature miRNAs (miR-106a, miR-
11
12 18b, miR-20b, miR-19b-2, miR-92a-2 and miR-363) in XRN1-KD (siRNA-XRN1) LAPC4-KD
13
14 cells after normalizing with the control siRNA (siRNA-Con). **(E)** Time-dependent change of
15
16 degraded native, SS⁶Mut and DSMut pre-miR-363 fragments after incubation with XRN1
17
18 protein at 37°C after normalizing with 0 min. (*p<0.05) **(F)** Time-dependent change of degraded
19
20 SS⁶Mut pre-miR-363 fragments after incubation with immunoprecipitated-XRN1 alone
21
22 (XRN1+Vec) or XRN1-IFIT5 complex (XRN1+IFIT5) at 37°C after normalizing with 0 min.
23
24 (*p<0.05) **(G)** Time-dependent change of degraded SS⁶Mut pre-miR-363 after incubation with
25
26 the immunocomplex derived from cells transfected with IFIT5 and control siRNA (IFIT5
27
28 w/siRNA-Con) or XRN1 siRNA (IFIT5 w/siRNA-XRN1) at 37°C after normalizing with 0 min.
29
30 (*p<0.05) **(H)** Dose-dependent recovery of mature miR-363 expression in IFIT5-expressing
31
32 LAPC4-Con cells transfected with XRN1 siRNA after normalizing with the control vector (Con:
33
34 control siRNA, *p<0.05).
35
36
37
38
39
40
41
42
43
44
45
46
47
48
49
50
51
52
53
54
55
56
57
58
59
60
61
62
63
64
65

Figure 5. The C-terminal TPR 7-8 domain of IFIT5 required for the interaction with pre-miR-363 and XRN1. **(A)** Relative expression level of mature miR-363 in LAPC4-Con and C4-2D2 cells transfected with wild type (WT) and mutant (Δ 7-8, K415A, K422A) IFIT5 after normalizing with the control vector. **(B)** Interaction between pre-miR-363 RNA molecule and wild type (WT) or mutant IFIT5 (Δ 7-8, K415A, K422A) proteins derived from LAPC4-Con (Upper panel) or C4-2D2 (lower panel) cells using RNA pull down assay. **(C)** Interaction

1
2
3
4 between XRN1 and wild type (WT) or Δ 7-8 mutant IFIT5 derived from LAPC4-Con cells using
5
6
7 IP. **(D)** The effect of SS⁶ Mut (upper panel) or DSMut pre-miR-363 RNA molecule (lower panel)
8
9 on the protein-protein interaction between XRN1 and IFIT5 using IP with Flag antibodies.

10
11
12
13
14 **Figure 6. The effect of miR-363 and IFIT5 on EMT in LAPC4 cells.** **(A)** Reduction of
15
16 Slug/SNAI2 mRNA levels in miR-363-expressing LAPC4-KD cells after normalizing with the
17
18 control vector (Vec). (*p<0.05, CL: miR-363 expressing stable clone) **(B)** Luciferase reporter
19
20 activities in LAPC4-KD cells co-transfected with siCHECK2-Slug-WT 3'UTR or -Slug Mut³⁶³
21
22 3'UTR and pCMV-miR363 or control vector. (RFU=Renilla to Firefly luciferase activity, each
23
24 bar represents mean \pm SD of four replicated experiments. * p<0.05) **(C)** Expression levels of E-
25
26 cadherin and Vimentin mRNA and protein in miR-363-expressing LAPC4-KD cell. **(D)** The
27
28 effect of miR-363 on cell migration of GFP-expressing LAPC4-KD cells. GFP-positive cells
29
30 were observed under microscope and migrated cells were stained with crystal violet and
31
32 quantified at O.D. 555nm. (Each bar represents mean \pm SD of three replicated experiments. *
33
34 p<0.05). **(E)** The effect of Slug on the expression levels of E-cadherin and Vimentin mRNA and
35
36 protein in miR-363 -expressing LAPC4-KD cells (CL3) after normalizing with the control vector
37
38 (Con). (*P<0.05). **(F)** The effect of SS⁶ Mut and DSMut pre-miR-363 on the expression levels of
39
40 mature miR-363, E-cadherin, Vimentin and Slug mRNA in LAPC4-KD cells after normalizing
41
42 with the control vector. **(G)** The effect of SS⁶ Mut or DSMut pre-miR-363 on cell migration or
43
44 invasion in LAPC4-KD cells. Migrated cells were stained with crystal violet and quantified at
45
46 OD 555nm. Each bar represents mean \pm SD of three replicated experiments. (* p<0.05, NS=no
47
48 significance)

1
2
3
4 **Figure 7. The impact of IFIT5 on EMT in liver and kidney cancer cell lines.** (A) The effect
5 of IFIT5 on the expression levels of E-Cadherin, Vimentin and Slug mRNA and protein in
6 LAPC4-Con cells after normalizing with the control vector (Vec). (B) Expression levels of E-
7 Cadherin, Vimentin and Slug mRNA and proteins in LAPC4-KD cells transfected with IFIT5
8 siRNA (+) compared to the control siRNA (-). (C) Cell invasion assay of LAPC4-KD cells
9 transfected with IFIT5 siRNA (+) compared to the control siRNA (-). (D, F, H) The expression
10 level of E-cadherin, Slug and Vimentin mRNA in IFIT5-shRNA knockdown (+) HepG2 (D),
11 293T (F) and 786O cells (H), compared to the control shRNA (-). (E) Transwell migration of
12 IFIT5-knockdown (+) HepG2 cells, compared to the control shRNA (-). (G) Transwell migration
13 of IFIT5-knockdown (+) 293T cells, compared to the control shRNA (-). (I) Transwell invasion
14 of IFIT5-knockdown (+) 786O cells, compared to the control shRNA (-). Migrated or invaded
15 cells at the lower chamber were stained with crystal violet and quantified at OD 555nm. Each bar
16 represents mean \pm SD of three replicated experiments (* p<0.05). (J) The impact of IFIT5 on
17 miR-363 maturation in LAPC4-KD cells transfected with SS⁶Mut or DSMut pre-miR-363
18 plasmids. Each bar represents mean \pm SD of three replicated experiments. (* p<0.05). (K) The
19 effect of IFIT5 and SS⁶Mut or DSMut pre-miR-363 on cell invasion of LAPC4-KD cells.
20 Invaded cells at the lower chamber were stained with crystal violet and quantified at OD 555nm.
21 Each bar represents mean \pm SD of three replicated experiments. (* p<0.05). (L) The effect of
22 XRN1 on the expression levels of E-cadherin, Vimentin and slug protein in IFIT5-expressing
23 LAPC4-Con cells after normalizing with the control vector (Vec) (Con: control siRNA).

24
25
26
27
28
29
30
31
32
33
34
35
36
37
38
39
40
41
42
43
44
45
46
47
48
49
50
51
52
53
54
55
56 **Figure 8. The effect of IFIT5-mediated miR-363 degradation on EMT and its clinical**
57 **correlation in PCa.** (A, B) Relative induction of IFIT5 mRNA and mature miR-363 level in
58
59
60
61
62
63
64
65

1
2
3
4 human PCa specimens derived from different grades including benign (N=10), G6 (N=9),
5
6 G7(N=9), G8(N=6) and G9(N=7) (*p<0.05, **p<0.0001). (C) Clinical correlation between miR-
7
8 363 and IFIT5 mRNA expression in human PCa specimens graded from G6 to G9 (N=31, R=-
9
10 0.3183, p=0.0405). (D) Clinical correlation between IFIT5 and SNAI2/Slug or Vimentin in PCa
11
12 from TCGA PCa dataset. (E) Schematic representation of IFIT5-mediated pre-miR-363 turnover
13
14 leading to EMT in cancer.
15
16
17
18
19
20
21
22
23
24
25
26
27
28
29
30
31
32
33
34
35
36
37
38
39
40
41
42
43
44
45
46
47
48
49
50
51
52
53
54
55
56
57
58
59
60
61
62
63
64
65

Figure 1.

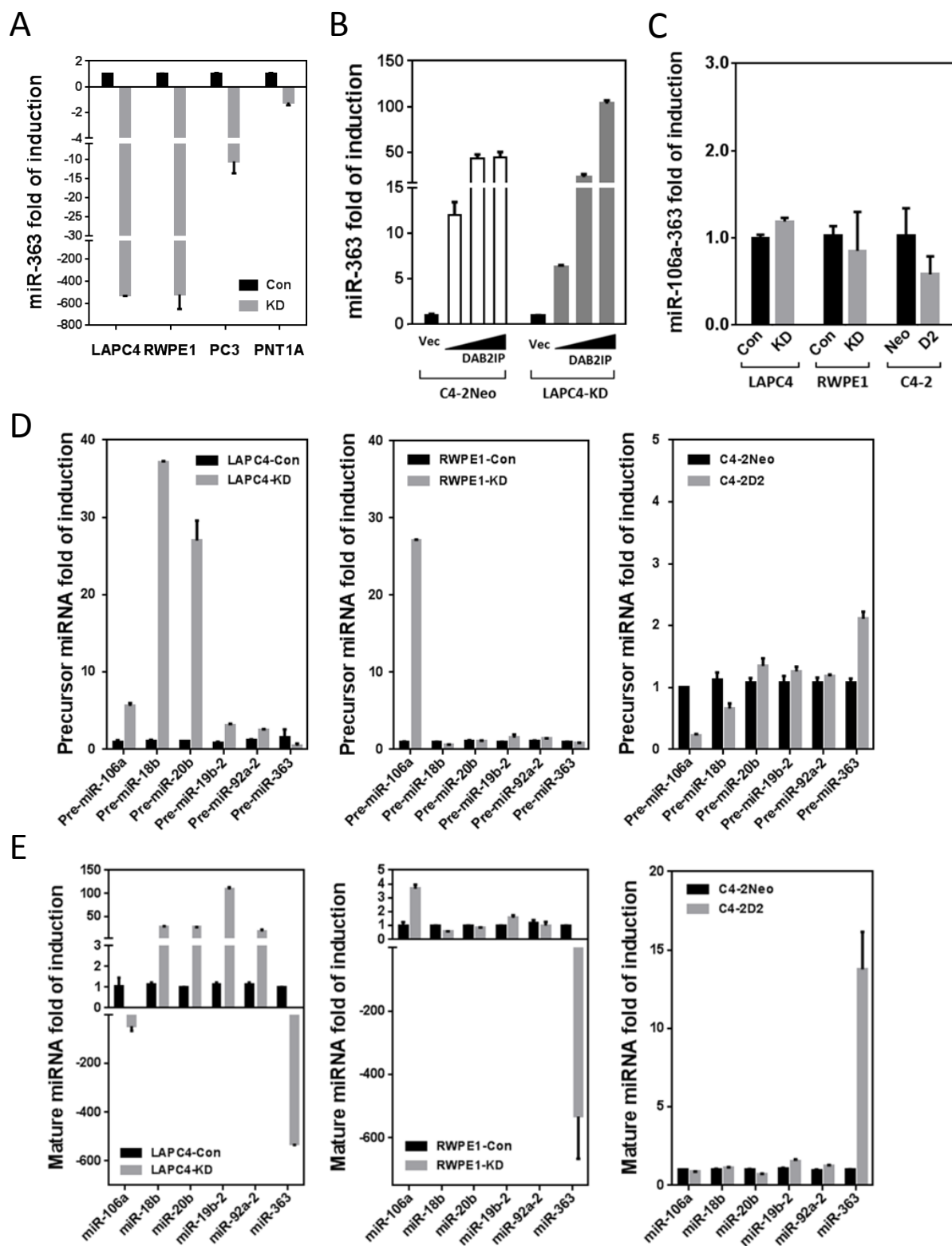


Figure 2.

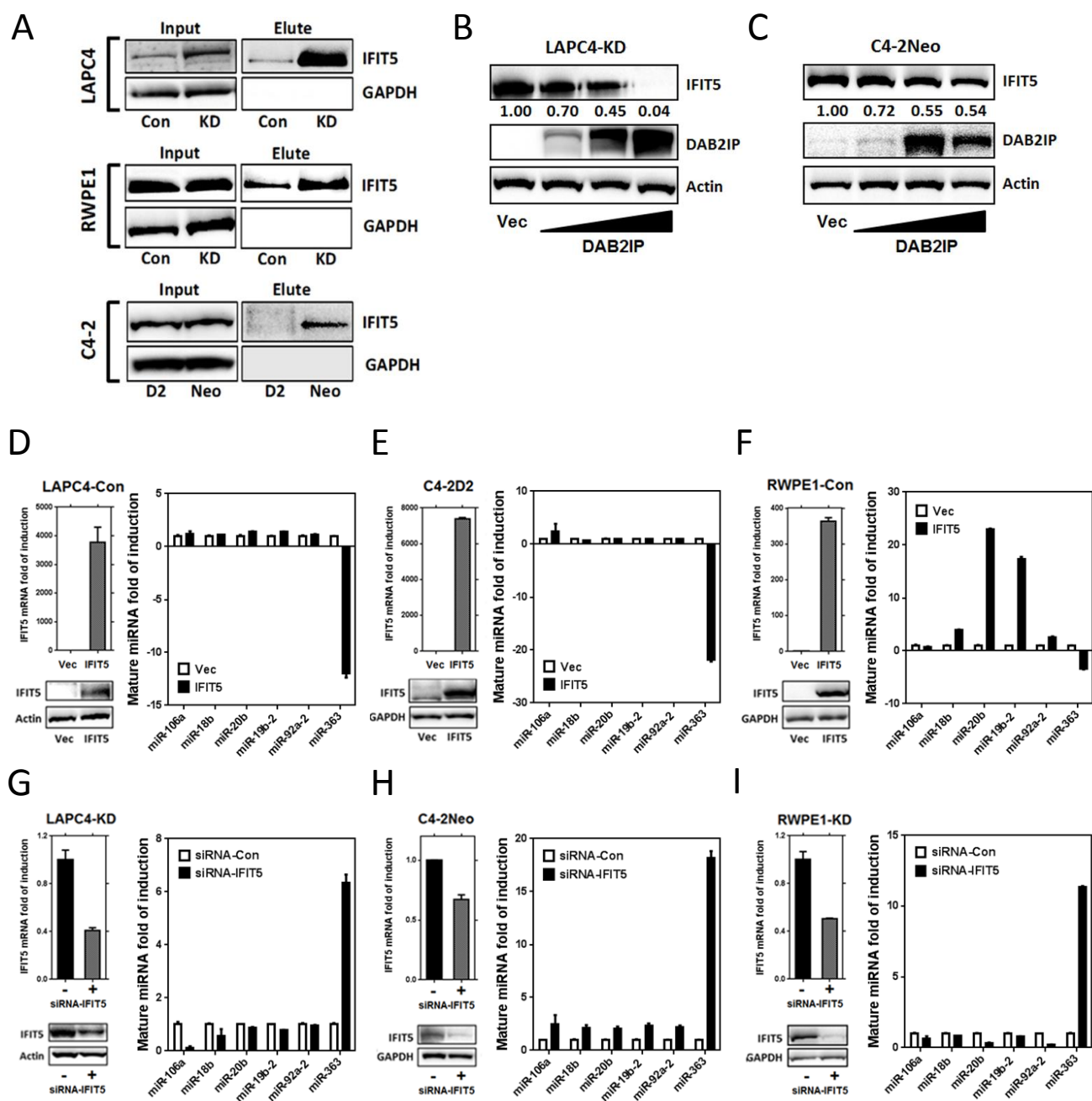


Figure 3.

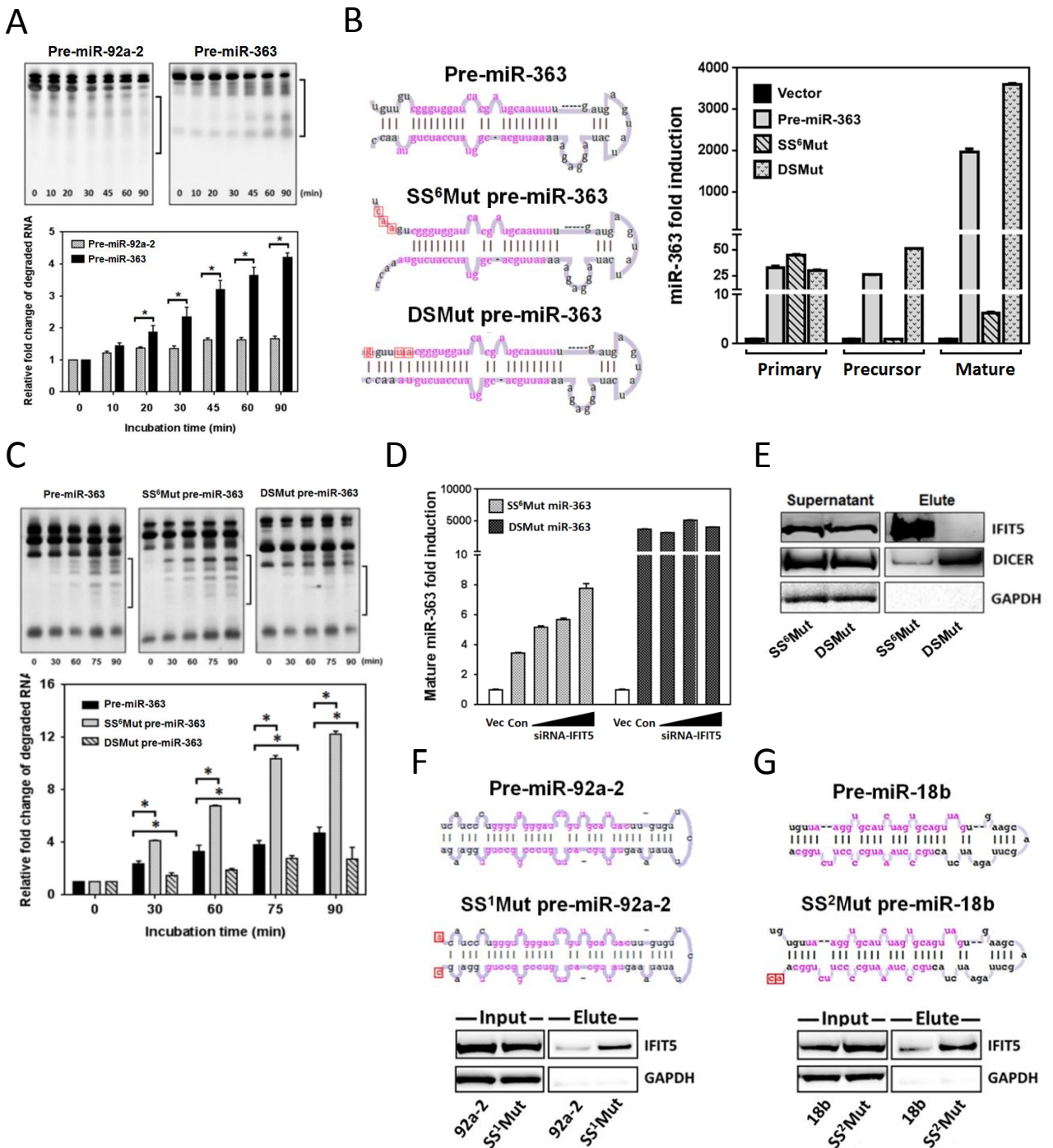


Figure 4.

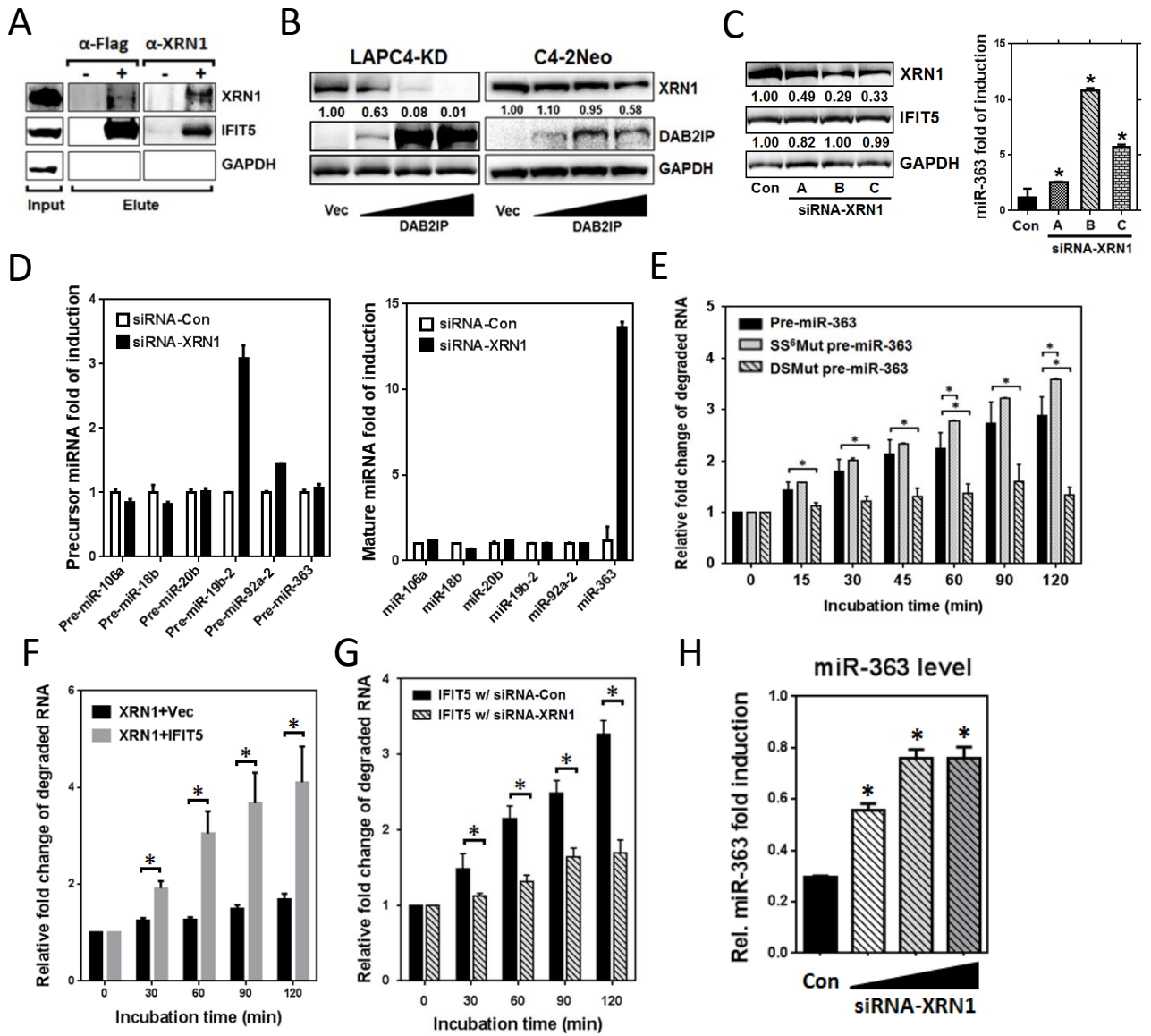


Figure 5.

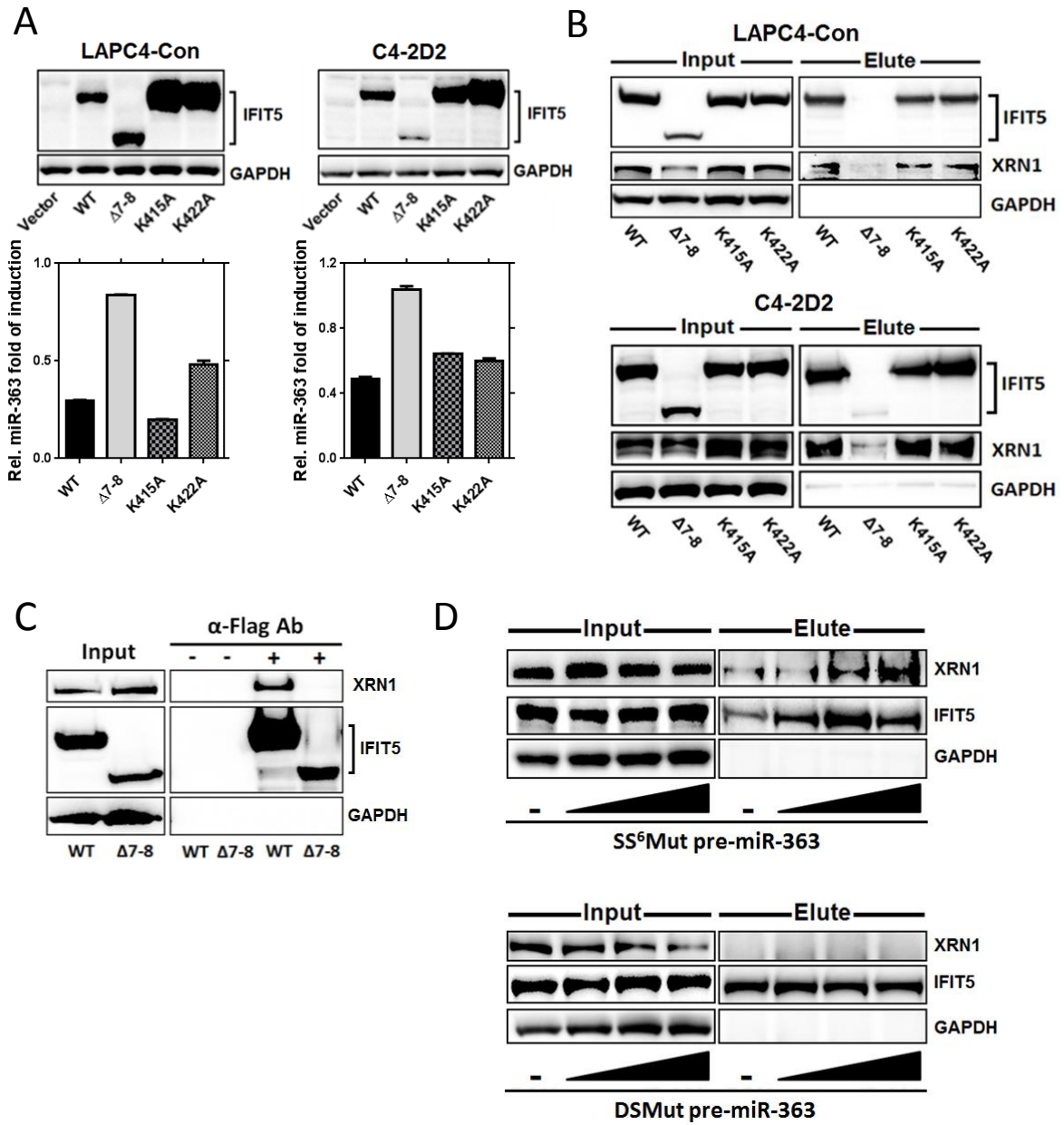


Figure 6.

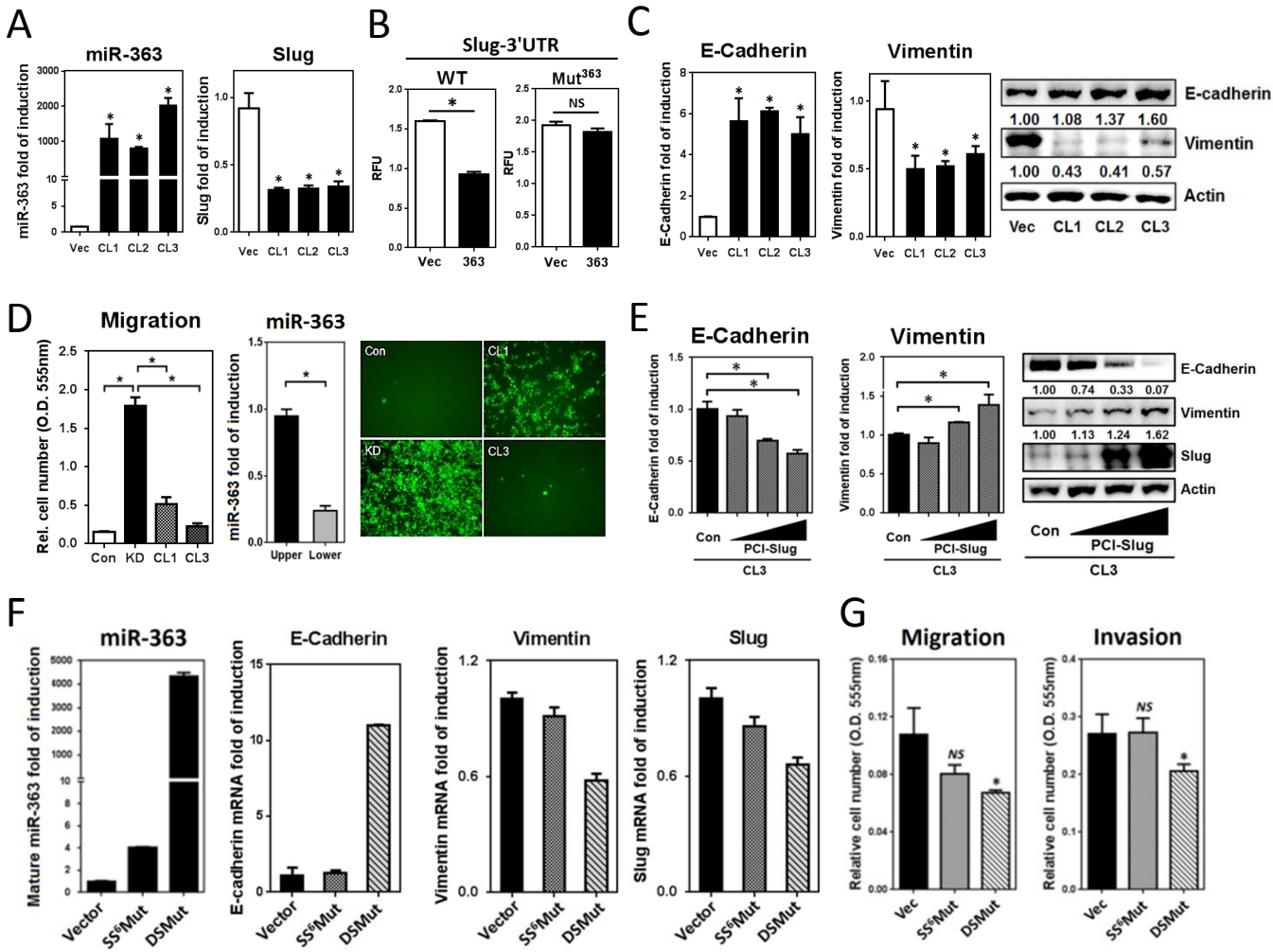


Figure 7.

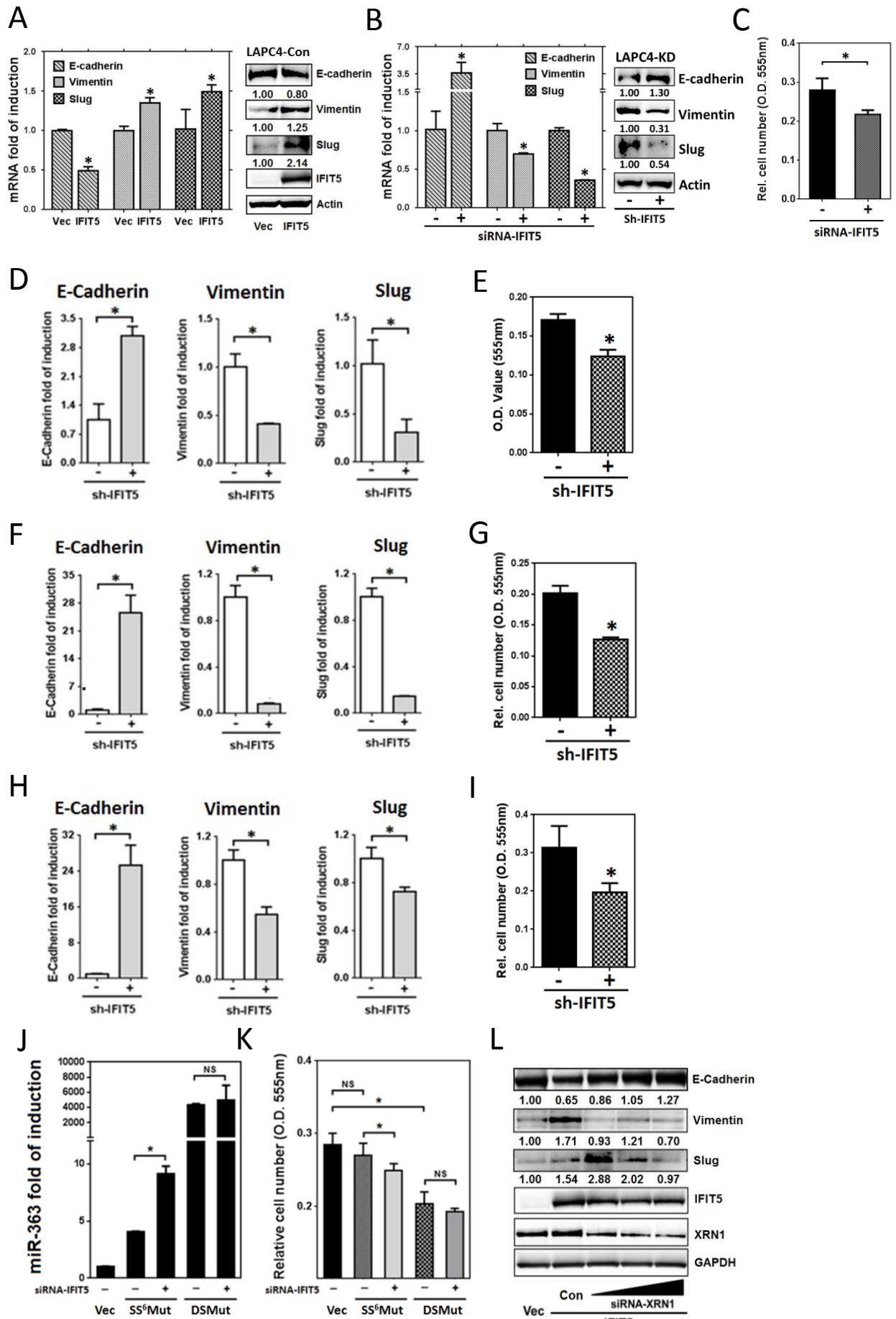
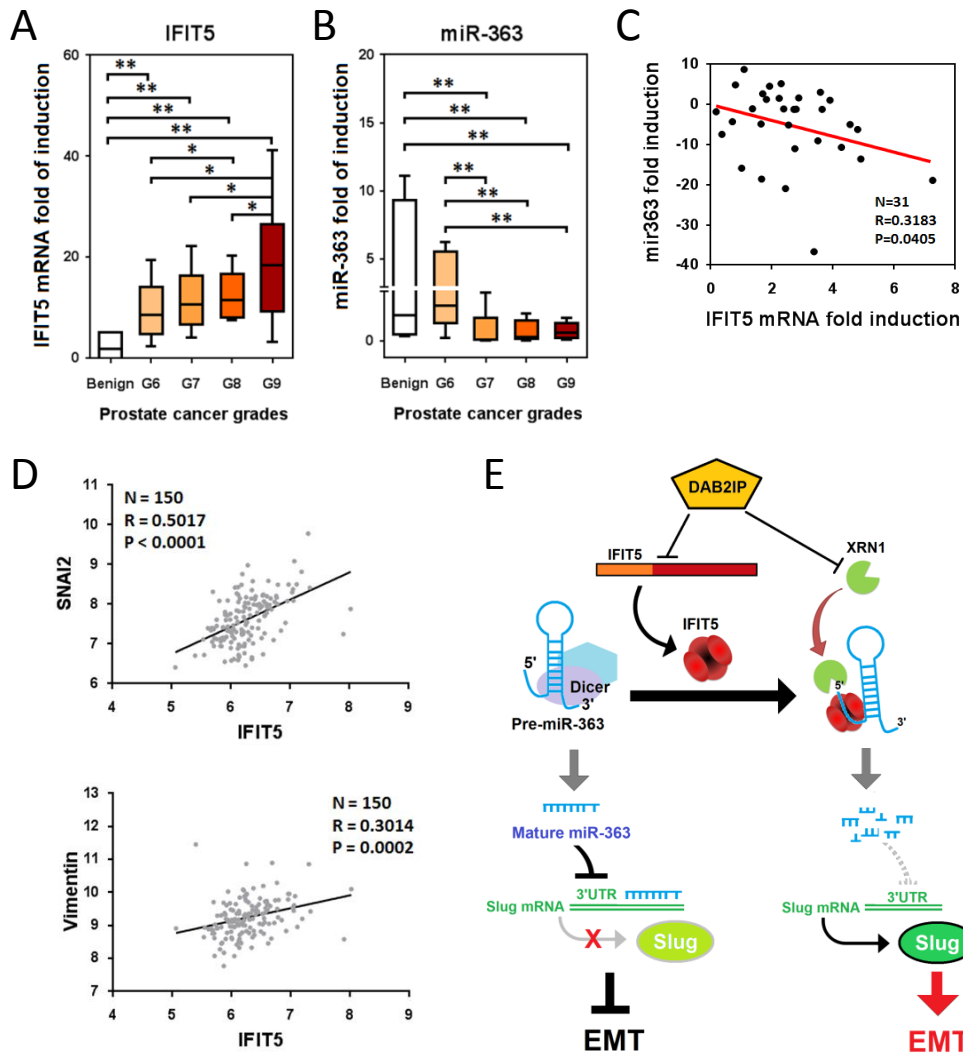
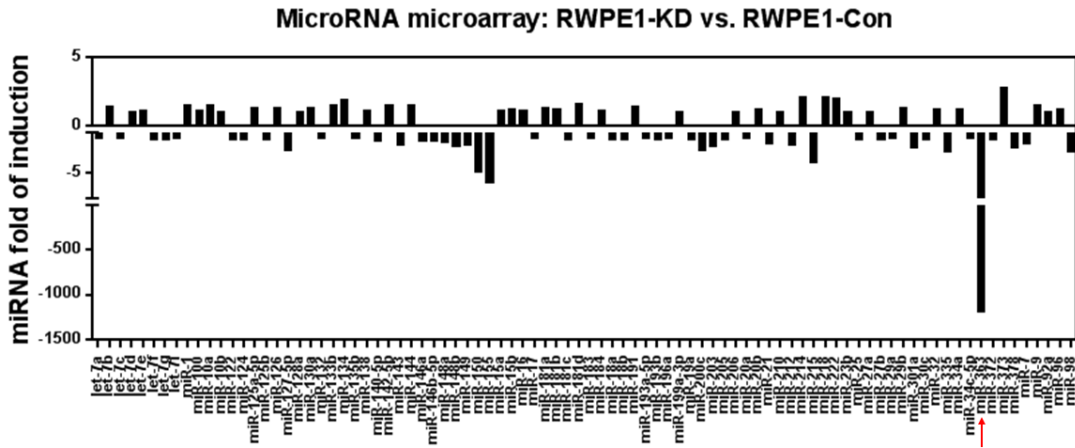


Figure 8.



Additional file 1

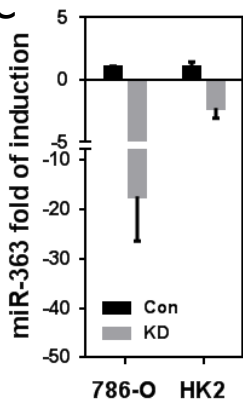
A



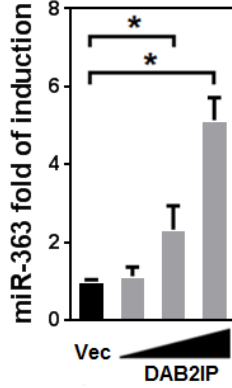
B

let-7a	-1.07
let-7b	1.41
let-7c	-1
let-7d	1.07
let-7e	1.15
let-7f	-1.23
let-7g	-1.15
let-7i	-1.07
miR-1	1.52
miR-100	1.15
miR-10a	1.52
miR-10b	1
miR-122	-1.23
miR-124	-1.15
miR-125a-5p	1.32
miR-125b	-1.15
miR-126	1.32
miR-127-5p	-2.46
miR-128a	1.07
miR-130a	1.32
miR-132	-1
miR-133b	1.52
miR-134	1.87
miR-135b	-1
miR-138	1.15
miR-140-5p	-1.41
miR-142-5p	1.52
miR-143	-1.74
miR-144	1.52
miR-146a	-1.41
miR-146b-5p	-1.41
miR-148a	-1.52
miR-148b	-2
miR-149	-1.74
miR-150	-4.92
miR-155	-6.06
miR-15a	1.15
miR-15b	1.23
miR-16	1.15
miR-17	-1.07
miR-181a	1.32
miR-181b	1.23
miR-181c	-1.15
miR-181d	1.62
miR-183	-1
miR-184	1.15
miR-18a	-1.23
miR-18b	-1.15
miR-191	1.41
miR-193a-5p	-1
miR-193b	-1.23
miR-196a	-1.07
miR-199a-3p	1
miR-19a	-1.15
miR-200c	-2.46
miR-203	-2
miR-205	-1.15
miR-206	1.07
miR-20a	-1.07
miR-20b	1.23
miR-21	-1.62
miR-210	1.07
miR-212	-1.87
miR-214	2.14
miR-215	-3.73
miR-218	2.14
miR-222	2
miR-23b	1.07
miR-25	-1.15
miR-27a	1
miR-27b	-1.15
miR-29a	-1.07
miR-29b	1.32
miR-301a	-2.14
miR-30c	-1.15
miR-32	1.23
miR-335	-2.64
miR-34a	1.23
miR-34c-5p	-1.07
miR-363	-1176.27
miR-372	-1.23
miR-373	2.83
miR-378	-2.14
miR-7	-1.62
miR-9	1.52
miR-92a	1.07
miR-96	1.23
miR-98	-2.64

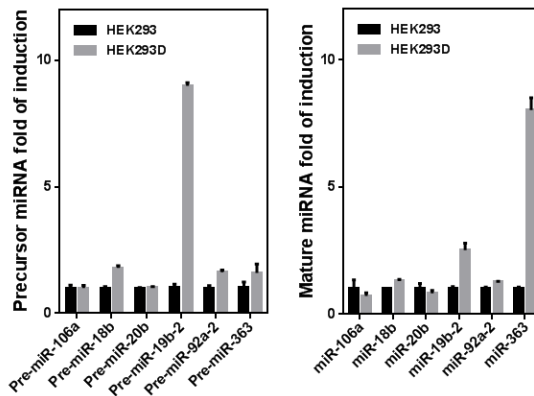
C



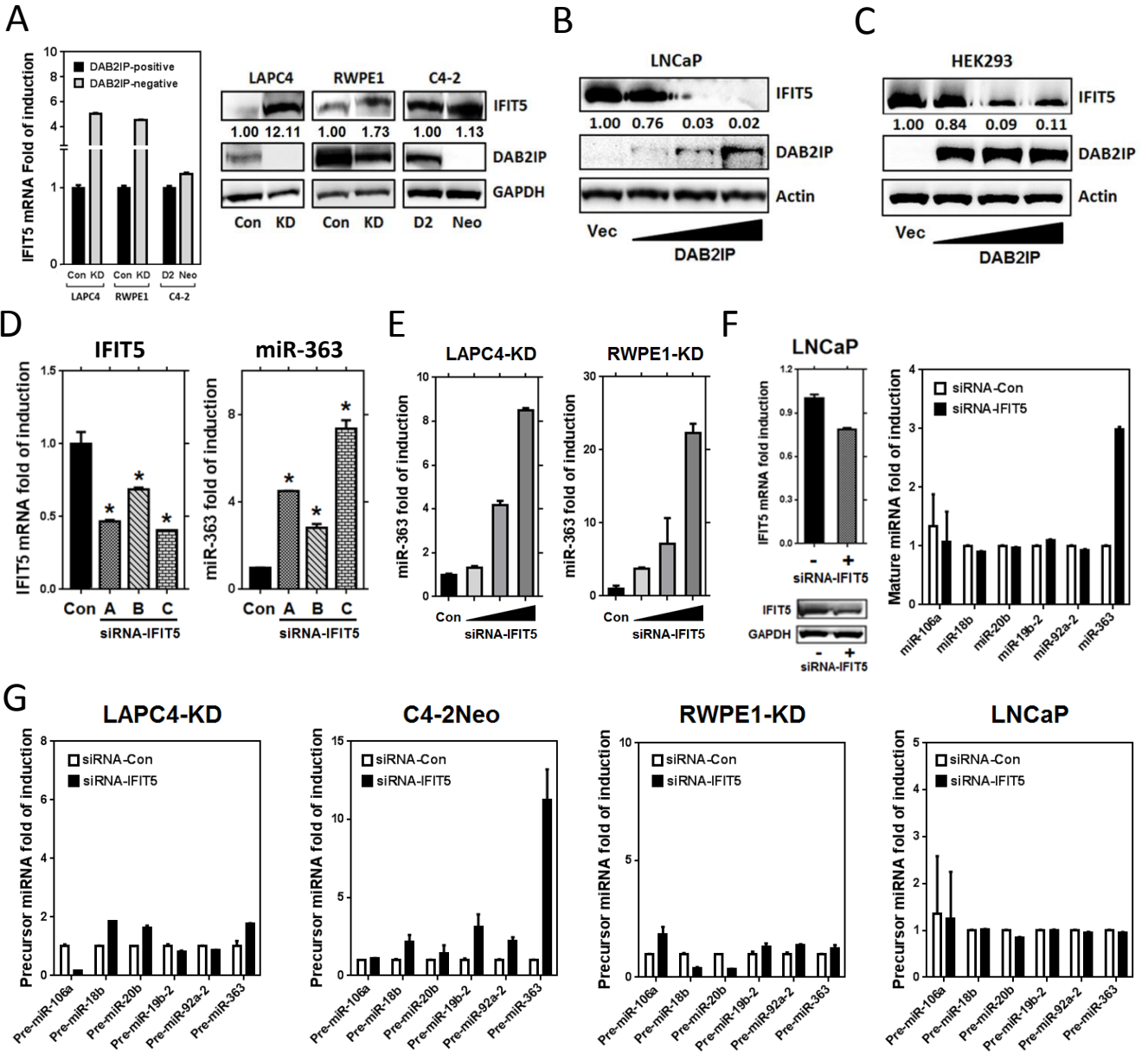
D



E

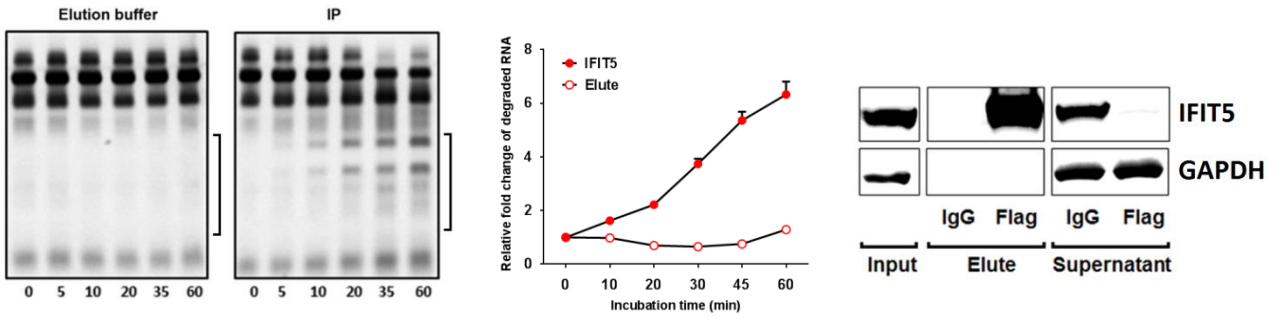


Additional file 2

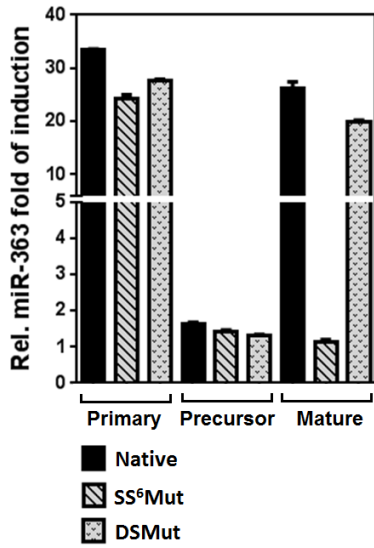


Additional file 3

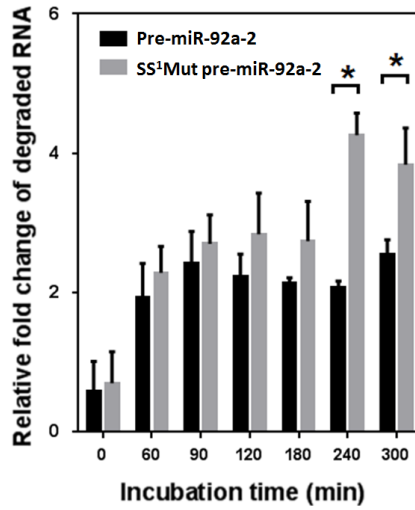
A



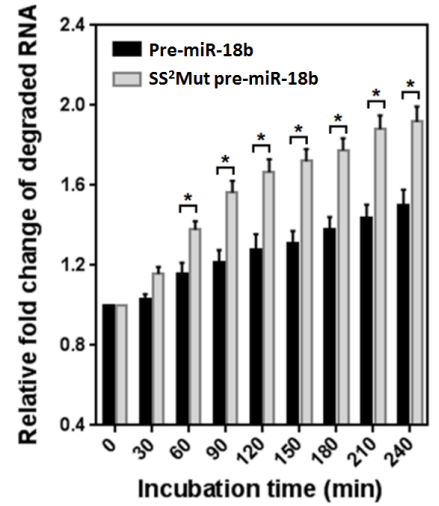
B



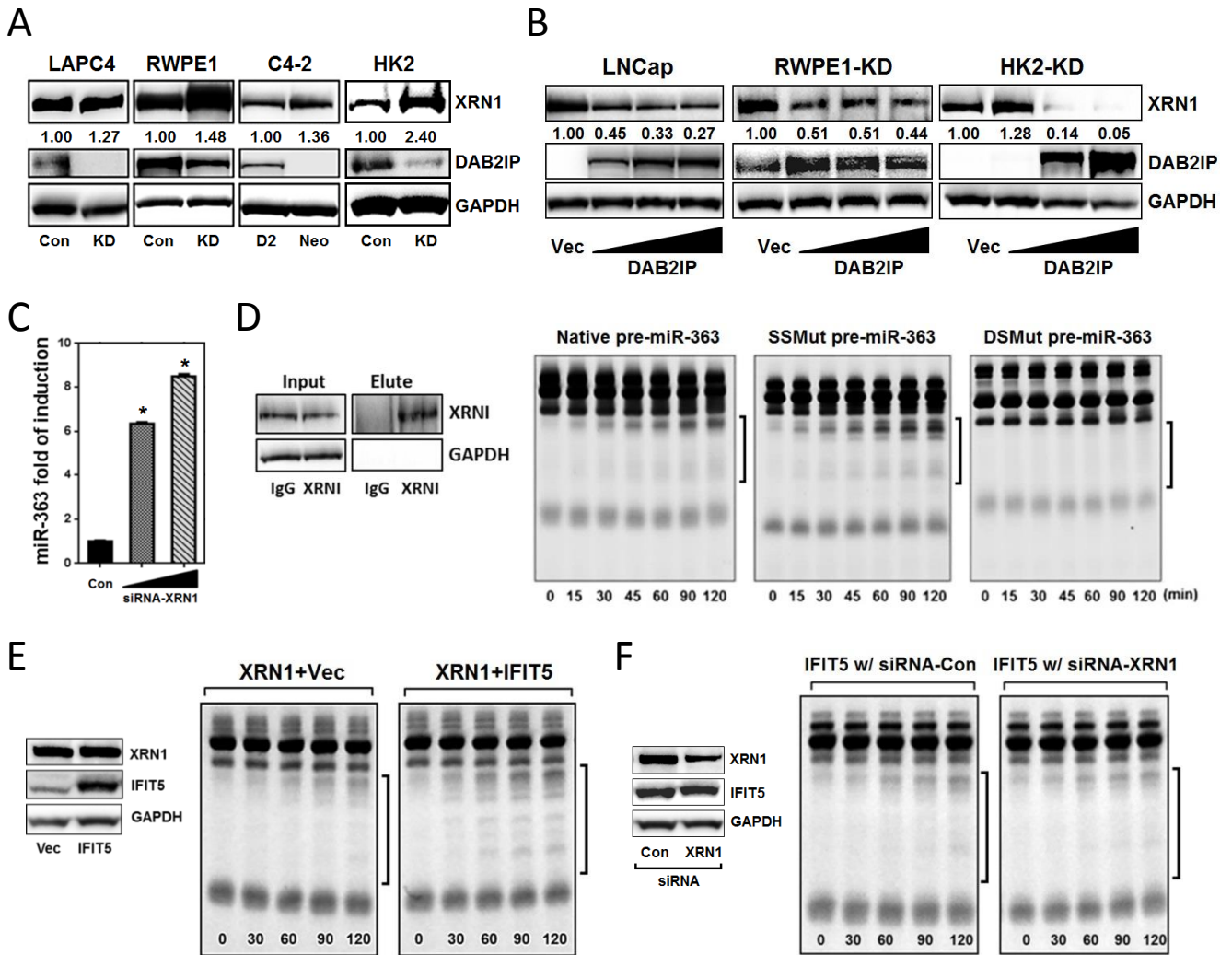
C



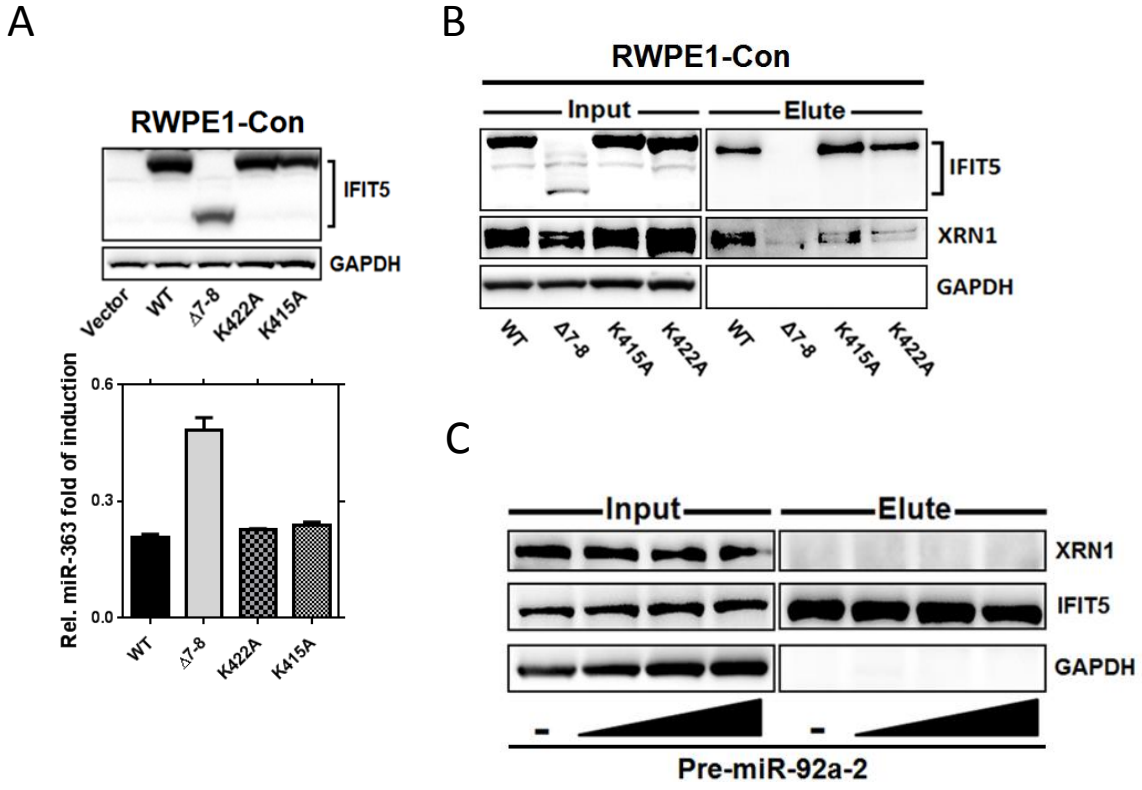
D



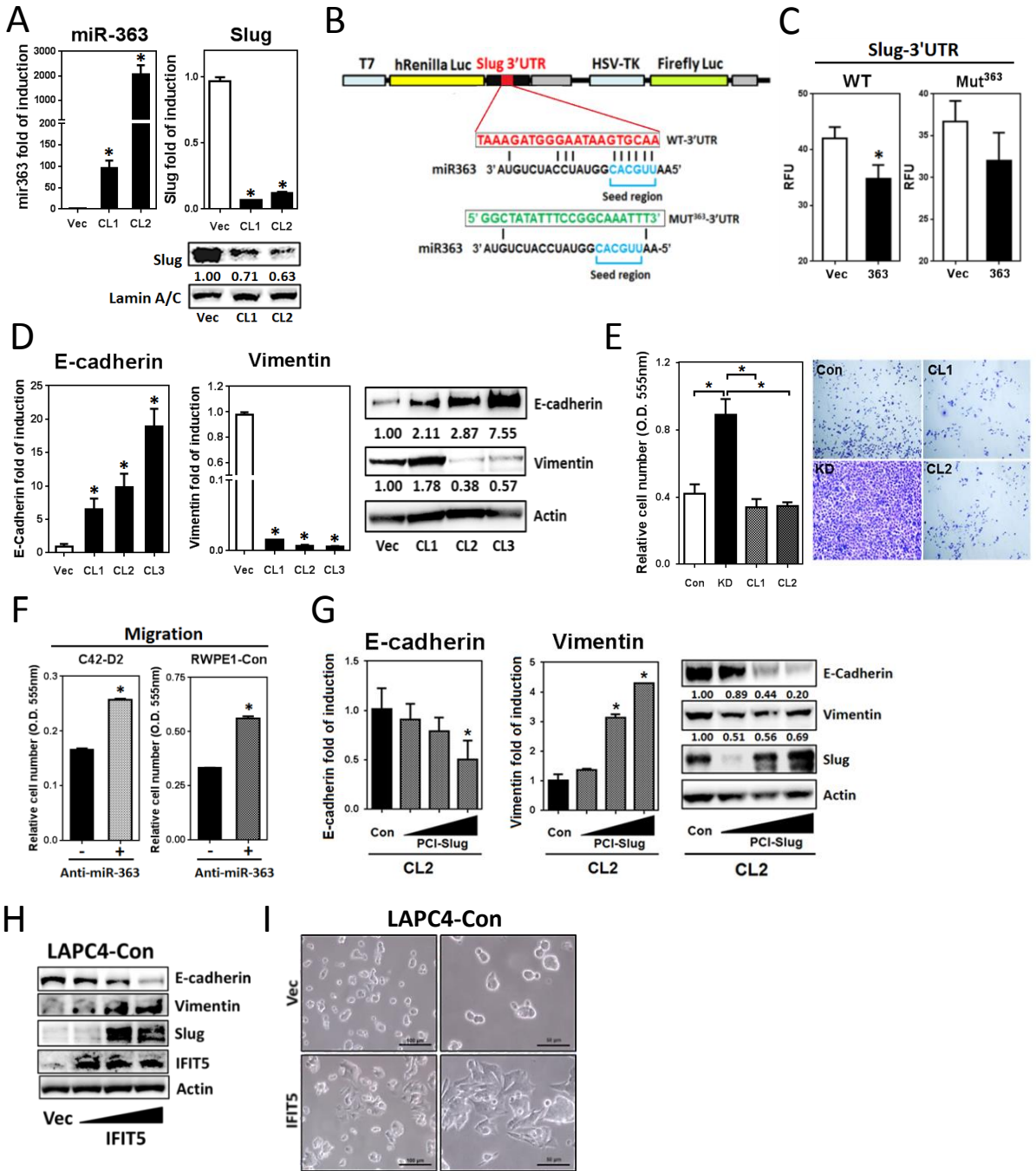
Additional file 4



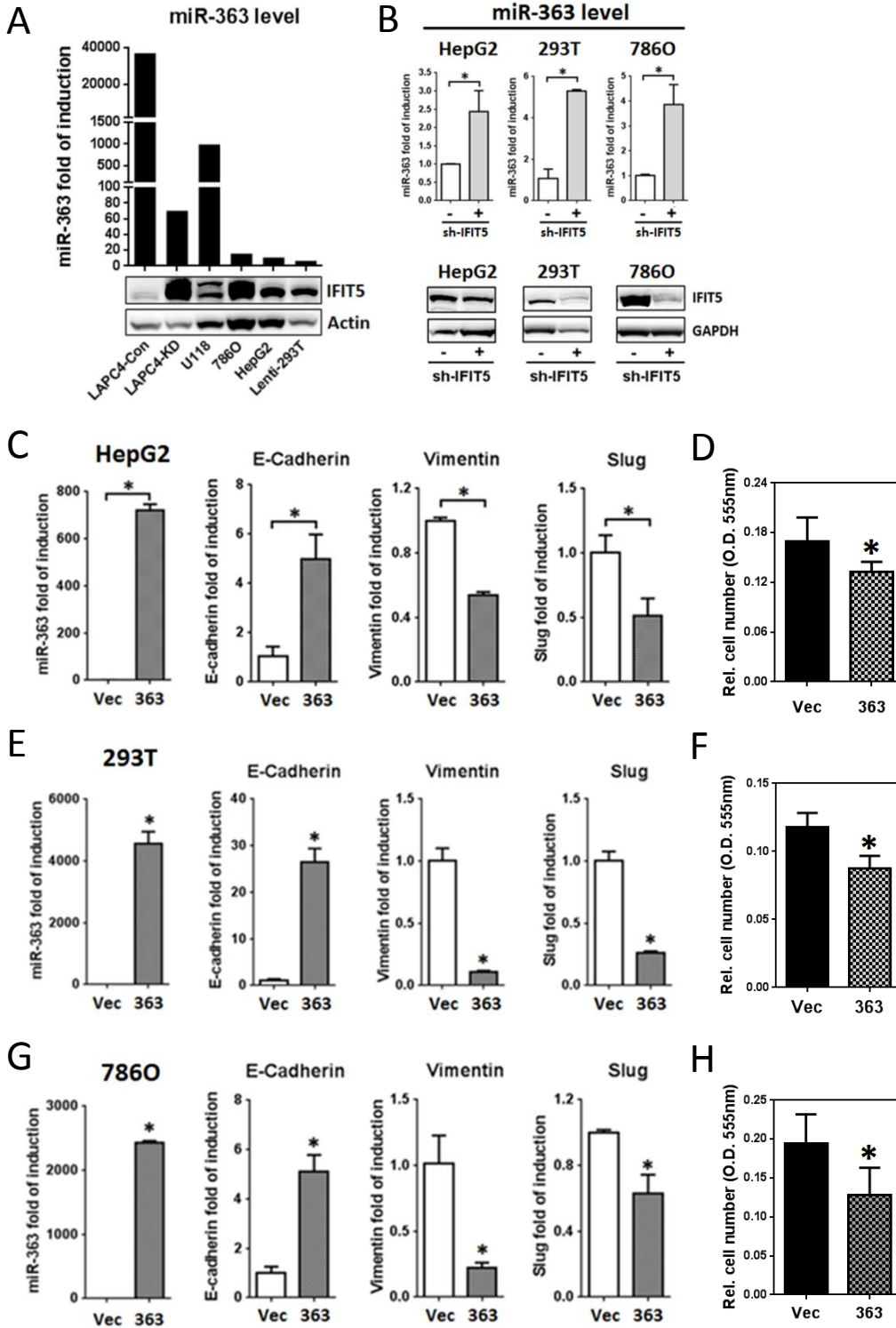
Additional file 5



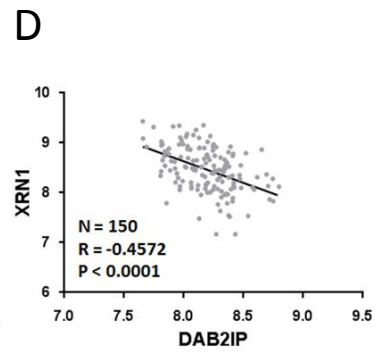
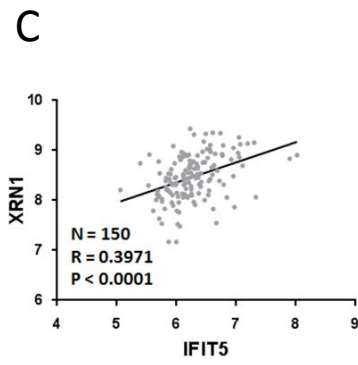
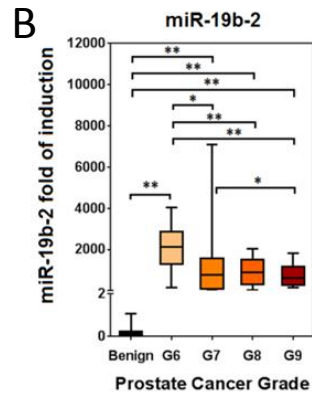
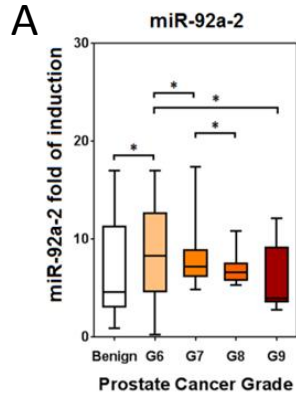
Additional file 6



Additional file 7



Additional file 8



Additional file 9

Table 1.

List of protein candidates derived from Mass Spectrometry after using precursor miR-363 to pull down protein complex in a variety of pairs (LAPC4, RWPE1 and C4-2) with or without DAB2IP expression.

Cell line	DAB2IP-/DAB2IP+ Ratio	PSMs	Peptide Seqs	% Coverage	S. COUNTS		S. INDEX (MIC SIn)	
					DAB2IP+	DAB2IP-	DAB2IP+	DAB2IP-
IFIT5_HUMAN Interferon-induced protein with tetratricopeptide repeats 5 OS=Homo sapiens GN=IFIT5 PE=1 SV=1								
LAPC4	LAPC4-KD Only	20	12	22.40		20.00		1.57E-06
RWPE1	1.28	152	18	39.60	62.50	90.50	2.63E-05	3.37E-05
C4-2	C4-2Neo Only	3	2	3.70		2.99		3.82E-07
B9A067_HUMAN Mitochondrial inner membrane protein OS=Homo sapiens GN=IMMT PE=2 SV=2								
LAPC4	0.11	5	5	8.60	4.00	1.00	1.22E-07	1.39E-08
RWPE1	0.28	5	3	7.30	3.00	2.00	3.57E-07	9.96E-08
C4-2	0.17	58	31	36.80	49.05	7.85	6.29E-06	1.05E-06
SNUT1_HUMAN U4/U6.U5 tri-snRNP-associated protein 1 OS=Homo sapiens GN=SART1 PE=1 SV=1								
LAPC4	0.40	14	10	14.80	9.00	5.00	2.37E-07	9.43E-08
RWPE1	0.90	17	10	13.50	8.00	9.00	7.93E-07	7.11E-07
C4-2	0.31	12	7	11.90	9.00	3.00	5.98E-07	1.88E-07
ADT2_HUMAN ADP/ATP translocase 2 OS=Homo sapiens GN=SLC25A5 PE=1 SV=7								
LAPC4	0.32	24	9	28.90	12.96	10.97	5.78E-06	1.82E-06
RWPE1	0.38	13	8	28.20	6.50	5.50	6.89E-06	2.63E-06
C4-2	0.35	18	11	28.90	11.02	6.00	8.09E-06	2.87E-06
PARP1_HUMAN Poly [ADP-ribose] polymerase 1 OS=Homo sapiens GN=PARP1 PE=1 SV=4								
LAPC4	0.68	135	40	40.80	73.00	62.00	3.38E-06	2.31E-06
RWPE1	0.48	10	5	6.90	6.00	4.00	3.33E-07	1.61E-07
C4-2	0.62	22	22	23.10	16.00	6.00	1.04E-06	6.42E-07
XRCC5_HUMAN X-ray repair cross-complementing protein 5 OS=Homo sapiens GN=XRCC5 PE=1 SV=3								
LAPC4	0.36	29	16	22.80	18.98	9.99	6.73E-07	2.45E-07
RWPE1	0.17	35	17	24.60	26.99	9.00	3.54E-06	6.10E-07
C4-2	C4-2D2 Only	6	6	8.30	6.00		4.04E-07	
SFPQ_HUMAN Splicing factor, proline- and glutamine-rich OS=Homo sapiens GN=SFPQ PE=1 SV=2								
LAPC4	0.54	176	34	46.10	115.41	59.73	1.50E-05	8.10E-06
RWPE1	0.69	11	6	12.00	5.00	6.00	7.40E-07	5.14E-07
C4-2	0.58	27	14	19.80	15.96	10.99	2.57E-06	1.49E-06
ATPA_HUMAN ATP synthase subunit alpha, mitochondrial OS=Homo sapiens GN=ATP5A1 PE=1 SV=1								
LAPC4	0.32	20	12	22.80	13.76	5.88	8.06E-07	2.55E-07
RWPE1	0.94	28	12	29.30	13.78	13.79	1.75E-06	1.65E-06
C4-2	0.88	97	25	41.60	49.17	46.19	1.13E-05	1.00E-05
VDAC2_HUMAN Voltage-dependent anion-selective channel protein 2 OS=Homo sapiens GN=VDAC2 PE=1 SV=2								
LAPC4	0.05	12	8	32.50	10.87	0.99	1.36E-06	6.52E-08
RWPE1	0.52	7	4	15.20	3.96	2.97	2.34E-06	1.21E-06
C4-2	0.13	36	11	48.80	27.70	7.92	2.40E-05	3.20E-06
H4_HUMAN Histone H4 OS=Homo sapiens GN=HIST1H4A PE=1 SV=2								
LAPC4	LAPC4-Con Only	5	3	31.10	5.00		2.46E-06	
RWPE1	0.70	7	4	40.80	5.00	2.00	3.79E-06	2.64E-06
C4-2	0.08	7	3	31.10	6.00	1.00	1.14E-05	9.59E-07
CKAP4_HUMAN Cytoskeleton-associated protein 4 OS=Homo sapiens GN=CKAP4 PE=1 SV=2								
LAPC4	0.41	6	3	6.00	3.00	3.00	8.02E-08	3.28E-08
RWPE1	0.73	28	13	27.20	16.00	12.00	1.93E-06	1.41E-06
C4-2	0.33	23	14	28.10	15.97	6.97	1.77E-06	5.76E-07
ILF2_HUMAN Interleukin enhancer-binding factor 2 OS=Homo sapiens GN=ILF2 PE=1 SV=2								
LAPC4	1.25	303	21	48.20	140.00	163.00	1.31E-04	1.63E-04
RWPE1	1.09	142	20	57.70	70.00	73.00	5.76E-05	6.29E-05
C4-2	1.47	28	8	20.00	13.00	15.00	2.89E-06	4.27E-06
ACACA_HUMAN Acetyl-CoA carboxylase 1 OS=Homo sapiens GN=ACACA PE=1 SV=2								
LAPC4	1.19	47	28	14.40	25.88	20.92	1.95E-07	2.32E-07
RWPE1	1.31	820	115	58.50	174.15	259.86	2.10E-05	2.74E-05
C4-2	8.98	16	122	43.40	5.94	9.44	8.89E-08	7.98E-07
I3L1L3_HUMAN Myb-binding protein 1A (Fragment) OS=Homo sapiens GN=MYBBP1A PE=4 SV=1								
LAPC4	LAPC4-Con Only	22	19	17.90	22.00		6.31E-07	
RWPE1	0.29	3	2	1.80	2.00	1.00	5.15E-08	1.47E-08
C4-2	C4-2D2 Only	2	2	1.60	2.00		3.41E-08	

Additional file 10

Table 2. Primers designed for site-directed mutagenesis and PCR.

Primers used for site-directed mutagenesis:	
Insertion of T7 promoter upstream to pre-miR-363 sequence in pCMV-miR-363 expression plasmid	
Pre363+T7m1-Forward	5'-AAGTTCCTGATATTTAGTCATTGTAATAATACGACTCAAATGATCTGTTTTGCTGTTGTGCG-3'
Pre363+T7m1-Reverse	5'-CGACAACAGCAAAACAGATCATTGAGTCGTATTATTACAATGACTAAATATCAGAACTT-3'
Pre363+T7m2-Forward	5'-TTAGTCATTGTAATAATACGACTCACTATAGGGCGAAATGATCTGTTTTGCTGTTGTGCG-3'
Pre363+T7m2-Reverse	5'-CGACAACAGCAAAACAGATCATTTCGCCCTATAGTGAGTCGTATTATTACAATGACTAA-3'
Generating Mutant form of T7-pre-miR-363 DNA templates	
SDM_T7-363-DS-Forward	5'-GGCGAAATGATCTGTTTTGCGGTTTACGGGTGGATCAC-3'
SDM_T7-363-DS-Reverse	5'-GTGATCCACCCGTAACCGCAAAACAGATCATTTCGCC-3'
SDM_T7-363-SS-Forward	5'-GGCGAAATGATCTGTTTTGCTCAAGTCGGGTGGATCAC-3'
SDM_T7-363-SS-Reverse	5'-GTGATCCACCCGACTTGAGCAAAACAGATCATTTCGCC-3'
Generating Mutant form of pre-miR-363 expression plasmids	
SDM_pCMV363-DS-Forward	5'-TTGTAATAATGATCTGTTTTGCGGTTTACGGGTGGATCAC-3'
SDM_pCMV363-DS-Reverse	5'-GTGATCCACCCGTAACCGCAAAACAGATCATTTTACAA-3'
SDM-pCMV363-SS-Forward	5'-TTGTAATAATGATCTGTTTTGCTCAAGTCGGGTGGATCAC-3'
SDM-pCMV363-SS-Reverse	5'-GTGATCCACCCGACTTGAGCAAAACAGATCATTTTACAA-3'
Insertion of ApaI upstream to pre-miR-92a-2 sequence in pGEM-pre-92a-2 plasmid	
T7-Apa1-mut-Forward	5'-ATTCGATTCTCTGGGCCCGCTTTCTTCCACAGGCCG-3'
T7-Apa1-mut-Reverse	5'-CGGCCTGTGGAAGAAAGCGGCCAGAGAATCGAAT-3'
Generating mutant miR-363 target site in siCHECK2-Slug 3'UTR	
SLUG-SDM-Forward	5'-CATTTTAATAATTTTGGAAATTAATGGCTATATTTCCGGCAAATTTAAGAGGATCTTAC-3'
SLUG-SDM-Reverse	5'-GTAAGAATCCTCTTAAATTTGCCGGAAATATAGCCATTAATTTTCAAAAATTATTAAAATG-3'
Insertion of NheI into pre-miR-92a-2 sequence in pCMV-miR-363 plasmid	
92a-2 SDM NheI-Forward	5'-TTCTATATAAAGTATTGCAGCTAGCCTTGTCCCGGCTGTGGAA-3'
92a-2 SDM NheI-Reverse	5'-TTCCACAGGCCGGGACAAGGCTAGCTGCAATACTTTATATAGAA-3'
Primers used for PCR:	
pre363wT7-Forward	5'-GTCATTGTAATAATACGACTCA-3'
pre363-Reverse	5'-GGTTTACAGATGGATACCG-3'
Pre92a-2-Forward	5'-GCCCATTCATCCCTGGGTGGGATTTGT-3'
Pre92a-2-Reverse	5'-CTCCTTTCTTCCACAGGCCGGGACAAGT-3'
T7_pre92a-2-Forward	5'-TGTAATACGACTCACTATAGGGCGAAT-3'
T7_pre92a-2-Reverse	5'-TCATCCCTGGGTGGGATTTGTTGCAT-3'
SDM_T7-363-DS-Forward	5'-GGCGAAATGATCTGTTTTGCGGTTTACGGGTGGATCAC-3'
SDM_T7-363-SS-Forward	5'-GGCGAAATGATCTGTTTTGCTCAAGTCGGGTGGATCAC-3'
Generating Mutant form of SN-A/C pre-miR-92a-2 DNA template	
X-92-5A-Fw	5'-TCTAGAACATCCCTGGGTGGGATTTGT-3'
X-92-3C-Rv	5'-TCTAGAGCTTCCACAGGCCGGGACAAGT-3'



AACR podium presentation

UT SOUTHWESTERN
MEDICAL CENTER



The specific regulation of miR-363 turnover from miR-106a-363 cluster by IFIT5 complex leading to epithelial-to-mesenchymal transition

U-Ging Lo, Rey-Chen Pong, Diane Yang, Leah Gandee, Jiancheng Zhou, Shu-Fen Tseng, Jer-Tsong Hsieh

Department of Urology

University of Texas Southwestern Medical Center

Dallas, TX

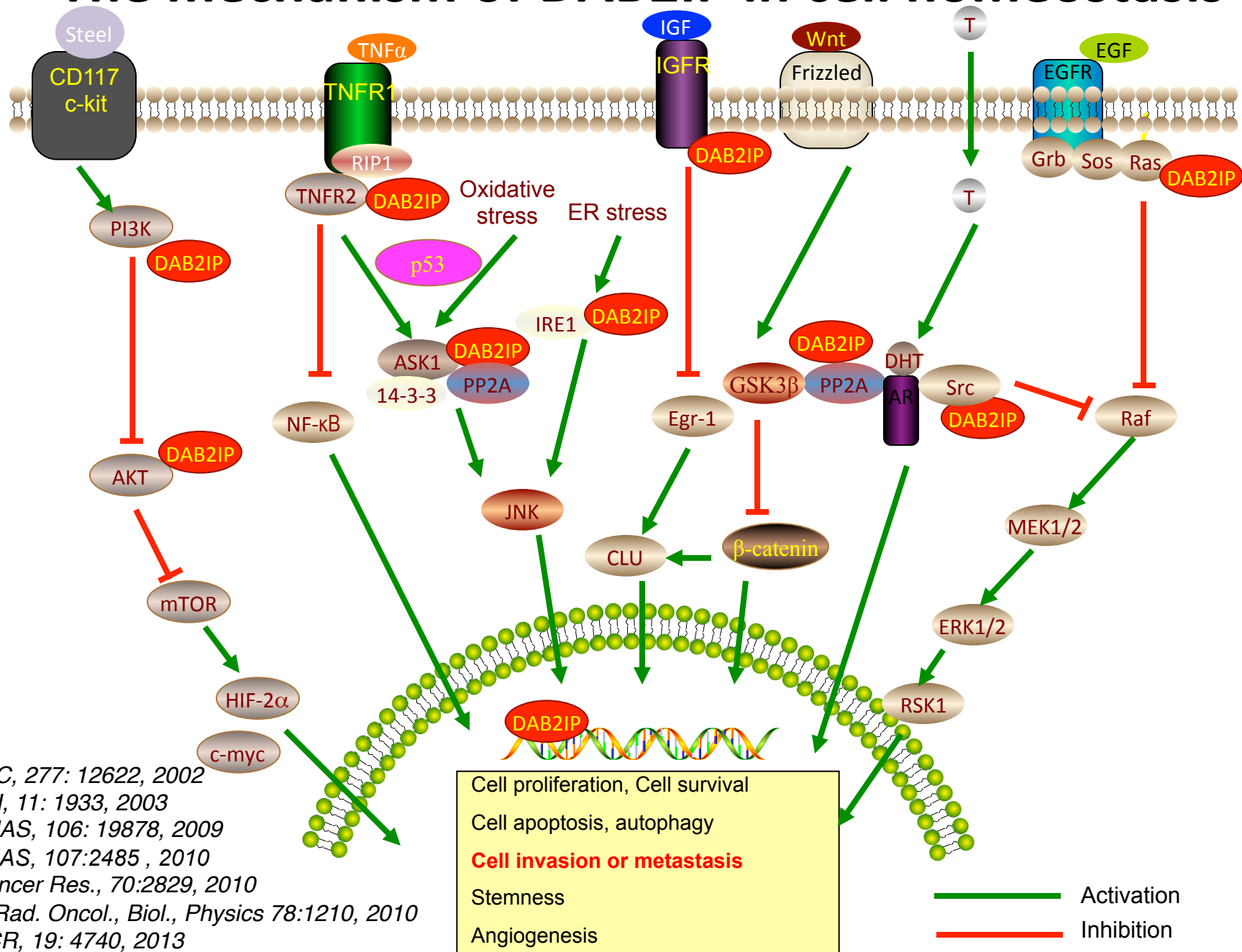
Disclosure Information

**2015 AACR Annual Meeting
U-Ging Lo**

I have no financial relationships to disclose.

I will not discuss off label use and/or investigational use in my presentation.

The mechanism of DAB2IP in cell homeostasis



JBC, 277: 12622, 2002

JCI, 11: 1933, 2003

PNAS, 106: 19878, 2009

PNAS, 107:2485, 2010

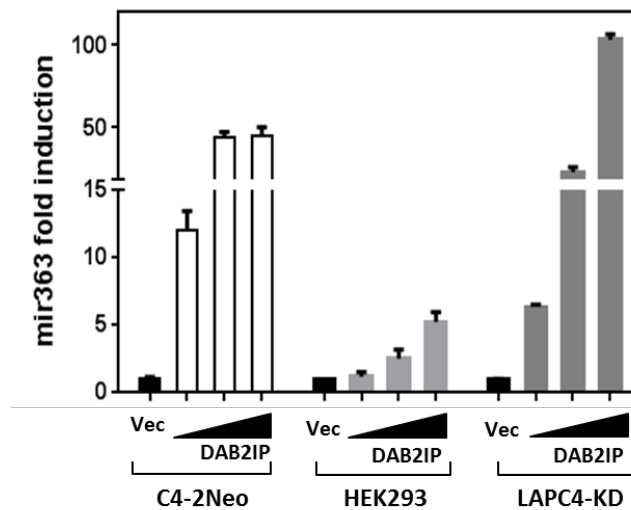
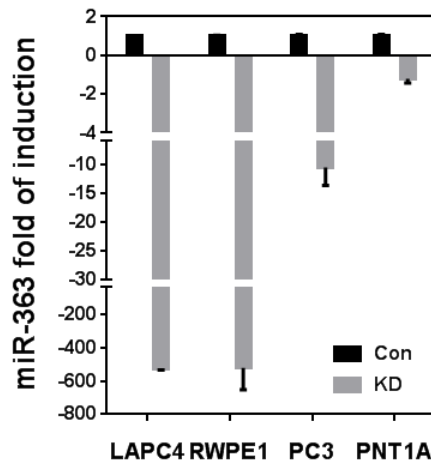
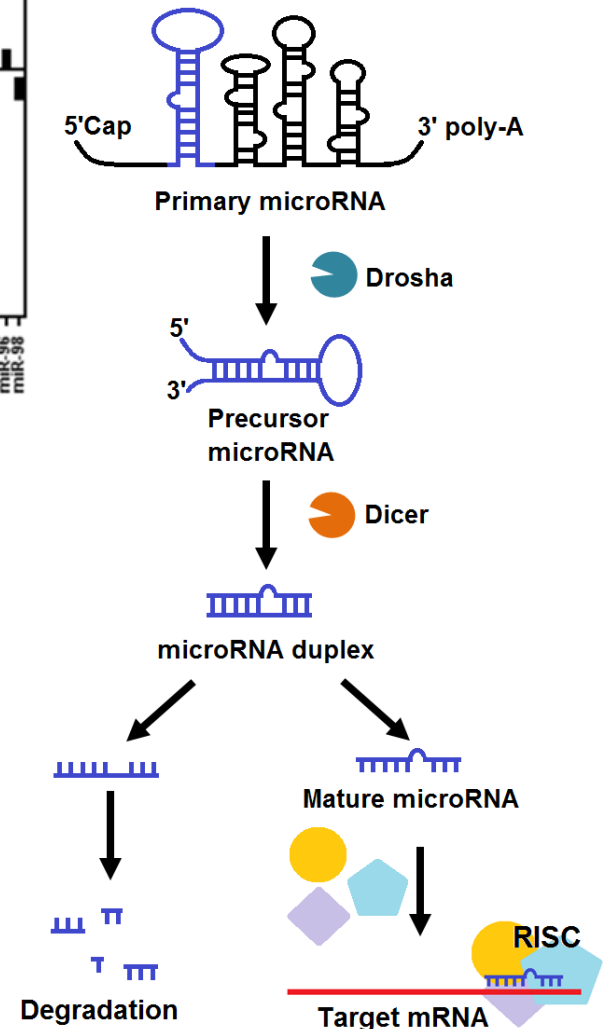
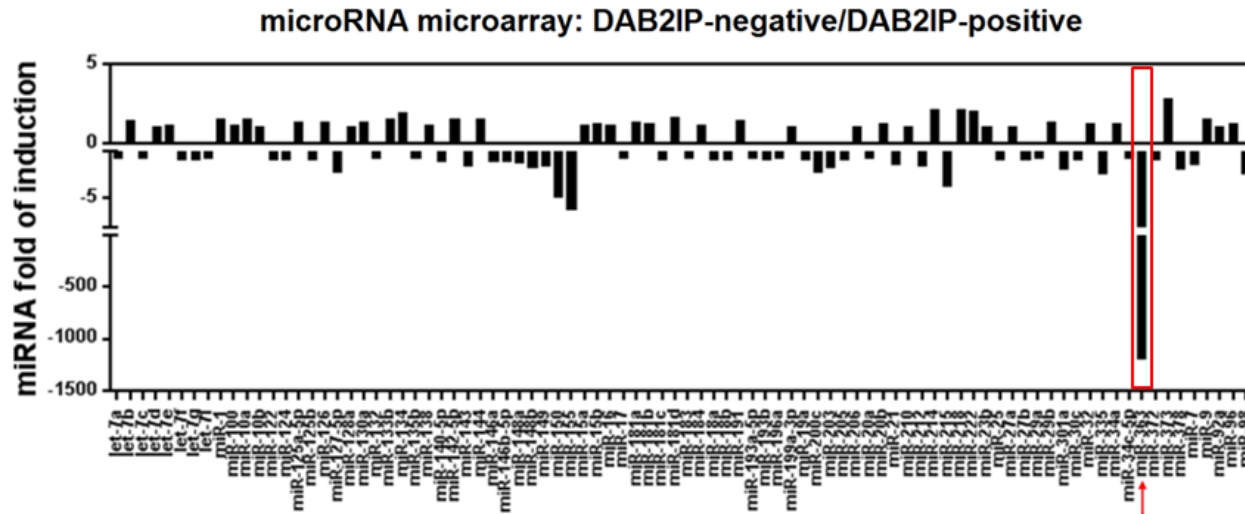
Cancer Res., 70:2829, 2010

J. Rad. Oncol., Biol., Physics 78:1210, 2010

CCR, 19: 4740, 2013

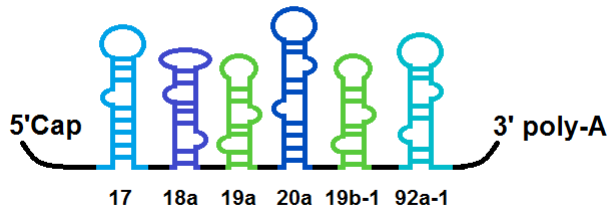
Oncogene, 33:1954, 2014

The positive correlation between DAB2IP and miR-363 expression

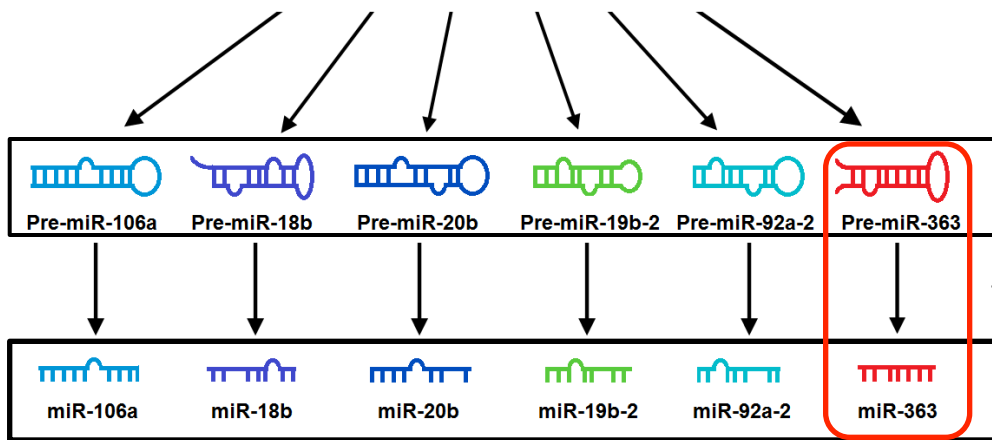
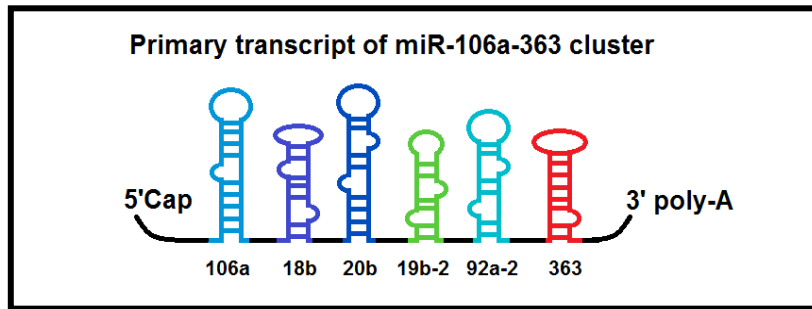


DAB2IP mediates a specific regulation of miR-363 from miR-106a-363 cluster

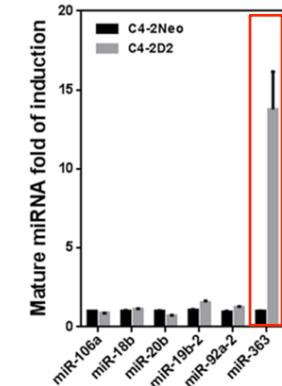
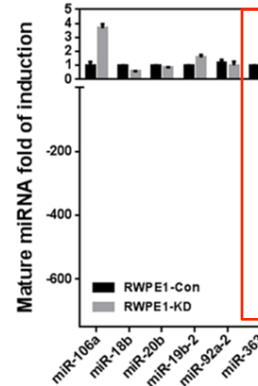
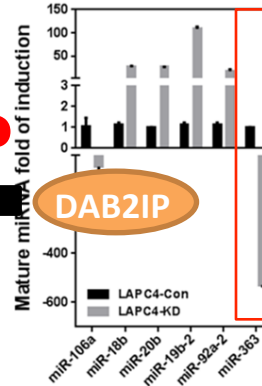
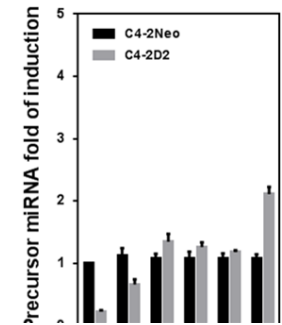
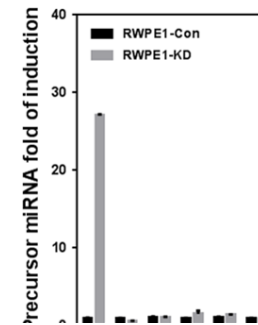
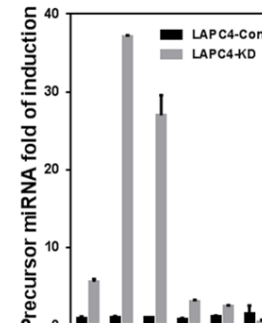
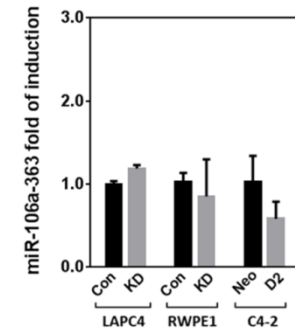
Primary transcript of miR-17-92 cluster



Resemble to miR-106a-363 in miRNA seed sequence



miR-106a-363 transcript



DAB2IP

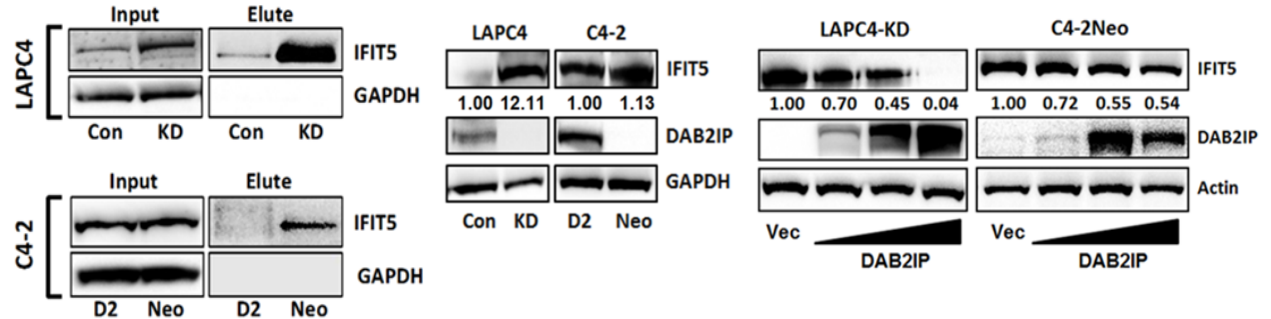
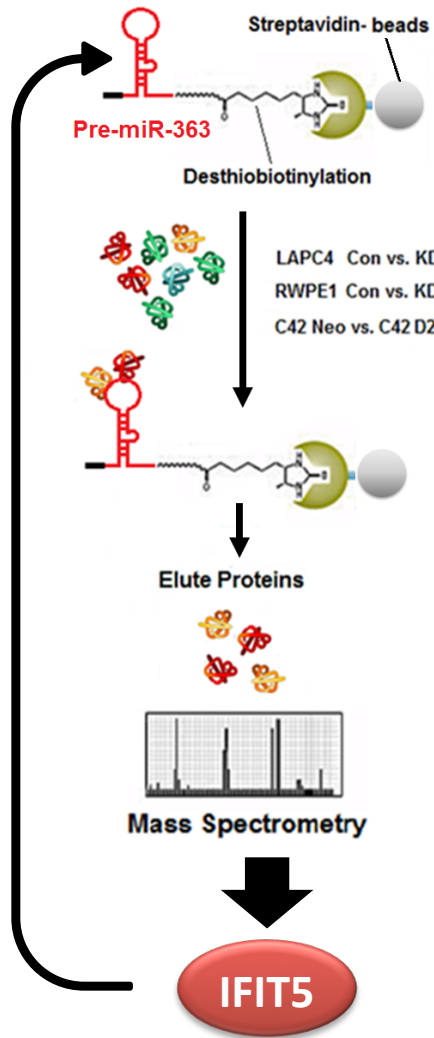


The impact of IFIT5 on miR-363 maturation distinct from miR-106a-363 cluster

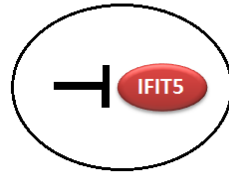
IFIT5: QMAQLVLPK Produced in vitro with tryptic proteolytic reagents 5 OS=Homo sapiens GN=IFIT5 PE=

Cell line	RATIO				S. COUNTS		S. INDEX (MIC SIn)	
	KD/Con	PSMs	Peptide Seqs	% Coverage	Con	KD	Con	KD
LAPC4	363_LP-kd Only	20	12	22.40		20.00		1.57E-06
C42	363_CNeo Only	3	2	3.70		2.99		3.82E-07

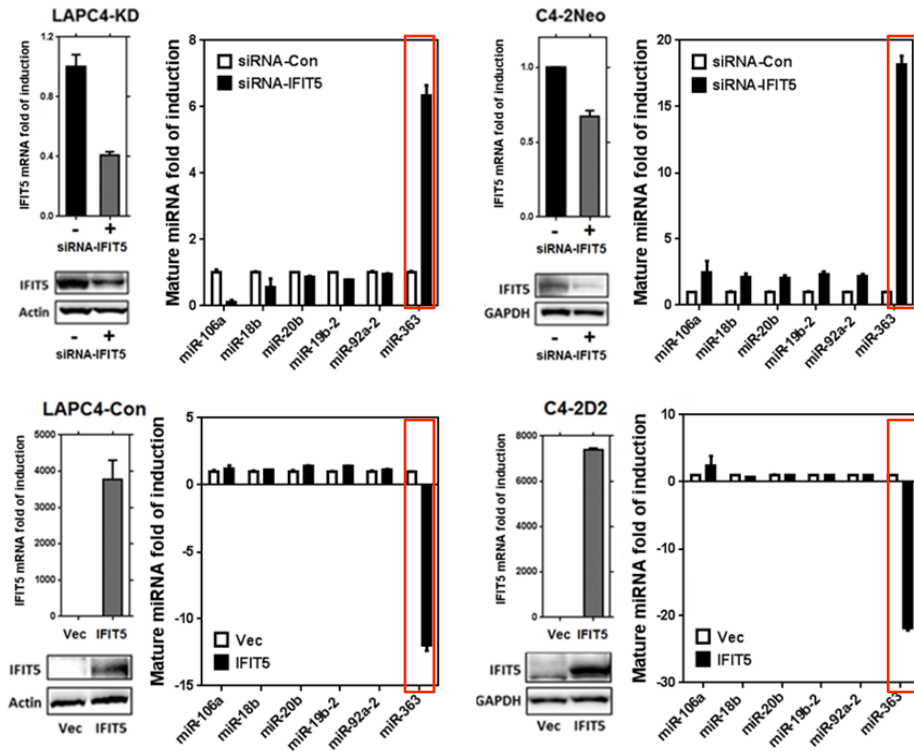
RNA pull-down assay



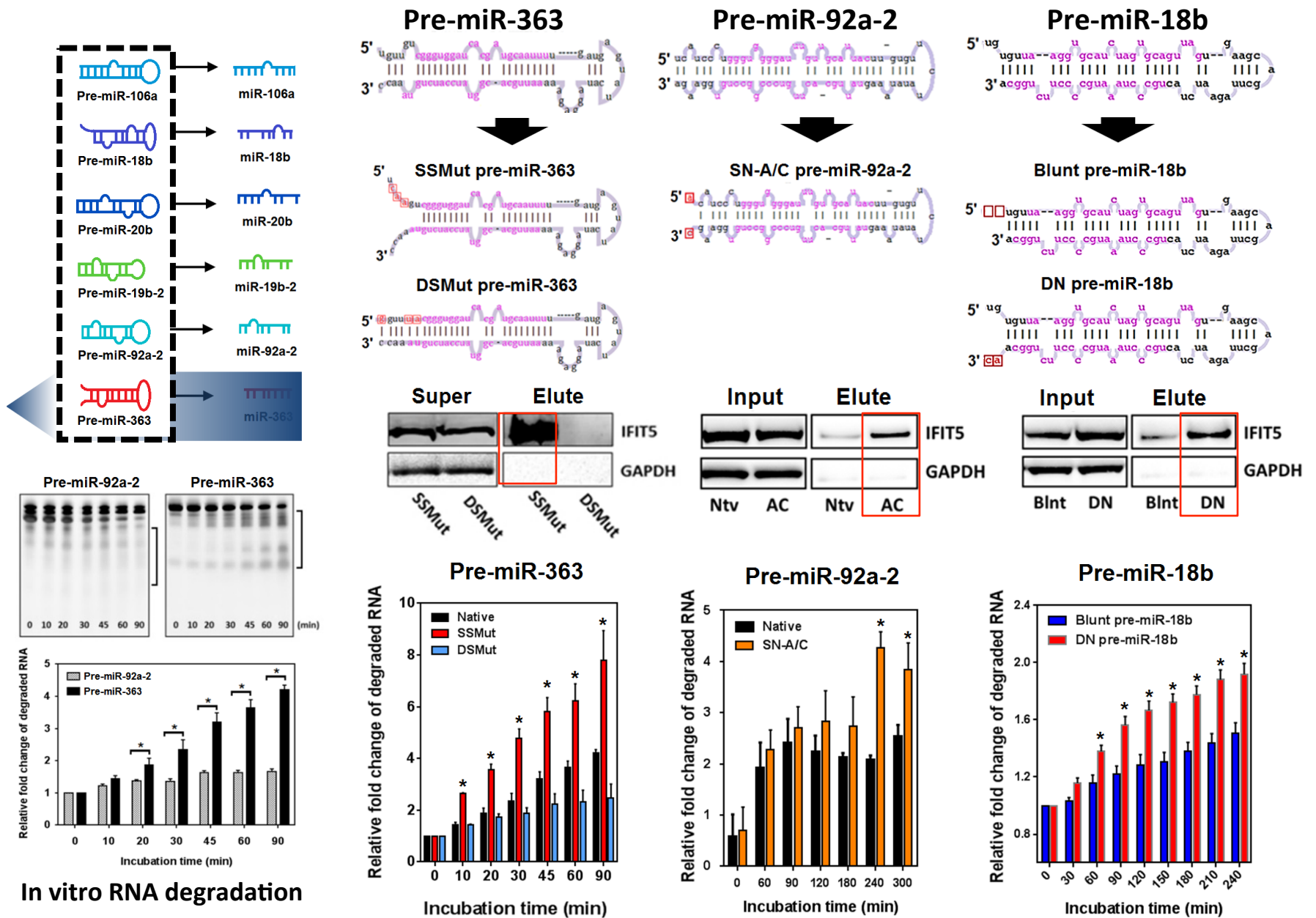
DAB2IP-negative



DAB2IP-positive



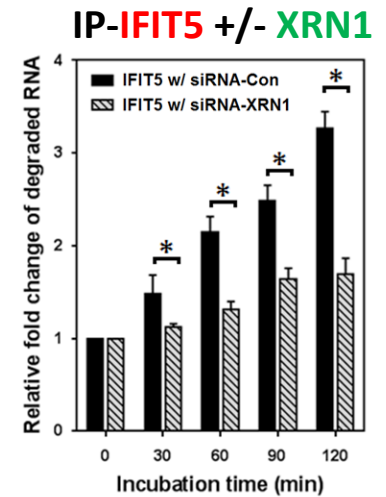
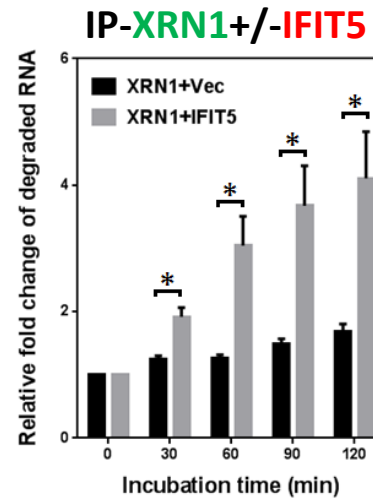
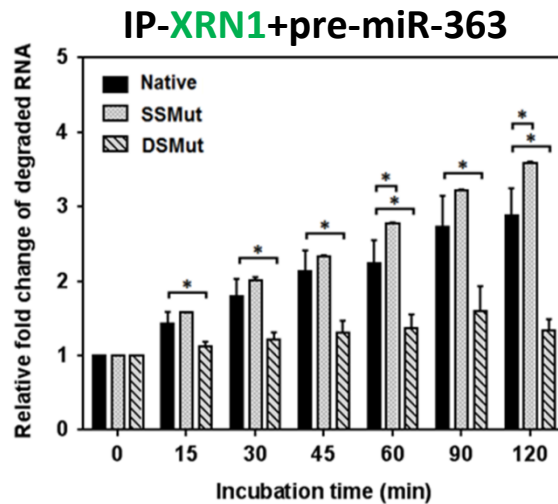
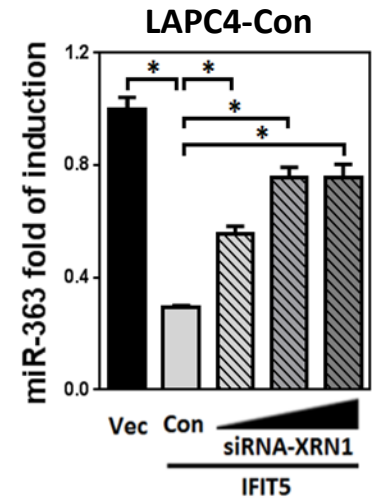
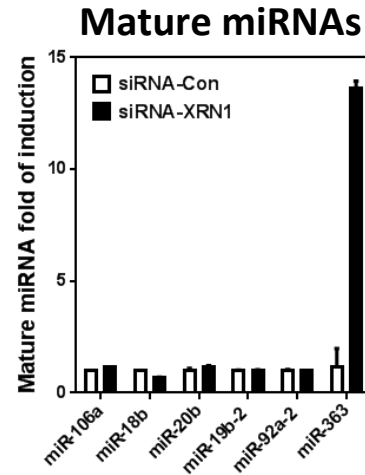
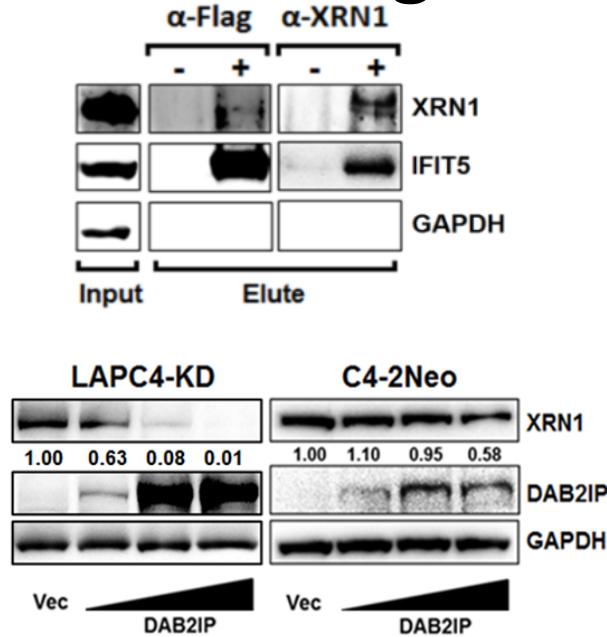
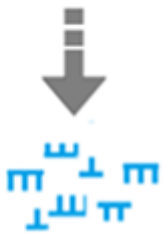
IFIT5 elicits miR-363 turnover at the precursor stage



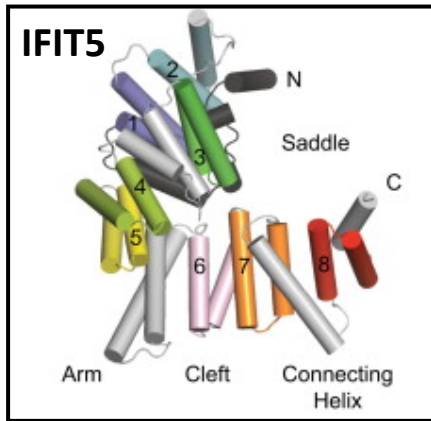
The role of XRN1 in IFIT5 complex in pre-miR-363 degradation



precursor miRNAs



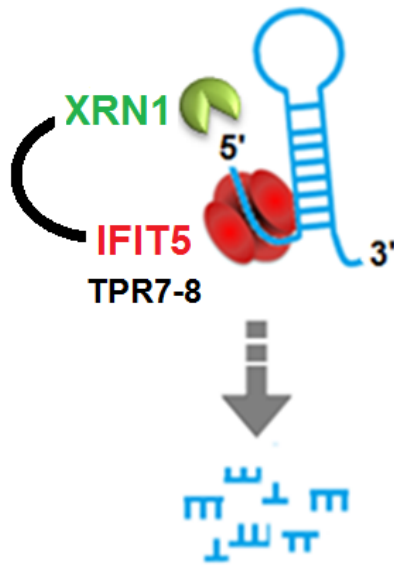
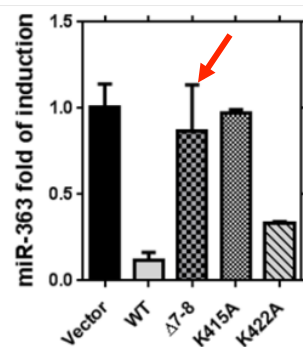
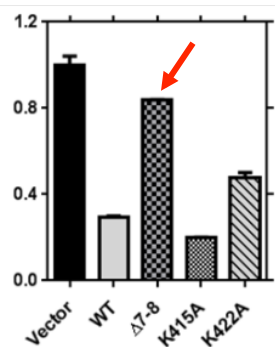
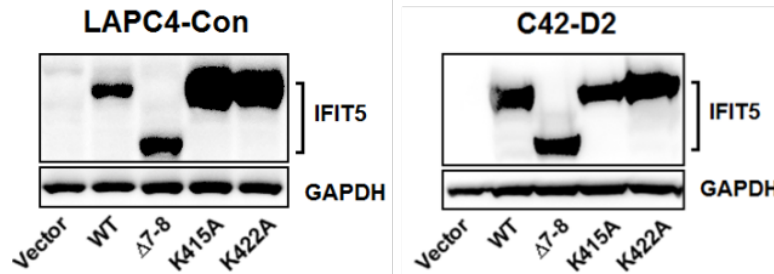
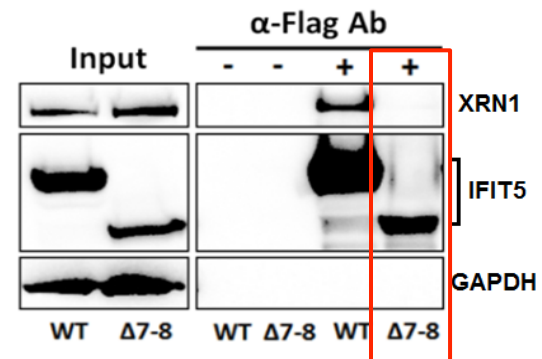
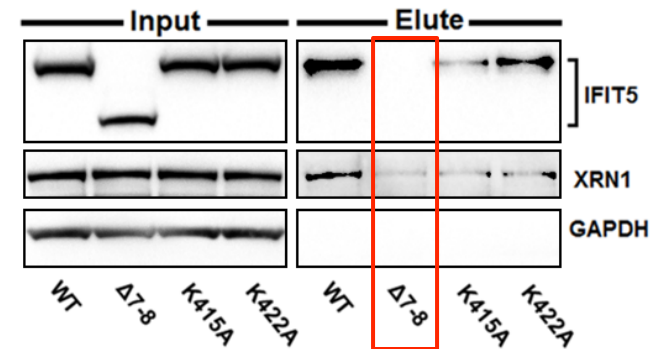
The TPR 7-8 domain of IFIT5 is required for docking XRN1 on pre-miR-363



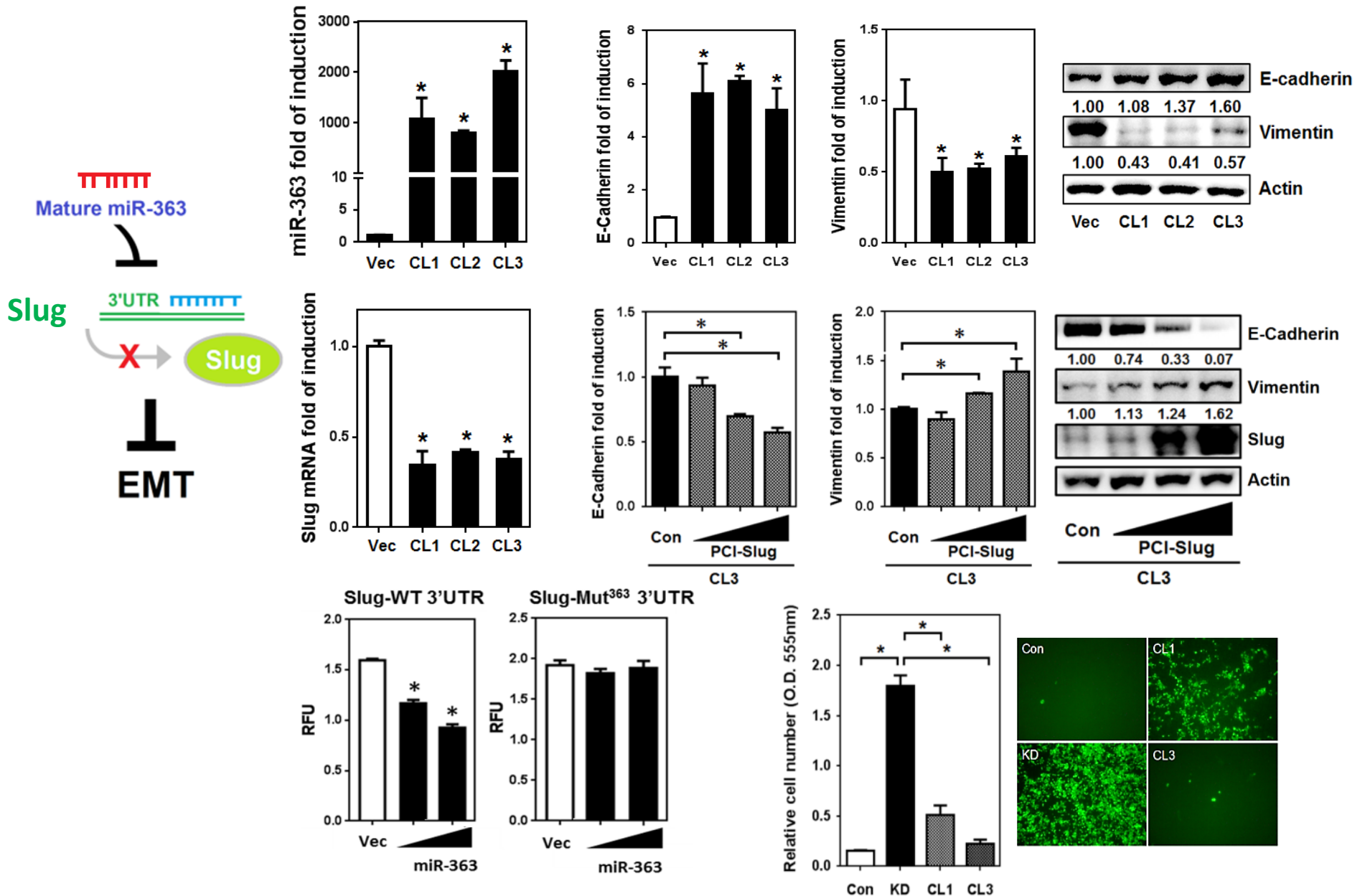
(Katibah et al., *Cell* 2012)



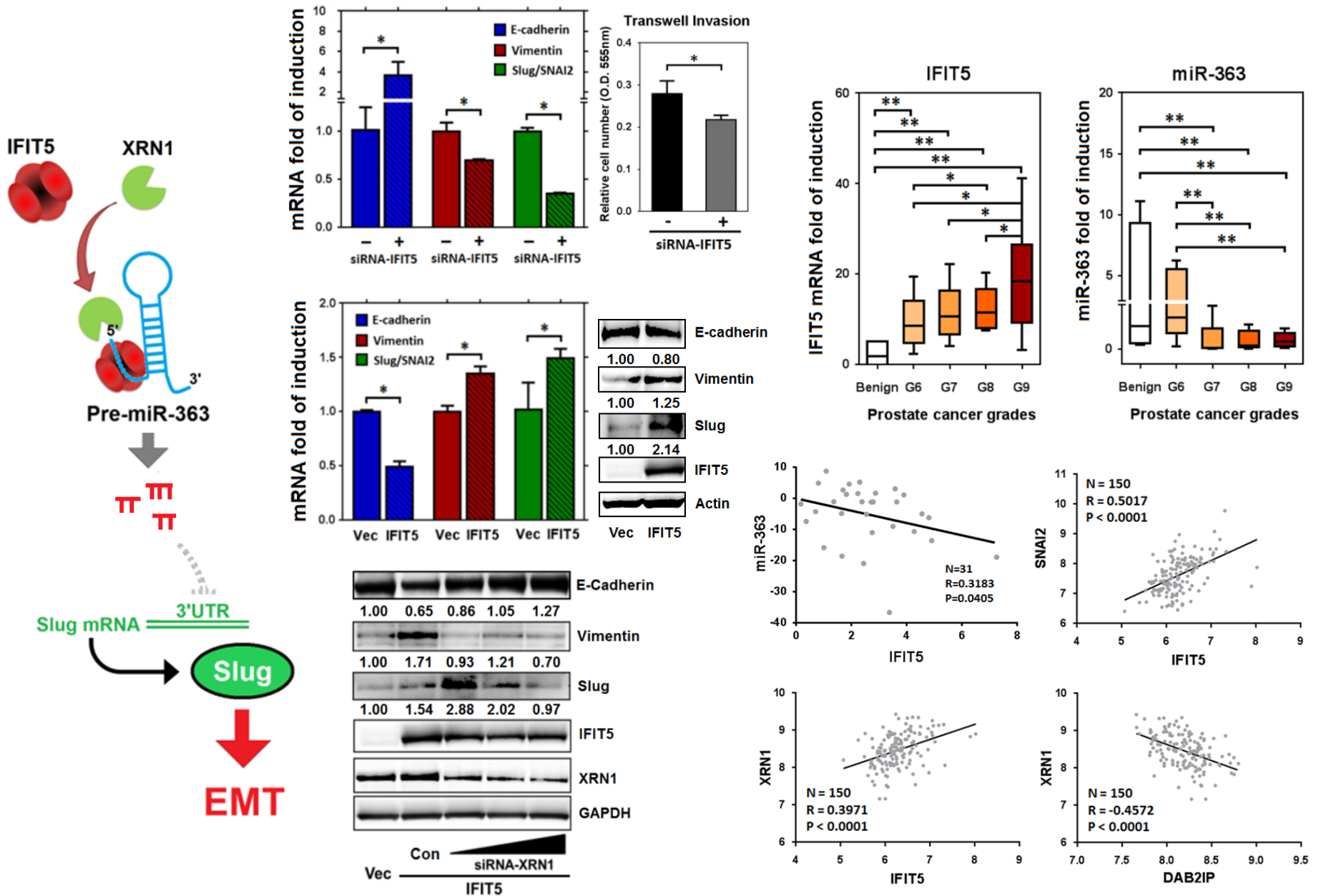
RNA pull down assay



miR-363 can suppress EMT by targeting Slug in PCa

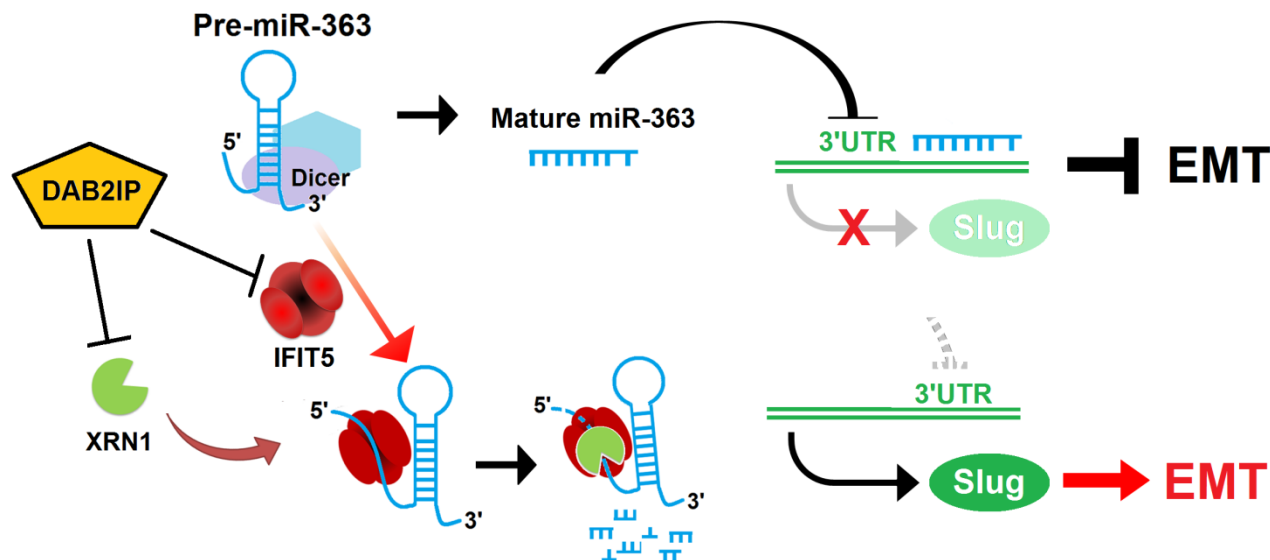


Clinical correlation of IFIT5 or miR-363 in PCa tissues



SUMMARY

- ✓ A differential expression profile of miR-363 from miR-106a-363 cluster is regulated by miRNA turnover.
- ✓ The **IFIT5-XRN1** complex is responsible for the specific miR-363 turnover.
- ✓ The **IFIT5 C' terminal TPR7-8** domain is required for (1) interaction with 5' end of precursor miR-363 and (2) recruitment of **XRN1**.
- ✓ **DAB2IP** play a critical role in regulating both **IFIT5** and **XRN1** expression.
- ✓ miR-363 perform tumor suppressive function and prevent EMT by targeting Slug.
- ✓ IFIT5 and miR-363 are inversely correlated in prostate cancer malignancies.



Acknowledgement



JT Hsieh Lab

Jer-Tsong Hsieh

Ray-Chen Pong

Eun-Jin Yun

Leah Gandee

Diane Yang

Jiancheng Zhou

Shu-Fen Tseng

Bin Wang

Cheng-Kuo Lai

Li-Chiung Lin

Chun-Jung Lin

Wai Chen

Elizabeth Hernandez

John Santoyo

Congressionally Directed Medical Research Programs

CDMRP



Department of Defense

The role of IFIT5 in miR-363 turnover

Short title: The function and regulation of miR-363

U-Ging Lo, Rey-Chen Pong, Diane Yang, Leah Gandee, Jiancheng Zhou, Shu-Fen Tseng, and Jer-Tsong Hsieh

Background: The majority of prostate cancer (PCa) mortality is due to the recurrent metastatic castration resistant PCa (mCRPC). The acquisition of epithelial-to-mesenchymal transition (EMT) in PCa cells increases their metastatic potential. Although several microRNAs (miRNAs) have been shown to be involved in EMT of PCa, the role of miR-363 has not been reported. This miR-363 belongs to the miR-106a-363 cluster containing additional miRNAs such as 106a, 18b, 20b, 19b-2, and 92a-2, which are closely resemble to the oncogenic miR-17-92 cluster characterized as an oncomir. However, no miR-363 homolog is found in this cluster and also its functional role is largely unknown. In addition, the regulation of miRNA expression becomes more complicated when a polycistronic primary transcript from a miRNA gene cluster generates each individual miRNA with different expression profile and functional role. In this study, we have unveiled a new protein complex responsible for the specific miR-363 turnover.

Methods: RNA pull down assay, immunoprecipitation assay, Liquid chromatography-tandem mass spectrometry, and *in vitro* RNA degradation assay were for determining miR-363 turnover. Real-time RT-PCR, luciferase reporter gene and cell invasion assays were for determining the function and mechanism of miR-363.

Results: Unlike other members characterized as oncomirs from the same cluster, miR-363 functions as an inhibitor of EMT by targeting Slug in PCa cells. Also, a dramatic down-regulation of mature miR-363 is found in PCa cells exhibiting EMT phenotypes, which is mediated by pre-miR-363 degradation. We further identify interferon-induced tetratricopeptide repeat 5 (IFIT5) as a key factor in mediating miR-363 turnover; which is also highly elevated in PCa tissues with high-grade tumor. IFIT5 is first characterized as a viral RNA binding protein, until now, there is no report indicating the role of IFIT5 in miRNA turnover. Nevertheless, IFIT5 was further characterized to unveil that it can recognize a unique structure at the 5'-end of pre-miR-363, which facilitates pre-miR-363 degradation by recruiting a 5'-3' exoribonuclease (i.e., XRN1). This regulation appears to be structure specific because IFIT5 fails to bind to other miRNAs from the same cluster to elicit their turnover. We also notice that IFIT5 can accelerate the turnover of miRNAs with the similar 5'-end structure of pre-miR-363. Meanwhile, the significant elevation of IFIT5 is detected in several PCa cell lines undergone EMT leading to highly metastatic potential. In addition, an inverse correlation between miR-363 and IFIT5 mRNA level was also found in PCa specimens.

Conclusion: miR-363 is a potent anti-EMT miRNA in PCa. IFIT5 complex represents unique post-transcriptional machinery for miR-363 turnover, which provide a new model of miRNA regulation from a cluster of miRNAs with different functions. Overall, this study provides a new insight of miRNA biogenesis machinery in cancer metastasis and potential new therapeutic target for mCRPC.